Department of Natural Resources and Mines
Geological Survey of Queensland

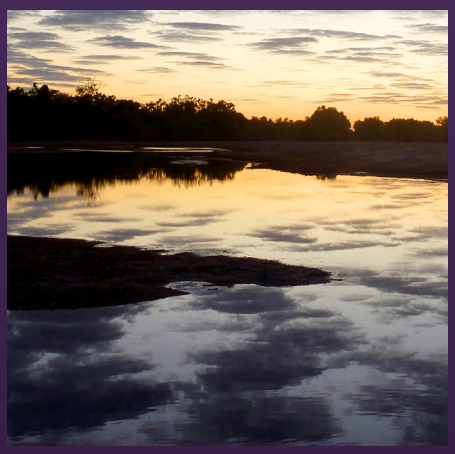

Queensland Geology 14

An assessment of the geothermal energy potential of northern and eastern Queensland

Coastal Geothermal Energy Initiative

B Talebi, S N Sargent and L K O'Connor

2014

Great state. Great opportunity.

Queensland Government

Acknowledgements

The Coastal Geothermal Energy Initiative team would like to thank Geoscience Australia for their in-kind contribution by providing analytical services for thermal conductivity analysis and precision temperature logging.

We are indebted to GSQ's field staff and Spatial and Graphics Services for their contribution.

Thank you also to J.L. McKellar, L.J. Hutton, I.W. Withnall, P.J.T. Donchak and, in particular, P.M. Green for their valuable comments and insights.

Address for correspondence:

Geological Survey of Queensland
Department of Natural Resources and Mines
PO Box 15216 City East 4002
Telephone: (07) 3006 4666; International +61 7 3006 4666
Email: geological_info@dnrm.qld.gov.au
Internet: www.dnrm.qld.gov.au

© State of Queensland (Department of Natural Resource and Mines) 2014

The Queensland Government supports and encourages the dissemination and exchange of its information. The copyright in this publication is licensed under a Creative Commons Attribution 3.0 Australia (CC BY) licence.

Under this licence you are free, without having to seek permission from DNRM, to use this publication in accordance with the licence terms.

You must keep intact the copyright notice and attribute the State of Queensland, Department of Natural Resource and Mines as the source of the publication.

For more information on this licence visit
http://creativecommons.org/licenses/by/3.0/au/deed.en

Cover photographs: Top to bottom, GSQ St Lawrence 1 site location; Gilbert River, Riverview Station at sunset; GSQ Gympie 7, on site core logging; GSQ Townsville 2-4R drilling operations ; GSQ Longreach 2 drill core with ammonite shell

ISSN 1039-4840
ISBN 978-1-922067-29-6
Issued: March 2014

Reference: TALEBI, B., SARGENT, S.N. & O'CONNOR, L.K., 2014: An assessment of the geothermal energy potential of northern and eastern Queensland, Coastal Geothermal Energy Initiative. *Queensland Geology* **14**.

Contents

FIGURE

TABLE

Abbreviation	Term
EGS	Enhanced or Engineered Geothermal System
HSA	Hot Sedimentary Aquifer
GSQ	Geological Survey of Queensland
CGEI	Coastal Geothermal Energy Initiative
GA	Geoscience Australia
HDR	Hot Dry Rocks Limited

Abbreviation	Unit
°	degrees
°C/km	degrees celsius per kilometre
°C	degrees celsius
EJ	exajoule or 10^{18} joules
GWh	gigawatt - hours
GWe	gigawatt electrical
g/cm³	grams per cubic centimetre
J/kg°C	joules per kilogram degree celsius
kg/m³	kilograms per cubic metre
kg/s	kilograms per second
km	kilometres
kWe	kilowatt electrical
MWe	megawatt electrical
m	metres
µW/m³	microwatts per cubic metre
mW/m²	milliwatts per square metre
mD	millidarcy
mg/L	milligram per litre
mm	millimetres
Ma	million years
%	per cent
PJ	petajoule
PJ/km³	petajoules per cubic kilometre
km²	square kilometres
W/mK	watt per metre-Kelvin

Executive summary

The Coastal Geothermal Energy Initiative (CGEI) was a $5 million program designed by the Queensland Government to investigate additional sources of geothermal energy close to existing electricity infrastructure. A structured drilling program, which ran from November 2010 to July 2012, was the key component of this initiative. Ten sites were drilled, from which temperature and thermal conductivity data were collected. These data were used to model heat flow and temperature to 5 km depth.

The CGEI program highlighted five areas prospective for geothermal energy within the Millungera, Surat, Hillsborough and Maryborough basins. A preliminary geothermal resource assessment of the areas quantified the stored thermal energy in-place and power generation potential of the inferred resources.

Modelling of data from these prospective areas indicates:

- modelled heat flow values between 67.0 and 113.0 mW/m^2
- modelled temperatures at 5 km between 187 and 240°C
- an estimated total stored thermal energy in-place between 88 000 and 402 000 PJ using a volumetric approach
- an electric power generation potential between 430 and 1980 MWe, which is sufficient to meet the state forecast demand over the next decade.

The high modelled heat flow and temperatures at depth are attributed to a variety of heat sources, including low, medium and high heat-producing intrusives; residual heat from rifting; and recent volcanism and crustal magmatism. Additionally, the coal-bearing strata within Surat, Hillsborough and Maryborough basins have a high insulating capacity allowing them to act as thermal blankets for intrusives, also contributing to the prospectivity of the areas.

All inferred resource areas are located within 100 km of Queensland's major population centres or existing transmission lines, allowing the geothermal energy to be utilised more efficiently.

This program has laid the groundwork for geothermal exploration in Queensland, facilitating the reduction of risk for future explorers by:

- collecting precompetitive data to redefine the state's potential resource areas
- expanding Queensland's exploration opportunities
- highlighting issues with, and suggesting solutions for, drilling heat flow bores in sedimentary basins in Queensland.

However, further investigation and detailed exploration is warranted for the inferred geothermal resource areas identified through the CGEI program.

1. Introduction

1.1 Rationale

With the growth of Queensland's population and heavy industries there is a need for new energy sources to meet future base-load electricity requirements. However, the environmental impact of any new energy sources must be considered; thus, a low emission alternative to fossil fuels would be advantageous. Geothermal energy can be utilised for power generation and direct-use application and as such has been identified as a potential future low emission energy resource for the State of Queensland.

Regional datasets such as OzTemp (Gerner & Holgate, 2010) are commonly used to highlight areas with geothermal energy potential, however the data is mainly based on existing petroleum data (Figure 1-1). OzTemp shows the southwest portion of the state to have anomalously high temperatures at 5 km depth, suggesting substantial geothermal energy potential. However, this potential is located

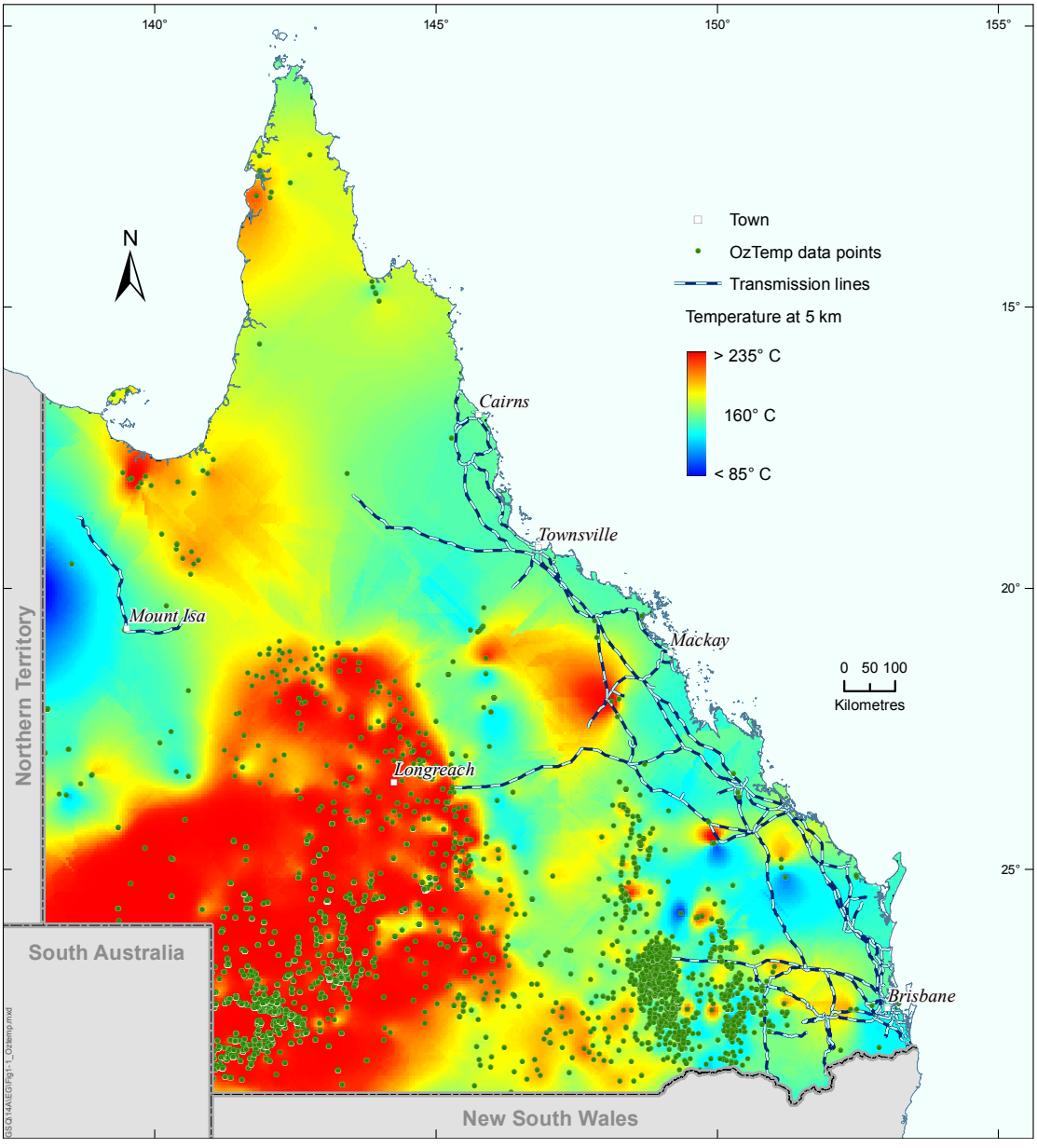

Figure 1-1. Geoscience Australia's OzTemp image.

away from existing infrastructure and energy markets, and the high cost of new infrastructure may limit the economic viability of its exploitation. Outside this portion of the state, data density and reliability diminish, limiting the ability to identify geothermal energy potential in Queensland's coastal regions. Thus, the collection of new data is critical for better assessment of the geothermal energy potential of Queensland.

Shallow drilling programs provide a means of assessing regional-scale geothermal potential for areas with limited data coverage. In lieu of direct measurements of temperature at depth, temperature and thermal conductivity data collected from shallow drilling may be used to determine heat flow—a useful tool through which temperatures can be estimated to depth. In 2011, Hot Dry Rocks Ltd used existing petroleum data to compile a heat flow map of Australia (Figure 1-2), which, as with the OzTemp data, highlights the southwest of Queensland as having anomalously high heat flow.

The Queensland Government's 'ClimateSmart 2050 – a cleaner energy strategy' allocated $5 million for a project designed to investigate additional sources of hot rocks for geothermal energy close to existing transmission lines. The Coastal Geothermal Energy Initiative (CGEI), implemented by the Geological Survey of Queensland, was the project undertaken to investigate these hot rocks.

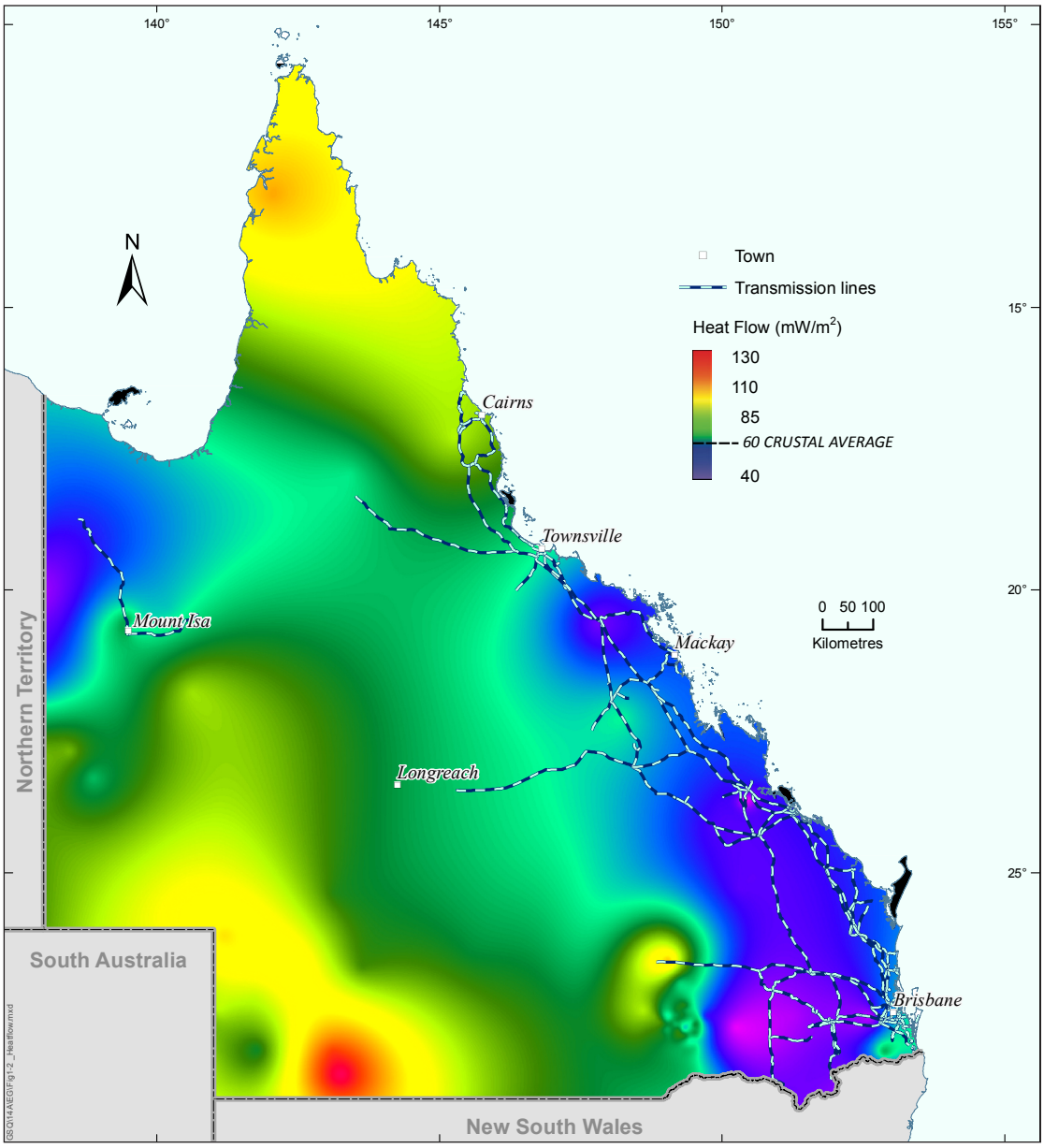

Figure 1-2. Hot Dry Rocks' heat flow map (Queensland portion)—highlighting high heat flow in southwest Queensland. Map available courtesy of Hot Dry Rocks Pty Ltd (personal communication, 2011).

The CGEI aimed to:

- identify areas within northern and eastern Queensland with geothermal energy potential
- collect new temperature and heat flow datasets through a structured drilling program
- provide an assessment of geothermal resource potential in Queensland
- provide pre-competitive data for use by the geothermal industry to reduce exploration risk.

1.2 Geothermal Energy Systems

Globally, geothermal energy is sourced from volcanically active regions. In the absence of active volcanism in Australia, geothermal exploration commonly targets areas with higher temperatures at depth in areas that are viable for the development of Enhanced Geothermal System and Hot Sedimentary Aquifer.

An **Enhanced Geothermal System (EGS)** is a man-made geothermal system, which differs from sedimentary and volcanic geothermal systems in that there is no natural, fluid-circulation path. The system is generally developed by targeting impermeable buried intrusives. EGS development requires the creation of an artificial fluid-flow path with suitable permeability using hydro-fracture stimulation. EGS heat sources are usually high heat-producing intrusives—intrusives with elevated concentrations of radioactive uranium (U), thorium (Th) and potassium (K) isotopes that generate anomalous radiogenic heat. These intrusives produce higher than average geothermal gradients. Under sufficient insulation, these intrusives can retain temperatures in excess of 160°C at 3–5 km depth.

One cubic kilometre of hot granite at 250ºC has the stored energy equivalent of 40 million barrels of oil when the heat is extracted to a temperature of 150ºC (Geodynamics, 2014a). Australia is estimated to have 22 000 EJ—5000 times its annual energy consumption—stored in EGS resources (Burns *et al.*, 2000). According to an estimate by the Energy Supply Association of Australia (Australian Geothermal Energy Group, 2007), EGS resources may provide up to 5.5 GWe, or 10% of present Australian electricity generation by 2030. Intrusives with EGS potential are currently being targeted for development in the Cooper Basin region, and it is predicted that EGS in this region will contribute 4000 MWe of base-load electricity by 2030 (Eghbal & Saha, 2011).

In EGS, two working fluids are used. A primary fluid, typically brine, is circulated in a continuous loop through the intrusive to the heat exchanger on the surface. In a heat exchanger, the heat is transferred to a secondary fluid with a lower boiling point, typically isopentane. This secondary fluid is then expanded through a turbine-generator to produce electricity. The brine and isopentane are both recirculated and the cycle repeated for continuous electricity generation (Figure 1-3). The best known example of an attempt to commercialise EGS in Australia is in northeastern South Australia, where the Innamincka Deeps project is targeting granites underlying the Cooper Basin. This project has progressed to the commissioning of a 1 MWe pilot plant and successful 5 month trial (Geodynamics, 2014b).

Geothermal reservoirs in sedimentary basins are referred to as **Hot Sedimentary Aquifer (HSA)** systems. In recent years, the Australian geothermal industry has targeted some sedimentary basins containing highly permeable aquifers at 1–3 km depth with temperatures in the range of 120°C to 160°C. Fluid-flow rates of between 80 kg/s and 200 kg/s per well make these reservoirs suitable for geothermal energy production. In Queensland, such developments focus on the Great Artesian Basin, the main aquifers being the Hutton Sandstone and Hooray Sandstone. These aquifers have excellent porosity (up to 25%) and permeability (up to 1000 mD), allowing natural fluid dynamics to drive HSA systems (Radke *et al.*, 2000). HSA is the source of heat for Australia's first geothermal power plant (at Birdsville, southwest Queensland), which has a gross generation capacity of 120 kilowatt (kWe). The plant uses water extracted at 98°C from a 1280 m deep bore penetrating the Great Artesian Basin.

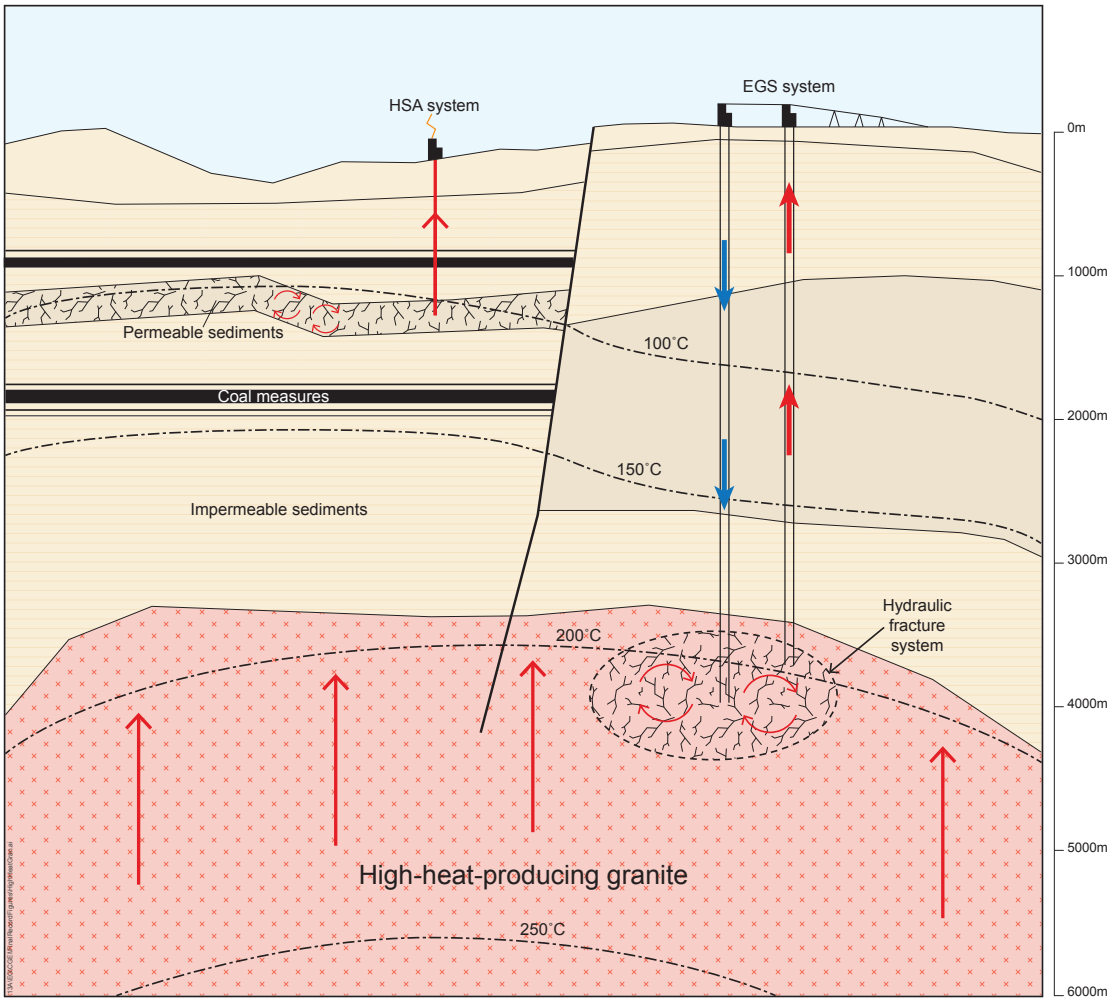

Figure 1-3. Enhanced Geothermal System (EGS) and Hot Sedimentary Aquifer (HSA) geothermal system, modified from Geodynamics Ltd.

2. Methodology

2.1 Drilling program and data collection

2.1.1 Site selection

Thirty-two potential targets (Figure 2-1) were identified based on the current understanding of the geological and tectonic history of eastern and northern Queensland. These targets were considered to have the potential for hot rocks at depth and elevated heat flow conditions, warranting further evaluation by drilling.

Each geothermal target was assessed using the following criteria where available:

i. inferred buried intrusives of felsic composition from geophysical surveys
ii. likely heat production values >5 $\mu W/m^3$ indicated from outcropping intrusives
iii. thickness of insulating cover (>1500 m)
iv. insulating capacity (thermal conductivity values of <3.5 W/mK) of overlying sedimentary cover
v. geothermal gradients >40°C/km in nearby boreholes
vi. presence of hot aquifers
vii. other geothermal indicators (e.g. ternary radiometric datasets highlighting high concentrations of radioactive U, Th and K; fluoride anomalies ≥4.0 mg/L; hydrothermal activity).

Once suitable target areas were identified, the site for each borehole was selected using the following criteria:

i. location away from any major topographic feature and relief
ii. within 100 km of a population centre and/or transmission line
iii. good access to site requiring minimal clearing and track preparation.

Twelve sites were then short-listed for drilling as part of Phase 1 of the program, with 11 sites drilled, one of which was abandoned due to difficult drilling conditions (Figure 2-2).

2.1.2 Drilling

Drilling of the 11 targets (Figure 2-2) commenced in mid-November 2010 with 10 boreholes completed by July 2012. The 11th target, GSQ Townsville 2-4R, was abandoned after multiple failed attempts to intersect consolidated ground before a depth of 150 m. A list of the boreholes drilled is shown in Table 2-1.

Upon reaching consolidated material, continuous coring was undertaken to total depth. Each borehole was cased to total depth with PVC or VAM steel casing and the annulus grouted with cement. After completion, the boreholes were left to thermally stabilise for a minimum of six weeks before precision temperature logs were run. A well completion report including all the collected data has been released for each borehole.

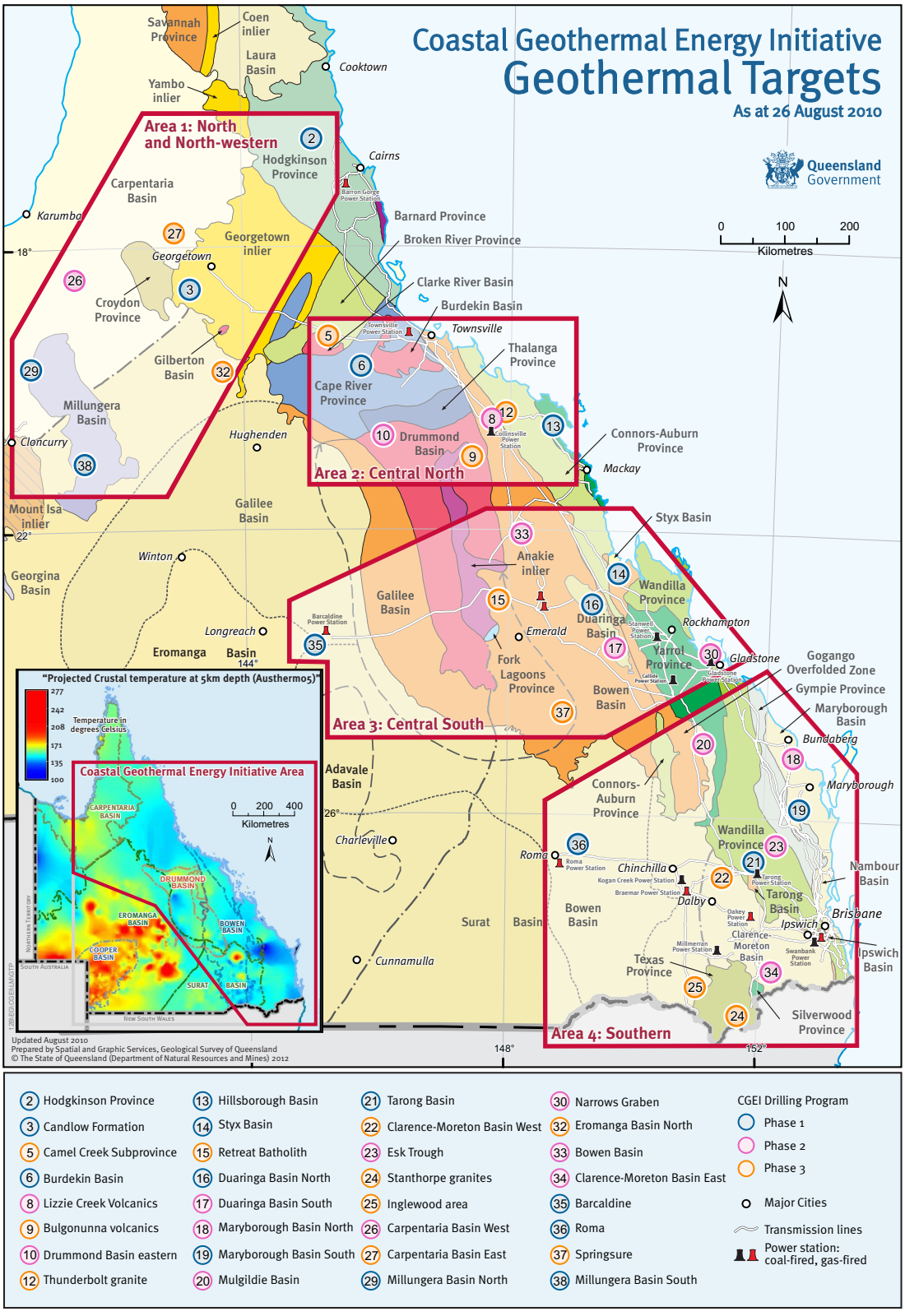

Figure 2-1. CGEI drill targets (32 sites).

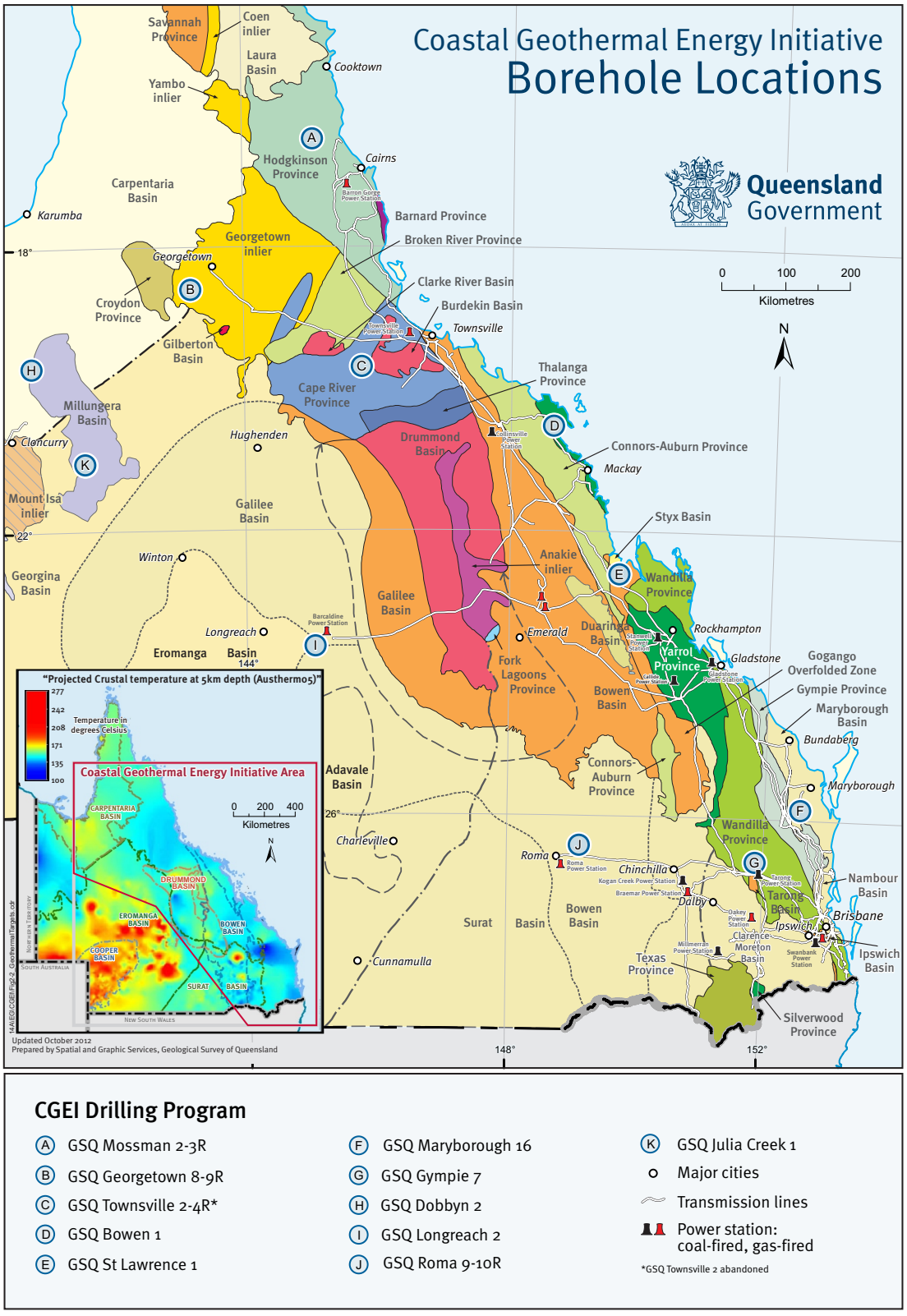

Figure 2-2. CGEI drilling program—Phase 1 (11 sites).

Table 2-1. Boreholes drilled in Phase 1 of the CGEI drilling program.

Tectonic unit	Age	Borehole name	Latitude*	Longitude*	Total depth (mGL)	Completion date	Queensland Geological Record no.
Nambour-Maryborough basins	latest Triassic – Early Cretaceous	GSQ Maryborough 16	-25.84517	152.44472	387.40	30 Nov 2010	2012/01
Tarong Basin	Late Triassic	GSQ Gympie 7	-26.69179	151.86641	338.60	21 Dec 2010 (1st) 22 Jan 2012 (2nd)	2012/12
Eromanga and Galilee basins	Late Triassic – Cretaceous	GSQ Longreach 2	-23.35250	145.23220	330.00	03 Feb 2011 (1st) 15 Jan 2012 (2nd)	2012/10
Surat Basin (Roma Shelf)	latest Triassic – Cretaceous	GSQ Roma 9 GSQ Roma 10R	-26.38600 -26.38598	148.97110 148.97115	335.90 344.16	24 Feb 2011 28 Mar 2012	2012/09
Styx Basin	Early Cretaceous	GSQ St Lawrence 1	-22.64077	149.66777	340.00	17 Mar 2011 (1st) 14 Dec 2011 (2nd)	2012/11
Millungera Basin - South	?Mesoproterozoic	GSQ Julia Creek 1	-20.90445	141.47260	500.02	08 Jun 2011	2012/05
Millungera Basin - North	?Mesoproterozoic	GSQ Dobbyn 2	-19.54532	140.88399	500.04	20 Jul 2011	2012/04
Etheridge Province	Proterozoic	GSQ Georgetown 8 GSQ Georgetown 9R	-18.40504 -18.40500	143.14143 143.14150	320.15 333.40	27 Aug 2011 05 Jul 2012	2012/16
Hodgkinson Province	Ordovician-Carboniferous	GSQ Mossman 2 GSQ Mossman 3R	-16.51796 -16.51797	145.03333 145.03100	67.10 339.70	02 Sep 2011 22 Sep 2011	2012/15
Burdekin Basin	Early Devonian – Carboniferous	GSQ Townsville 2 GSQ Townsville 3R GSQ Townsville 4R	-19.70069 -19.70072 -19.70075	145.85989 145.85989 145.85989	78.50 150.00** 150.00**	18 Oct 2011 18 Oct 2011 18 Oct 2011	2012/18
Hillsborough Basin	Cenozoic	GSQ Bowen 1	-20.28725	148.46589	321.00	10 Nov 2011	2012/08

* Datum: GDA94

** Abandoned due to problematic ground condition

2.1.3 Thermal conductivity analysis

Core samples of the dominant rock types at each site were collected for thermal conductivity analysis. Duplicate samples, approximately 150 mm in length, were taken from the core approximately every 20 m, and labelled 'A' and 'B'. 'A' samples were covered with a wet cloth until they could be wrapped in plastic and duct tape to maintain *in situ* moisture content and preserve their structural integrity. The 'A' samples were dispatched to Hot Dry Rocks Pty Ltd (HDR) for analysis. The 'B' samples were sent to Geoscience Australia (GA) to be analysed under dry/saturated conditions as a quality control measure.

All samples were analysed in accordance with American Society for Testing and Materials Standard E1225 using a divided bar device. Where possible, testing was carried out on three sections of each sample to determine a harmonic mean value.

2.1.4 Precision temperature logging

Precision temperature logs were run after each borehole had returned to a stabilised thermal condition. The temperature logs were run by GA and HDR. The initial logs of GSQ Gympie 7, GSQ Roma 9, GSQ Longreach 2 and GSQ St Lawrence 1 indicated that fluid circulation between coal seams, aquifers, or minor permeable units had destabilised the temperature gradient. Consequently, the boreholes were recompleted by cementing the annulus to isolate any permeable intervals. The temperature logs from the recompleted boreholes reflected a thermally equilibrated condition.

2.2 Heat flow modelling

2.2.1 Principle

The principle aim of geothermal exploration is to locate anomalously high temperatures at an economically and technically viable drilling depth. Investigation of the thermal state in a target area provides a firm basis for identifying regions with anomalously high temperatures. The thermal state of the crust can be expressed at the surface in the form of heat flow (q_s), which is a function of heat actively generated within the crust by the decay of radioactive isotopes (q_c) plus the heat supplied from the mantle (q_m) (Turcotte & Schubert, 1982):

$$q_s = q_c + q_m$$

The average vertical conductive heat flow can be calculated following Fourier's expression (equation 1) from measurements of thermal conductivity and temperature gradient parameters over one or several intervals within a borehole.

$$q = k \cdot dT/dz \qquad (1)$$

Where: q = heat flow, in W/m^2
dT/dz = temperature gradient in K/m
k = rock thermal conductivity in W/mK.

Therefore, heat flow is a calculated value from these two measured parameters. Equation (1) shows that the temperature gradient has an inverse relationship with thermal conductivity, one decreasing as the other increases.

2.2.2 One-dimensional modelling

Steady-state vertical conductive heat flow models for each of the CGEI boreholes were built using 1D heat flow modelling computer code (HF1D) that was developed by the project team based on an inversion modelling technique. Required input data are precision downhole temperature logs recorded at thermally equilibrated conditions, and thermal conductivity data of the core samples. HDR values were chosen as they better represent the thermal conductivity of the rocks under *in situ* conditions.

The thermal conductivity data and an arbitrary magnitude of heat flow were put into the model to compute a theoretical temperature profile to match the recorded temperature log in each borehole. The magnitude of the heat flow was adjusted until the computed temperature profile best matched the recorded temperature log. The results of this modelling are highlighted in Section 3.1.

2.3 Data estimation to depth

2.3.1 Thermal conductivity at depth

For each target drilled, the geological succession to 5 km was inferred from geological and geophysical data to estimate the thicknesses of the stratigraphic units and their representative rock types to that depth (see Sections 4 and 5 for details). Thermal conductivity values were assigned to formations with uniform rock types using either the measured values or those reported in the literature. Where a mixture of rock types were present in a formation, a representative thermal conductivity was calculated from the weighted harmonic mean of the component rock types (Beardsmore & Cull, 2001). These established thermal conductivity profiles were then used to estimate temperatures to 5 km.

2.3.2 Temperature estimations to depth

Estimation of the temperature profile to 5 km is a key factor in assessing the geothermal energy potential of an area. In lieu of deep drilling and direct measurements at depth, heat flow modelling provides a firm basis for reasonably accurate estimation of temperatures to depth. This estimation needs to reflect variations in thermal resistance through the 5 km section where thermal resistance is a measurement of a temperature difference by which an object or material resists the flow of heat. In this context, thermal resistance is defined as the thickness of an interval divided by its thermal conductivity. The incorporation of thermal resistance more accurately represents the thermodynamic principles of heat transfer. Therefore, the estimated temperatures are more reliable than those generated through the traditional method of temperature gradient extrapolation.

In a purely conductive heat regime, downward estimation of steady-state temperature to a depth z can be performed by:

$$T_z = T_0 + q_0 \cdot \int_0^z \frac{d_z}{k_z} \tag{2}$$

Where: k_z = thermal conductivity of the interval
d_z = thickness of the interval
q_0 = heat flow at the top of the interval
T_0 = temperature at the top of the interval
T_z = temperature at the bottom of the interval.

The heat flow at the top of the interval is assumed to be purely conductive and therefore constant with depth z. Although this linear relationship is a simplification of a complex dynamic system, it is a reasonable first order approximation in the absence of direct measurements at depth.

Equation (2) implies that most prospective regions for geothermal exploration are those that have geological units of sufficient thickness and with low thermal conductivity (i.e. high thermal resistance) in the cover sequence combined with high heat flow.

Using equation (2), the temperature was then estimated to greater depths using the 1D heat flow models for each borehole. The results of this estimation are highlighted in Section 3.2.

2.3.3 Depth estimation to isotherms

Heat flow modelling allows the estimation of depth-to-isotherm targets using equation (2). Depths to isotherms of 80, 100, 120, 150 and 200°C were estimated under each CGEI borehole. Temperatures of 80–120°C are favourable for direct use applications of geothermal energy, whereas 150–200°C is a desirable range for electricity generation purposes. The results of this estimation are highlighted in Section 3.3.

A high prospectivity region is defined as an inferred resource area where the 150°C isotherm is present at a depth around 4000 m to allow for a sufficient reservoir thickness. The 150°C isotherm is assumed to be the minimum temperature of the geothermal resource, which could allow commercial deliverability from a production well. This temperature is defined as the cut-off temperature based on which an Organic Rankine Cycle (ORC) binary plant can be operated commercially.

2.4 Stress regime

In order to maximise the efficiency of thermal energy extraction, the permeability of the reservoir rocks needs to be enhanced through a hydro-fracturing stimulation process. A critical factor in the successful development of EGS is the response of the fracturing process to the *in situ* stress field. *In situ* stress

fields also exert significant control on fluid-flow patterns in fractured rocks. Knowledge of both the regional and prospect scale stress regimes is important to understand the effects of stress-dependent fracture permeability. In EGS, knowledge of the stress regime is critical in predicting reservoir growth direction when undertaking hydro-fracturing stimulation (Department of Trade and Investment of NSW, 2010). Stress fields are defined in simplified terms by three mutually perpendicular principal axes of stress; being the maximum, intermediate and minimum stress axes.

Anderson (1951) introduced a scheme that related the three major styles of faulting in the crust to the three major arrangements of the principal axes of stress; the vertical principal stress (SV), and the maximum (SH) and minimum (Sh) horizontal principal stresses, in the following relationships for:

i. normal faulting stress regime where SV>SH>Sh
ii. strike-slip faulting stress regime where SH>SV>Sh
iii. reverse or thrust faulting stress regime where SH>Sh>SV.

In the case of EGS development, the induced fractures may grow in three major directions:

i. vertical to steeply dipping fractures that strike orthogonal to Sh in a normal faulting stress regime (SV>SH>Sh)
ii. vertical to steeply dipping fractures that strike <45° to the direction of SH in a strike-slip faulting stress regime (SH>SV>Sh)
iii. horizontal to shallow dipping fractures that strike approximately parallel to Sh in a thrust faulting stress regime (SH>Sh>SV).

Therefore, a stress regime that facilitates horizontal fracture growth is considered optimal for development of EGS reservoirs. This requirement has been considered when investigating stress regime of the CGEI targets.

2.5 Preliminary resource assessment

2.5.1 Principle

An important factor in the assessment of geothermal energy potential of a target area is the evaluation of the volume of the geothermal system in question. A volumetric approach has been used as the preferred method for preliminary assessment of the inferred geothermal energy resources identified through the CGEI program. This approach is based on the methodology used by the United States Geological Survey to assess the geothermal energy resources of the United States (Muffler, 1979).
In the application of the volumetric method, it is assumed that the volume has a surface area A in the x-y plane and thickness z_1-z_0 along the z-axis, where z_1 and z_0 are respectively the lower and upper limits of the geothermal system. For simplicity, the heat capacity and temperature are assumed to be homogeneous in the x-y plane and are only dependent on depth. The thermal energy content of the system can be calculated by integrating the product of the estimated heat capacity per unit-volume (C_z), and the difference between the estimated temperature curve (T_z) in the system and the reference (base) temperature (T_0).

$$Q = A \int_{z_0}^{z_1} C_z [T_z - T_0] d_z$$

If one assumes that the temperature curve is close to being linear in the z direction, then a constant temperature can be inferred for the resource. The constant temperature of the resource is the average between the minimum temperature of the system, which could allow commercial deliverability from a production well (known as cut-off temperature), and the temperature at the base of the system. The

thermal energy content of the geothermal system containing a single phase fluid, for example water, can be estimated by the equation:

$$Q = [(1 - \Phi) \cdot \rho_r C_r + \Phi \rho_w C_w] \cdot V \cdot (T_R - T_r)$$

where: Q = total thermal energy, Joule (J)
Φ = rock porosity, (%)
ρ_r = rock density, kg/m^3
ρ_w = water density, kg/m^3
C_r = rock specific heat capacity, J/kg°C
C_w = water specific heat capacity, J/kg°C
V = rock (resource) volume, m^3, (=AH) where:
A = rock (resource) surface area, m^2
H = rock (resource) thickness, m
T_R = rock (resource) average temperature, °C
T_r = reference (base) temperature, °C.

Sanyal & Sarmiento (2005) indicated that heat in the rock is known to strongly dominate the above equation, even for high porosity rocks with fluid content. Therefore, the inferred resource rocks are assumed to have negligible porosity and, hence, negligible fluid content. A more simplistic equation can be used for the thermal energy estimates:

$$Q \approx \rho_r C_r V (T_R - T_r) \quad (3)$$

2.5.2 Estimation of stored thermal energy in-place

The constraints on the parameters used in the estimation of stored thermal energy in a geothermal resource are outlined below:

- *Resource cut-off temperature*: as described earlier, the minimum temperature of the geothermal resource that could allow commercial deliverability from a production well. For the purposes of this assessment, a cut-off temperature of 150°C is assumed based on which an ORC binary plant can be operated commercially.
- *Resource mean temperature (T_R)*: the average between the cut-off temperature (150°C) and the temperature at the base of the resource (5 km).
- *Reference (base) temperature (T_r)*: the temperature relative to which the stored thermal energy will be estimated. The choice of the reference temperature is very important, since it has a large effect on the estimation of stored thermal energy. In a geothermal power plant, the reference temperature is typically defined as the average temperature between the reinjection and production wells (Williams, 2007). However, for the purposes of this assessment, the reference temperature is assumed to be the average of the cut-off temperature (150°C) and the rejection temperature (the temperature of the geothermal fluid after the heat extraction process in the power plant). The rejection temperature is set at 70°C, this being the typical temperature for rejected fluid by an ORC binary plant with an air cooling system. For the purposes of this assessment, the reference temperature is assumed to be 110°C.
- *Specific heat capacity (C_r)*: estimated to be between 900 and 1000 J/kg°C for the CGEI inferred resource rock, at the cut-off temperature of 150°C and above, based on data presented by Vosteen & Schellschmidt (2003) for plutonic, metamorphic and sedimentary rocks (Figure 2-3).
- *Density (ρ_r)*: of the CGEI inferred resource rock is taken between 2600 and 2900 kg/m^3, which is a reasonable approximation for many inferred resource rocks within the highlighted areas, based on the current geological knowledge.
- *Surface area of the resource (A)*: ideally, a resource area should be defined as the areal extent of the 150°C isotherm (cut-off temperature). As there are insufficient data to map the areal extent of this isotherm, the surface area of the geothermal energy resource is defined as the lateral extent of the intrusive or the area of optimal sedimentary thickness as determined from geophysical data.

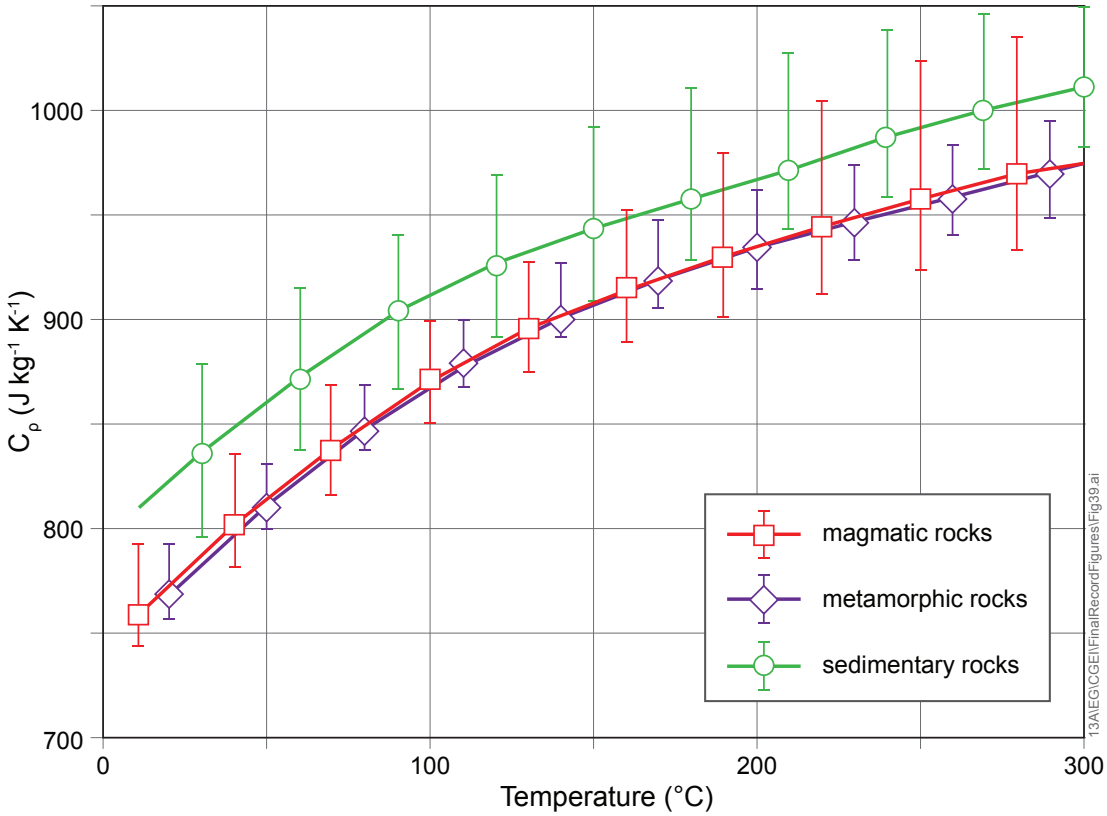

Figure 2-3. Mean values and ranges of variation of specific heat capacity (C_ρ) at constant pressure as a function of temperature for magmatic, metamorphic and sedimentary rocks (Vosteen & Schellschmidt, 2003).

- *Resource thickness (H)*: the resource thickness is estimated by the depth at which the cut-off temperature of 150°C is exceeded to the base of the resource, which is defined as being at 5 km depth.

Using equation (3), the total thermal energy content of an inferred resource area has been estimated and reported in petajoules (PJ). The results of this estimation are highlighted in Section 6.1.

2.5.3 Electric power generation potential

The estimated stored thermal energy of CGEI inferred resources is reported in terms of equivalent electric power generation potential in megawatt (MWe) and annual electricity generation potential in gigawatt-hour (GWh). There are a few parameters that govern the conversion process of thermal energy to electricity. These parameters are discussed and rationalised below.

- *Recovery factor*: only a small fraction of the total stored thermal energy in a geothermal system is recoverable and can be converted to electricity. While conceptually simple, recovery factor is very difficult to predict and is hard to define. Even in convective geothermal reservoirs with long production histories, there is no definitive guideline as to how the recovery factor should be defined or determined (Australian Geothermal Energy Group, 2010). Generally, recovery factors vary between 5 and 50% depending on the geological conditions, mainly porosity, with an average value of 25% for hydrothermal resources (Muffler, 1979) and 40–50% for EGS resources (Sanyal & Butler, 2005). Williams (2007) used a theoretical approach and suggested a range of 5–20% as a recovery factor for both natural fracture dominated and EGS resources. At this stage, there is no sound basis for predicting the net recovery factors for the thermal energy estimates calculated for the CGEI inferred resource areas. Therefore, a conservative value of 5% has been assumed as the recovery factor in the calculations for the areas.

- *Thermal conversion efficiency*: only a small portion of the recoverable thermal energy from the geothermal system can be converted to electricity, and this is determined by the thermal conversion efficiency of the power plant in use. The conversion efficiency of geothermal power plants is mainly dependent upon the temperature of the geothermal fluid. Compared with conventional fossil-fuel or nuclear power plants, which operate with superheated steam over a temperature of about 550°C, geothermal power plants operate over lower temperature ranges, generally between 150 and 250°C. At these relatively low temperatures, thermal conversion efficiencies are inherently lower than conventional power plants. With the low temperatures generally around 150°C and the use of ORC binary power plants, the conversion efficiency of geothermal plants can vary between 7% and 12%. For higher temperatures, the conversion efficiency can reach well over 12% (Figure 2-4). Given the fact that the inferred resource temperature has not been measured directly, the net thermal conversion efficiency cannot be determined at this stage. However, 7% has been assumed as a conservative value for thermal conversion efficiency in the calculations for the areas.

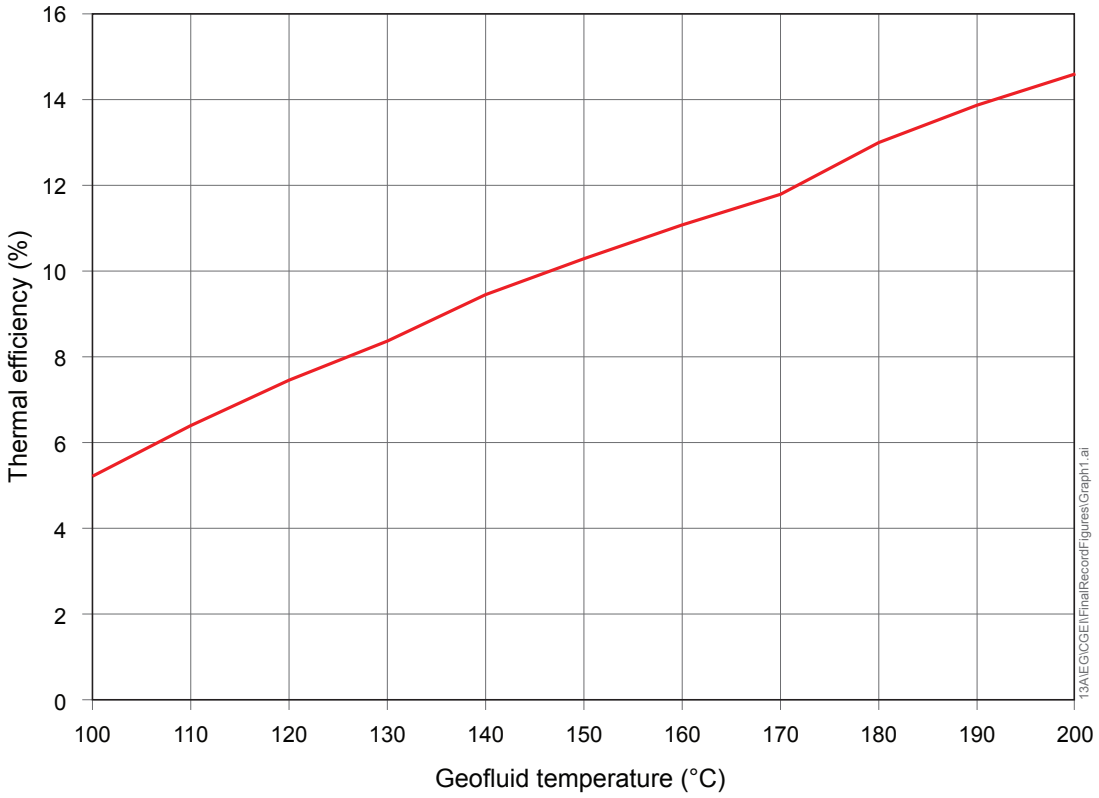

Figure 2-4. Level of typical thermal efficiencies for electricity generation of ORC binary plants (Bertani, 2010).

- *Plant capacity factor*: the portion of time a power plant operates is the plant's capacity factor. Base-load geothermal power plants typically produce electricity about 90% of the time, but can be operated up to 98% of the time in some cases. The Birdsville geothermal power plant with net generation capacity of 80 kWe and a capacity factor of greater than 95% provides all of the town's electricity needs at night and during the cooler winter months (Chopra, 2005). A capacity factor of 90% is normal in a new geothermal electricity plant, whereas the current world average is 74.5% (Tzimas *et al*., 2011), regardless of site-specific constraints and the technology, and size and age of the power plants. It is therefore assumed that 90% would be a reasonable capacity factor when calculating electric power generation potential of the inferred resource areas from the estimated recoverable thermal energy.

- *Plant/project economic lifetime*: the economic lifetime of a geothermal plant/project is the period it takes the whole investment to be recovered within its targeted internal rate of return. This is usually between 25 and 30 years. Therefore, it is a common practice to assess the potential of a geothermal resource over an economic lifetime of 25 years.

In summary, the assumptions used to convert the estimated thermal energy to equivalent electric power generation potential in the inferred resource areas are:

- thermal energy recovery factor: 5%
- plant thermal conversion efficiency: 7%
- plant capacity factor: 90%
- plant/project economic lifetime: 25 years.

2.6 Uncertainty distribution

Because of the limited data and large uncertainty associated with the assumptions made, some degree of caution and conservatism has also been taken into account in the estimates. This approach, which accounts for a risk factor, can be quantified with reasonable approximation using the Monte Carlo simulation. It applies a probabilistic method of evaluating the estimated thermal energy or equivalent power output that captures uncertainty. Given the complexity and heterogeneity of the geological formations of most geothermal systems, this method is preferred over the usual deterministic approach, which assumes a single value for each parameter to represent the whole system. Instead of assigning a 'fixed' value to an input parameter, numbers within the range of the distribution model are randomly selected and drawn for each cycle of calculation. Sampling is usually done through 1000 iterations to obtain a good representation of the distribution. The results are then analysed in terms of the probability of occurrence of the estimated thermal energy or equivalent power output in the range of values over the resulting population.

Whilst the availability of sufficient quantitative data is required to justify the application of the probability approach, for this study a Monte Carlo simulation has been used to provide an indication of likely uncertainties in the estimates. The assigned input parameters have been categorised as "most likely", "minimum", and "maximum" scenarios, by assuming 10% uncertainty for each input parameter, except for the resource mean temperature which inherits its actual uncertainty from the heat flow error. The Monte Carlo simulation result is then presented as a plot of relative and cumulative frequency distribution against the estimated thermal energy or equivalent power output. The results of this simulation are presented in Section 6.2.

There is no doubt that the reliability of the results from a Monte Carlo simulation depends on the type, amount, and quality of the geoscientific data, which are in turn dependent on the stage of development and maturity of the target area. Generally, the reliability increases as the target area is drilled, with direct measurements and more quantitative data becoming available.

3. Modelling results

3.1 Heat flow

A graphical representation of the heat flow model for each CGEI borehole is presented in Appendix 1. A summary of the heat flow modelling results is shown in Table 3-1. The uncertainty in the heat flow is calculated by propagating the relative uncertainty of the average thermal conductivity of the rock units intersected.

3.2 Temperature to depth

Results of the temperature estimation at 5 km below the CGEI boreholes are tabulated in Table 3-2. Estimated temperatures range from 106 to 240°C under the CGEI boreholes. The uncertainty in the estimated temperatures at depth is calculated solely from the propagated uncertainty in the heat flow models. Graphical representations of estimated temperatures to 5 km are included in Appendix 2.

3.3 Depth to isotherms

The depth estimates to isotherms 80, 100, 120, 150 and 200°C for each borehole are also presented in Table 3-2 and Figure 3-1. The estimated formation or rock type that may be intersected at the isotherm depth is also shown in Table 3-2.

Table 3-1. Modelled heat flow values for the CGEI boreholes

Borehole name	Latitude*	Longitude*	Total depth (mGL)	Modelled interval (m)	Harmonic mean conductivity (W/mK)	Mean temp. gradient (°C/km)	Heat flow (mW/m²)
GSQ Maryborough 16[1]	-25.84517	152.44472	387.40	61–380	1.97 ± 0.13	34.37	67.0 ± 2.9
GSQ Gympie 7[2]	-26.69179	151.86641	338.60	54–337	1.18 ± 0.08	31.78	37.5 ± 1.4
GSQ Longreach 2[3]	-23.35250	145.23220	330.00	84–310	1.40 ± 0.06	41.75	60.0 ± 2.5
GSQ Roma 9-10R[4]	-26.38600	148.97110	335.90	106–335	2.11 ± 0.10	39.04	82.5 ± 2.4
GSQ St Lawrence 1[5]	-22.64077	149.66777	340.00	90–338	1.51 ± 0.04	42.66	64.5 ± 1.1
GSQ Julia Creek 1[6]	-20.90445	141.47260	500.02	120–480	2.19 ± 0.08	52.82	113.0 ± 2.9
GSQ Dobbyn 2[7]	-19.54532	140.88399	500.04	91–500	1.68 ± 0.04	66.31	107.5 ± 1.7
GSQ Georgetown 8-9R[8]	-18.40550	143.14143	320.15	43–320	3.48 ± 0.30	15.26	48.5 ± 2.3
GSQ Mossman 2-3R[9]	-16.51797	145.03100	339.70	62–265	3.96 ± 0.08	19.80	77.0 ± 0.9
GSQ Bowen 1[10]	-20.28725	148.46589	321.00	89–321	2.14 ± 0.11	33.06	71.0 ± 2.3

*Datum: GDA94
[1] Sargent *et al.*, 2012a;
[2] Sargent *et al.*, 2012b;
[3] Brown *et al.*, 2012a;
[4] Faulkner *et al.*, 2012b;
[5] Troup *et al.*, 2012;
[6] Faulkner *et al.*, 2012a;
[7] Fitzell *et al.*, 2012;
[8] Maxwell *et al.*, 2012;
[9] Brown *et al.*, 2012b;
[10] O'Connor *et al.*, 2012

Table 3-2. Estimated isotherm depth and temperature at 5 km beneath the CGEI boreholes

Borehole name		Heat flow (mW/m²)	Estimation at 5000 m		Estimation to 80°C isotherm		Estimation to 100°C isotherm		Estimation to 120°C isotherm		Estimation to 150°C isotherm		Estimation to 200°C isotherm	
			Temperature (°C)	Formation / rock type	Depth (m)	Formation / rock type	Depth (m)	Formation / rock type	Depth (m)	Formation / rock type	Depth (m)	Formation / rock type	Depth (m)	Formation / rock type
GSQ Maryborough 16		67.0 ± 5.3	178 ± 14	Gympie Group (undiff) – slate	2 147	Brooweena Formation – siltstone	2 881	Brooweena Formation – siltstone	3 586	Brooweena Formation – siltstone	4 355	Gympie Group (undiff) – slate	5 512	Gympie Group (undiff) – slate
	*Inferred resources area	67.0 ± 4.9	207 ± 15	Brooweena Formation – siltstone	1 598	Maryborough Formation: Gregory Sandstone member – sandstone	2 233	Grahams Creek Formation – andesite	2 681	Grahams Creek Formation – andesite	3 357	Tiaro Coal Measures – siltstone	4 784	Myrtle Creek Sandstone – sandstone
GSQ Gympie 7		37.5 ± 3.1	106 ± 9	Boondooma Igneous Complex – granite	3 094	Boondooma Igneous Complex – granite	4 568	Boondooma Igneous Complex – granite	5 978	Boondooma Igneous Complex – granite	8 063	Boondooma Igneous Complex – granite	10 038	Boondooma Igneous Complex – granite
GSQ Longreach 2		60.0 ± 5.6	140 ± 13	Thomson Orogen – metasandstone	2 334	Thomson Orogen – metasandstone	3 250	Thomson Orogen – metasandstone	4 135	Thomson Orogen – metasandstone	5 407	Thomson Orogen – metasandstone	7 511	Thomson Orogen – metasandstone
GSQ Roma 9-10R		82.5 ± 6.0	187± 14	Timbury Hills Formation – metasiltstone	1 924	Roma granites – granite	2 599	Roma granites – granite	3 218	Timbury Hills Formation – metasiltstone	4 041	Timbury Hills Formation – metasiltstone	5 319	Timbury Hills Formation – metasiltstone
GSQ St Lawrence 1		64.5 ± 6.0	171 ± 16	Glenprairie beds – sandstone	1 483	Boomer Formation – mudstone	2 262	Back Creek Group undiff. – sandstone	3 078	Glenprairie beds – sandstone	4 235	Glenprairie beds – sandstone	6 032	Glenprairie beds – sandstone
GSQ Julia Creek 1		113.0 ± 8.7	238 ± 18	Soldiers Cap Group – metasediments	1 546	Williams Supersuite – granitoid	2 038	Williams Supersuite – granitoid	2 510	Soldiers Cap – metasediments	3 190	Soldiers Cap – metasediments	4 245	Soldiers Cap – metasediments
GSQ Dobbyn 2	Area A	107.5 ± 8.0	232 ± 17	Soldiers Cap Group – metasediments	1 520	Williams Supersuite – granitoid	2 037	Williams Supersuite – granitoid	2 532	Williams Supersuite – granitoid	3 239	Soldiers Cap – metasediments	4 347	Soldiers Cap – metasediments
	*Area B	107.5 ± 6.8	240 ± 15	Soldiers Cap Group – metasediments	1 267	Millungera Basin – sandstone	1 898	Williams Supersuite – granitoid	2 393	Williams Supersuite – granitoid	3 098	Williams Supersuite – granitoid	4 189	Williams Supersuite – granitoid
GSQ Georgetown 8-9R		48.5 ± 2.4	109 ± 5	Bernecker Creek Formation – metasediments	3 257	Interpreted granite	4 452	Bernecker Creek Formation – metasediments	5 701	Bernecker Creek Formation – metasediments	7 574	Bernecker Creek Formation – metasediments	10 694	Bernecker Creek Formation – metasediments
GSQ Mossman 2-3R		77.0 ± 0.3	138 ± 1	Hodgkinson Province – greywacke	2 531	Hodgkinson Province – greywacke	3 419	Hodgkinson Province – greywacke	4 263	Hodgkinson Province – greywacke	5 462	Hodgkinson Province – greywacke	7 363	Hodgkinson Province – greywacke
GSQ Bowen 1		71.0 ± 5.6	204 ± 16	Campwyn Volcanics – basalt	1 553	Campwyn Volcanics – sandstone	2 324	Campwyn Volcanics – sandstone	3 064	Campwyn Volcanics – Basalt	3 880	Campwyn Volcanics – Basalt	4 913	Campwyn Volcanics – Basalt

* projected to north of original borehole location

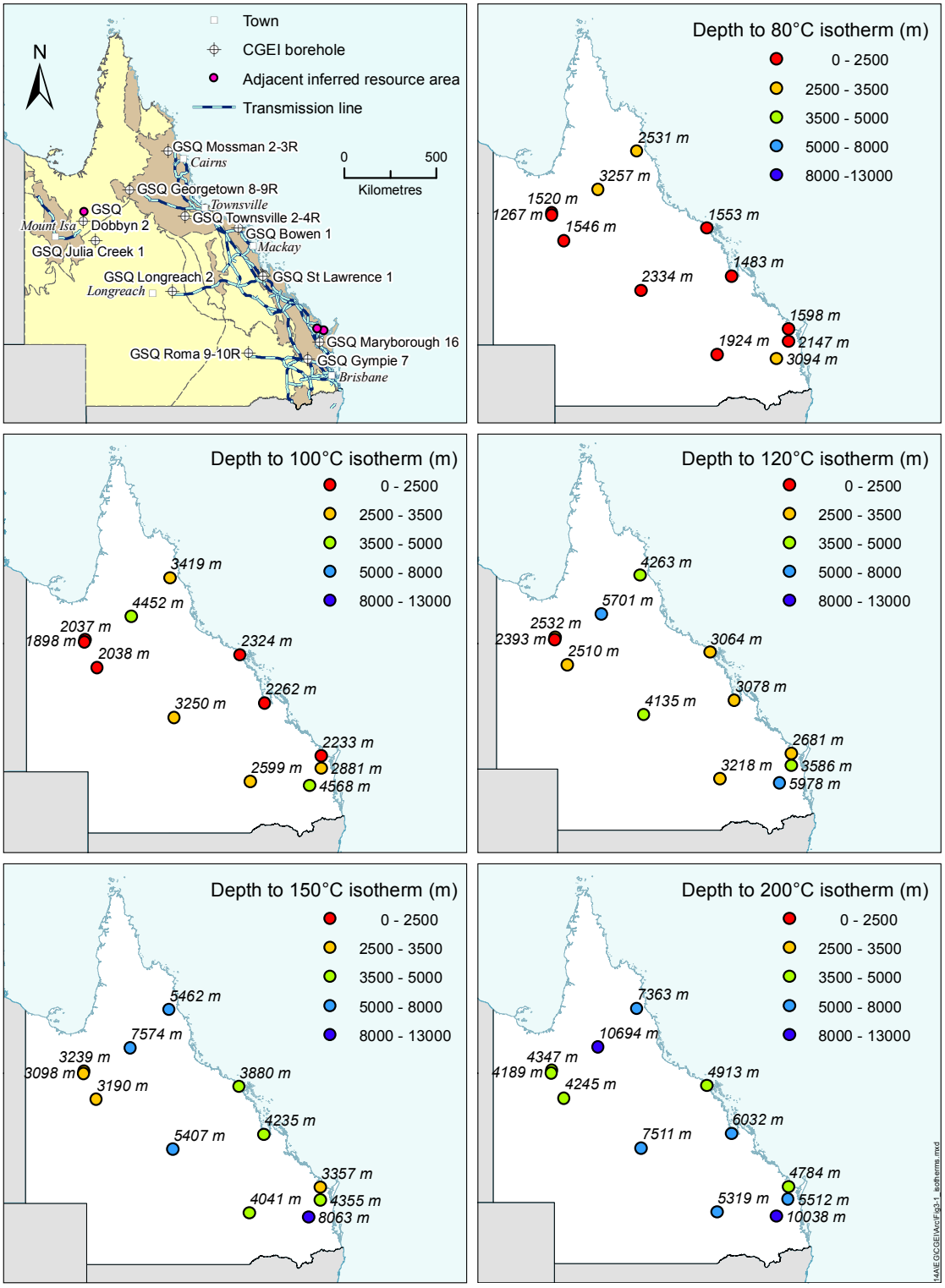

Figure 3-1. A compilation of depth estimates to isotherms 80, 100, 120, 150 and 200°C.

4. High prospectivity regions

4.1 Millungera Basin

Two GSQ boreholes were drilled in the Millungera Basin region targeting the Williams Supersuite. The heat production of the targeted intrusives is high, and the insulation is moderate. High heat flow was modelled for both—GSQ Dobbyn 2 and GSQ Julia Creek 1—107.5 ± 1.7 mW/m^2 and 113.0 ± 2.9 mW/m^2 respectively. Thermal modelling estimates temperatures of 232–240°C at 5 km depth.

4.1.1 Geological framework

The **Soldiers Cap Group** of the Eastern Fold Belt Subprovince of the Mount Isa inlier is postulated to underlie the Millungera Basin (Withnall & Hutton, 2013) (Figure 4-1). The Group comprises metasiltstone with graphite, meta-chert, marble, iron formation, metabasalt, quartzite, and numerous metadolerite dykes and sills (Queensland Department of Mines and Energy *et al.*, 2000). The Soldiers Cap Group has undergone multiple phases of deformation and intrusion; the youngest of these intrusions produced the Mesoproterozoic Williams Supersuite.

The **Williams Supersuite** is dominated by the Williams and Naraku plutons. The plutons were emplaced after the Isan Orogeny deformation event and are both I-type and A-type granites. Geochemical analysis indicates a lower crustal derivation (Wyborn, 1998). The plutons are enriched in U, Th and K, with calculated heat production values of 6.72–7.50 μW/m^3 (Geological Survey of Queensland, 2011). Interpretation of deep crustal seismic sections (Geological Survey of Queensland, 2011) has identified several potential plutons beneath the Millungera Basin that have been attributed to the Williams Supersuite (Korsch *et al.*, 2011). Anomalous fluoride concentrations >4.00 mg/L recorded across the southern Carpentaria Basin, attributed to the interactions of aquifers with fluoride-rich granitic basement (Evans, 1996), also suggest the presence of granites in the region.

The **Millungera Basin** has been inferred from aeromagnetic and gravity data to be about 280 km long and 95 km wide (Korsch *et al.*, 2011; Withnall & Hutton, 2013). The basin lies east of Cloncurry and is overlain by the Eromanga and Carpentaria basins. The age of this basin is unknown, but geochronology and stratigraphy provide some constraints. The underlying Soldiers Cap Group is Palaeoproterozoic, and detrital zircon population dating of the Millungera Basin succession gave a maximum depositional age of 1540 Ma (Korsch *et al.*, 2011). Preliminary Rb-Sr dating of illite from the core in GSQ Dobbyn 2 indicates that the basin infill was affected by intermediate temperature (250–300°C), tectonic and hydrothermal events at 1100 Ma (Tonguç Uysal, University of Queensland, unpublished data). These data indicate that the Millungera Basin succession is likely to be Mesoproterozoic.

The seismic sections show that the basin infill thickens to the east, in three distinct sedimentary sequences, with a maximum preserved thickness of ~3370 m (Korsch *et al.*, 2011).

Sequence 2 of the basin is interpreted to have been intersected by GSQ Julia Creek 1 (Faulkner *et al.*, 2012a) and GSQ Dobbyn 2 (Fitzell *et al.*, 2012) and comprises highly siliceous sandstone to quartzite. Several drill holes to the south have penetrated similar rock types, which may be attributed to the Millungera Basin (Korsch *et al.*, 2011). Thrust faults truncate both the eastern and western margins of the Millungera Basin and an angular unconformity is present at the base of the Eromanga and Carpentaria basins.

The Jurassic to early Late Cretaceous **Carpentaria Basin** occupies an area of 550 000 km^2 of onshore northern Queensland and the Northern Territory, and extends offshore under the Gulf of Carpentaria (Figure 4-1). It is an epeirogenic intracratonic basin (Bradshaw *et al.*, 2009; Doutch, 1973). Unlike the largely contemporaneous Eromanga and Surat basins, which overlie large and thick older sedimentary basins, the Carpentaria Basin mainly overlies an erosional surface of deformed

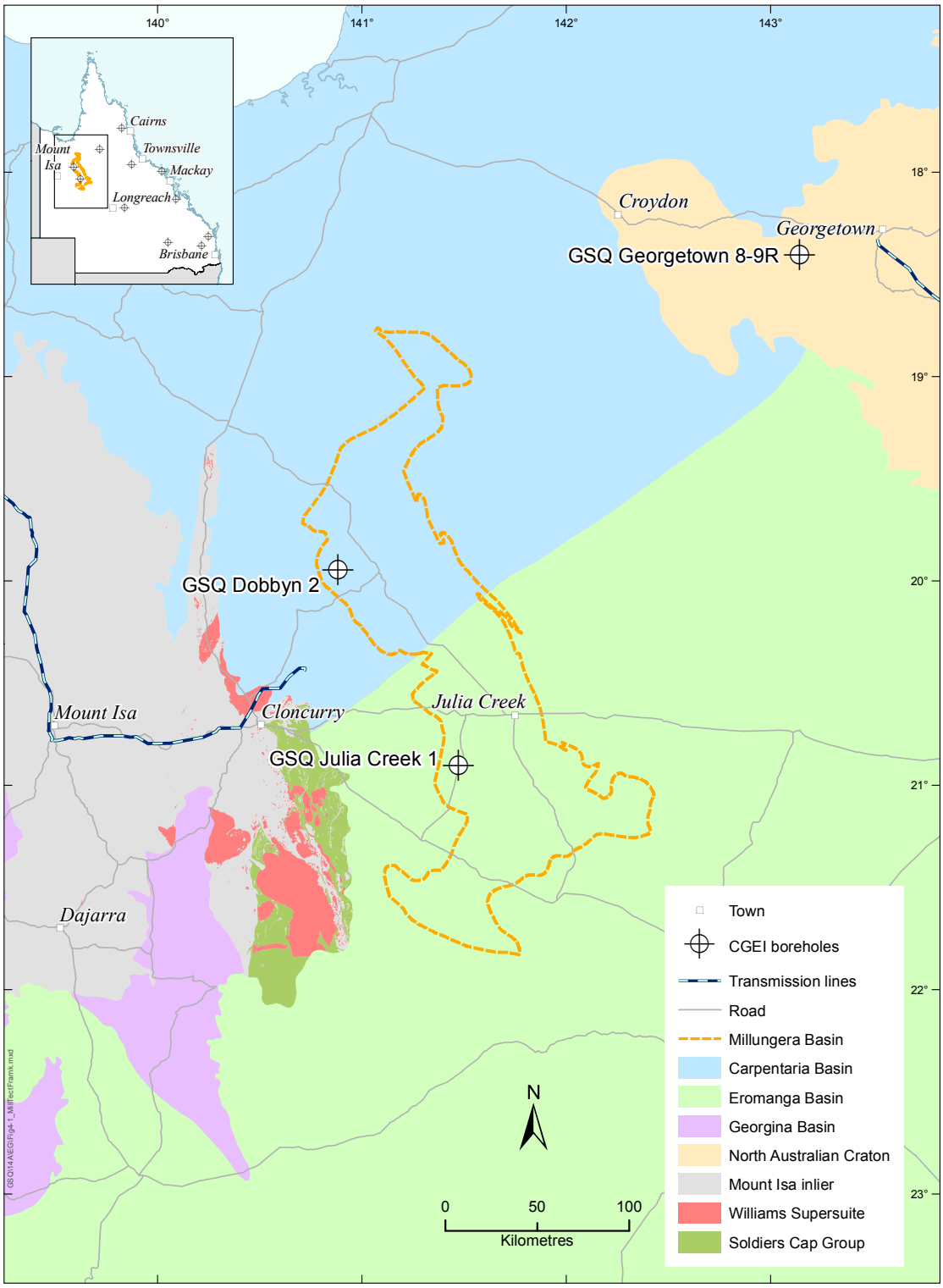

Figure 4-1. Tectonic framework of the Millungera Basin region

Proterozoic rocks (Geoscience Australia, 2008a) and crystalline basement (Cook *et al*., 2013). Onshore, strata of the Carpentaria Basin are laterally extensive and relatively undeformed, with a maximum thickness of 1800 m (Bradshaw *et al*., 2009). The basin underwent only minor tectonism during deposition, as interpreted from seismic data, but variations in basement type do impose a structural control on deposition, where infill of continental sediments was restricted to structurally controlled erosion hollows (McConachie *et al*., 1990). This was followed by the deposition of marine mudstone sequences, then paralic sediments (Doutch, 1973) (Figure 4-2). The basin is overlain by the Paleogene–Neogene Karumba Basin.

The latest Triassic to Early Cretaceous **Eromanga Basin** is a large intracratonic basin that covers 1 000 000 km^2 of central-eastern Australia, of which more than 600 000 km^2 lies in Queensland (Figure 4-1) (Bradshaw *et al*., 2009). The Eromanga Basin connects with the Carpentaria Basin over the Euroka Arch and with the Surat Basin over the Nebine Ridge. It overlies the Cooper Basin in southwest Queensland, the Adavale, Drummond and Galilee basins in southern and central Queensland, and the Millungera and Georgina basins in the northwest. The maximum thickness of the Eromanga Basin is greater than 2500 m, approximately where it overlies the Cooper Basin, and thins to about 300 m over the Euroka Arch. The Eromanga Basin strata are predominantly flat-lying (Vine, 1973).

Locally, sedimentation commenced in the Late Triassic, and by the lower Jurassic an extensive braided fluvial system covered the Eromanga, Carpentaria, and Surat basins. Throughout the Middle and Late Jurassic, a series of fluvial, lacustrine and paludal sequences were deposited. During the Early Cretaceous, the depositional environment turned from paralic to marine, followed by a regression, which brought about paralic, fluvial, and lacustrine deposition in the Late Cretaceous (Cook *et al*., 2013). Figure 4-2 shows the stratigraphy of the Eromanga Basin.

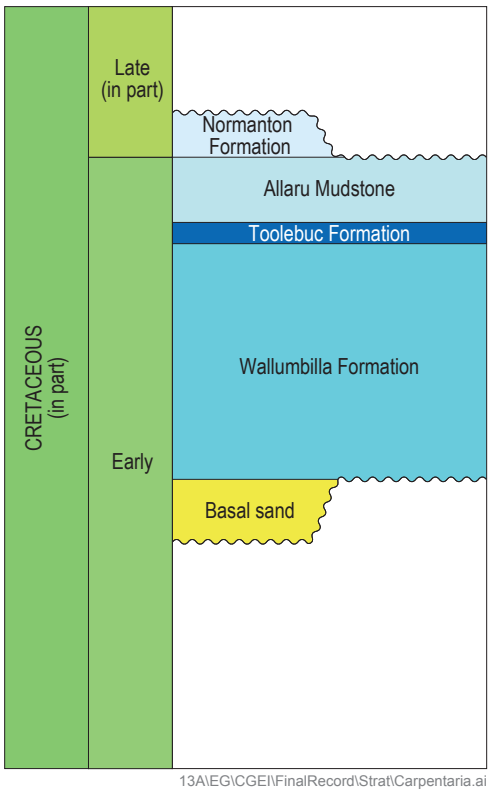

Figure 4-2. Stratigraphy of the Carpentaria and Eromanga basins over the Euroka Arch (adapted from Cook et al., 2013).

4.1.2 Resource investigation

Potential heat source and insulation

Precision downhole temperature logging shows elevated bottom-hole temperatures in the Millungera Basin region, and there are several potential sources of heat.

The targeted heat source for the Millungera Basin is high heat producing intrusives underlying the basin. Granitic bodies have been inferred from geophysical data to underlie the Millungera Basin and are possible Williams Supersuite equivalents (Korsch *et al*., 2011). The plutons of the Williams Supersuite exhibit a high response on ternary radiometric images (Figure 4-3), and geochemical analysis has shown them to be enriched in U, Th and K. The Williams and Naraku plutons have average heat production values of 6.72 and 7.50 µW/m^3 respectively (Geological Survey of Queensland, 2011).

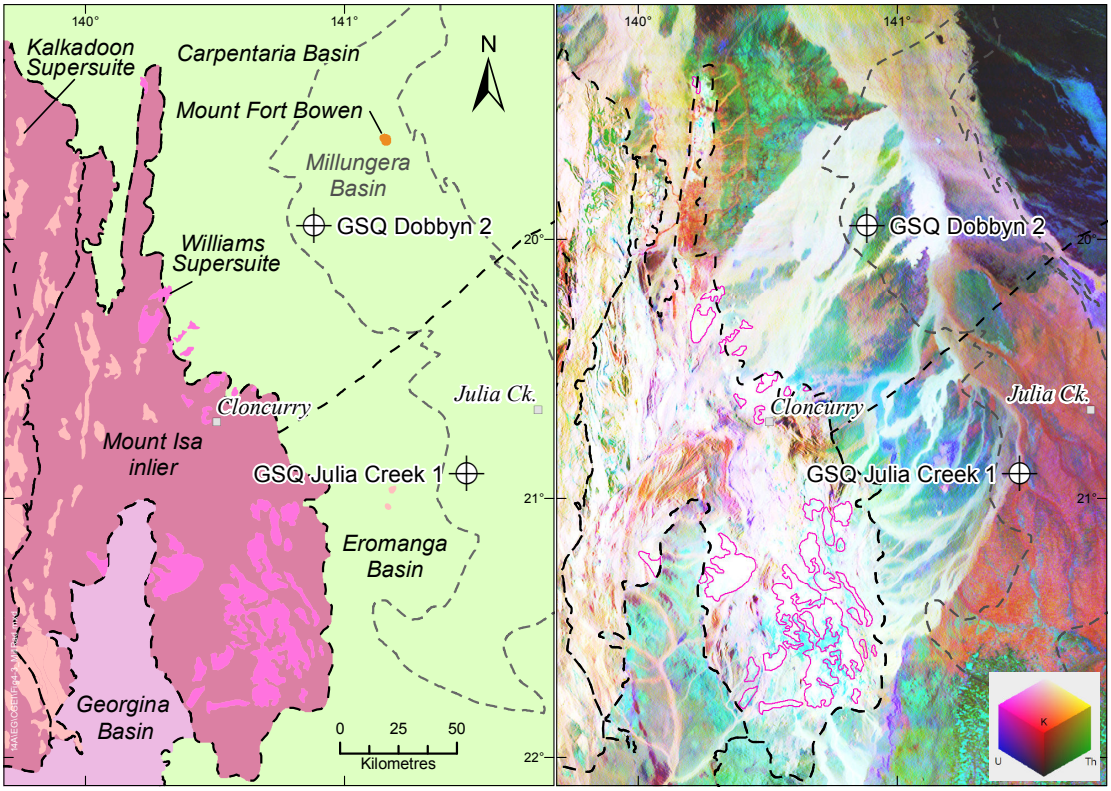

Figure 4-3. Radiometric ternary image of the Millungera Basin region. The Williams Supersuite intrusives show a high response, seen here in white, indicating enrichment in all three radioactive elements.

Other potential heat sources include increased mantle heat flow, with thinned crust under the basin highlighted in the 2006–2007 deep crustal seismic surveys, potentially also increasing the geothermal gradient across the region. Additionally, heat diffracting around the thick Mount Isa inlier may also contribute to the high observed heat flow. Seismic tomography images generated by Saygin *et al*. (2013) also suggested the nature of high heat flow underlying the Millungera Basin may vary, with GSQ Dobbyn 2 and GSQ Julia Creek 1 coinciding with a 'hot spot'.

The insulation capacity of the overlying Eromanga, Carpentaria, and Millungera basins is highly variable. Korsch *et al*. (2011) divided the Millungera Basin into three seismic sequences, based on their seismic character. The highly conductive, homogenous sandstones intersected in GSQ Dobbyn 2 and GSQ Julia Creek 1 have been interpreted to represent the second, non-reflective seismic sequence. Thermal conductivity values obtained from these boreholes indicate this Millungera Basin sequence has a very low insulation capacity. However, the vast difference in the seismic characteristics of sequences 1 and 3 suggest a distinct change in rock type to that of sequence 2. In contrast, the low thermal conductivity of the overlying Eromanga and Carpentaria basins (<2.0 W/mK) highlights good insulation capacity.

Inferred geothermal resource area

Millungera Basin – North

The inferred resource area for the Millungera Basin – North has been defined as the interpreted area of the Williams Supersuite underlying the basin. In the northern Millungera Basin there are two inferred resource areas (Area A and Area B), defined by this subsurface extent of the Williams Supersuite, as inferred from gravity, seismic, and magnetotelluric survey data. Area A (Figure 4-4) and Area B (Figure 4-5) are interpreted intrusive units, each defined by a distinct gravity low and over 565 km^2 and 339 km^2 respectively.

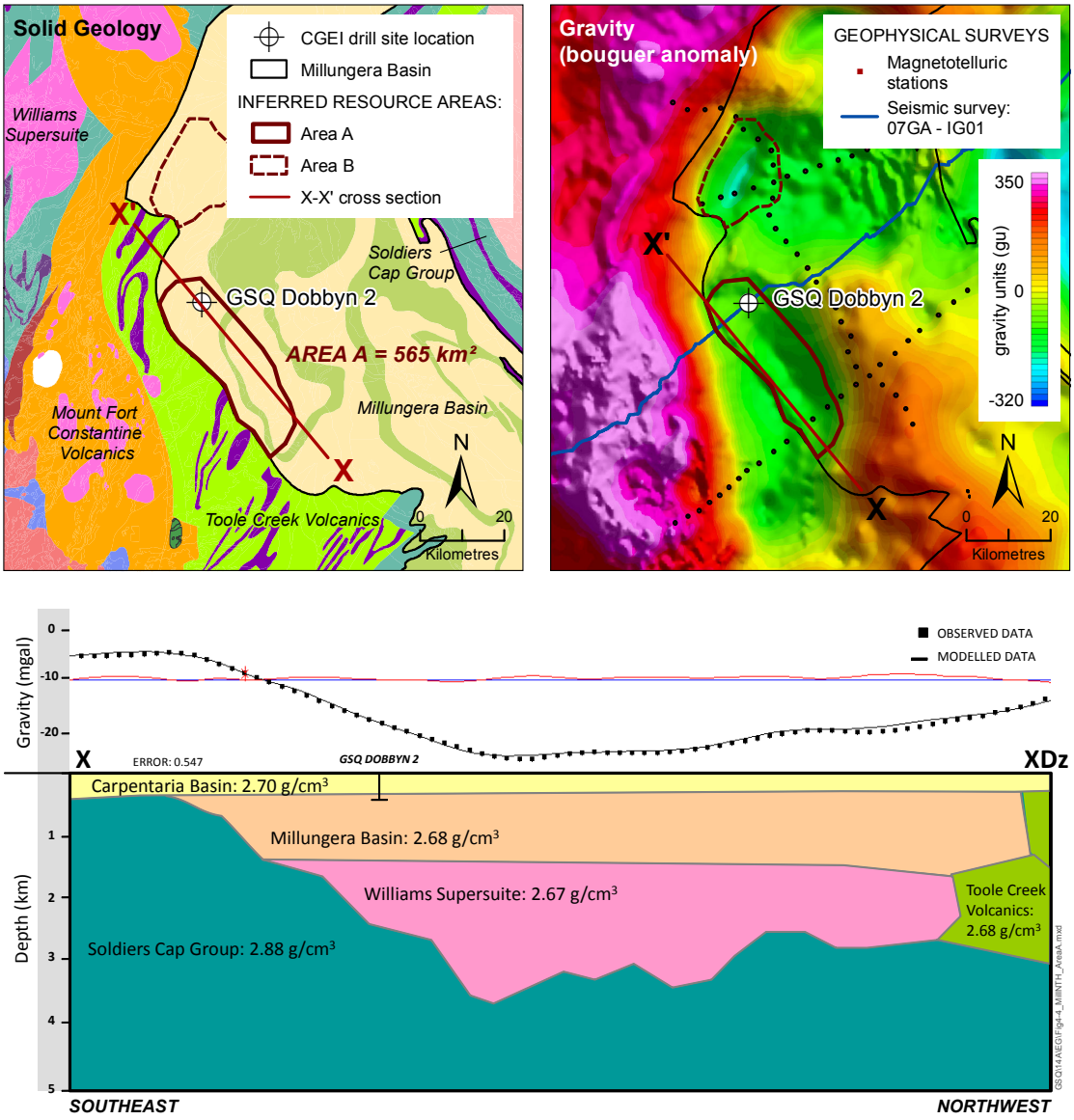

Figure 4-4. Inferred resource area and cross section through Area A, in the Millungera Basin – North.

Area A

Stratigraphic estimations to 5 km were used to estimate depth to the 150°C cut-off temperature, in order to define the thickness of the resource (Table 4-1). In GSQ Dobbyn 2344 m of Carpentaria Basin strata were intersected, with *in situ* measured thermal conductivity values used to assign thermal properties. Based on seismic interpretation, the Millungera Basin is estimated to extend to 1500 m in Area A.

An intrusive unit equivalent to the Williams Supersuite is interpreted to underlie the basin. Using an averaged density value of Williams Supersuite (2.67 g/cm^3), gravity modelling suggests the intrusion is on average 1000 m thick.

The Soldiers Cap Group is then interpreted to be present to 5 km based on seismic and MT interpretation. The Soldiers Cap Group predominantly comprises metasedimentary and metavolcanics, while the Toole Creek Volcanics consist primarily of metavolcanics.

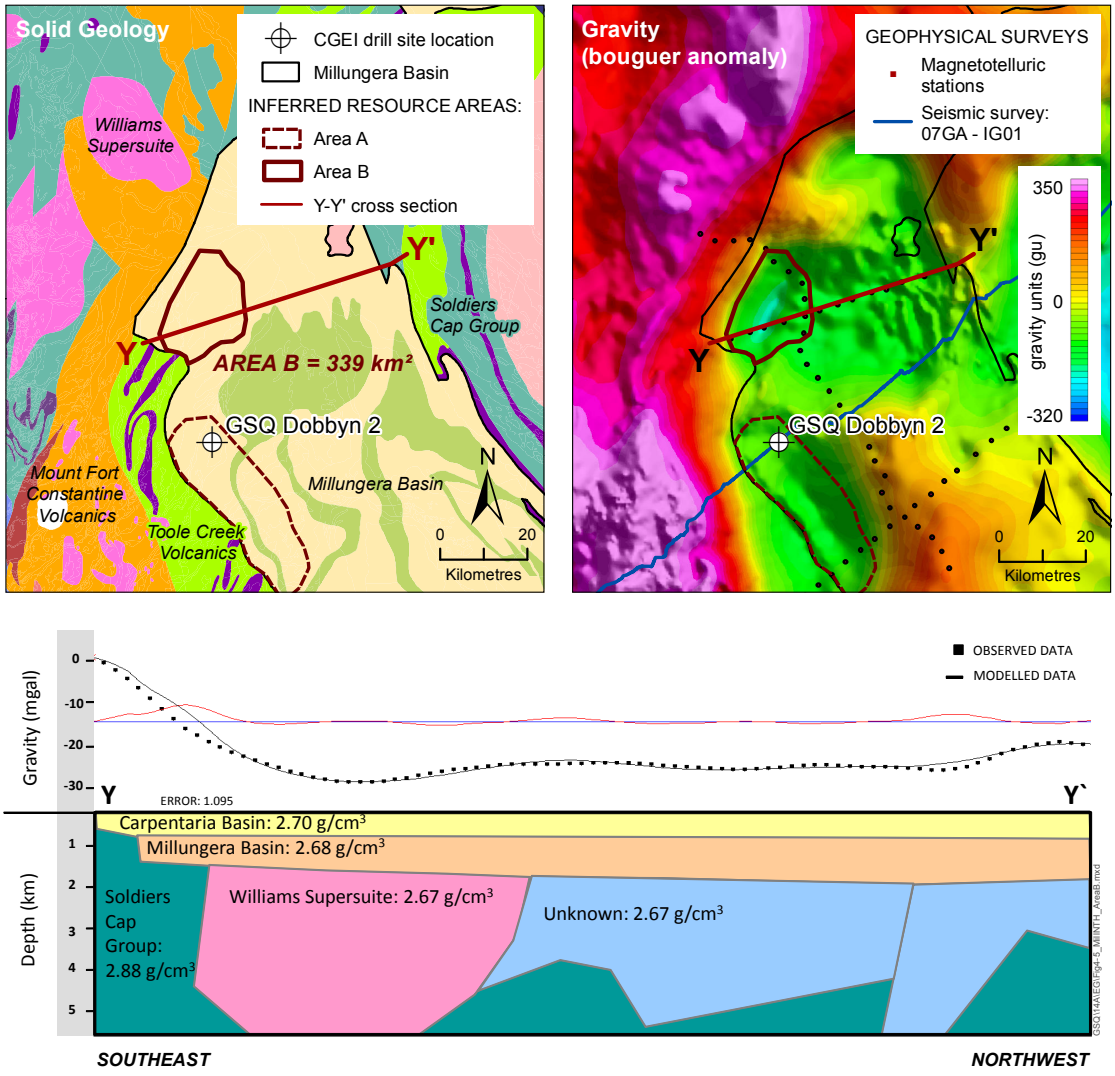

Figure 4-5. Inferred resource area and cross section through Area B, in the Millungera Basin – North.

Table 4-1. Estimated stratigraphy to 5 km depth beneath GSQ Dobbyn 2, Millungera Basin – North, Area A inferred resource area

Borehole name	Depth interval (m)	Tectonic unit	Formation	Rock type	Thermal conductivity (W/mK)
GSQ Dobbyn 2	0–146[1]	Carpentaria Basin	Allaru Mudstone[1]	Mudstone, sandstone[1]	1.14 ± 0.02[1]
	146–226[1]		Allaru Mudstone[1], Toolebuc Formation[1]	Mudstone, calcareous mudstone, sandstone[1]	1.14 ± 0.02[1]
	226–390[1]		Wallumbilla Formation[1]	Mudstone, sandstone[1]	1.13 ± 0.05[1]
	390–1500[2, 3]	Millungera Basin	Millungera Basin (Undiff.)[1,2]	Sandstone[1]	6.64 ± 0.18[1]
	1500–3000[3]	Mount Isa Province	Williams Supersuite[3]	Granitoid[4]	3.20 ± 0.73[5]
	3000–5000[3]		Soldiers Cap Group (Undiff.)	Metasediments[4]	3.26 ± 0.87[5]

[1] GSQ Dobbyn 2 (Fitzell *et al*., 2012)
[2] Korsch *et al*. (2011)
[3] GSQ gravity modelling
[4] Geological Survey of Queensland (2011)
[5] GSQ unpublished database

Area B

Stratigraphic estimations to 5 km are highlighted in Table 4-2. A thickness of 390 m was assigned to the Carpentaria Basin strata, which overlies 1210 m of the Millungera Basin. The quartzose sandstones intersected in GSQ Dobbyn 2 were used to predict the thermal properties of the entire Millungera Basin sequence. Gravity modelling over Area B suggests an underlying intrusive unit, correlative to the Williams Supersuite, extends to at least 5 km.

Table 4-2. Estimated stratigraphy to 5 km depth beneath the Millungera Basin – North, Area B inferred resource area

Borehole name	Depth interval (m)	Tectonic unit	Formation	Rock type	Thermal conductivity (W/mK)
GSQ Dobbyn 2**	0–146[1]	Carpentaria Basin	Allaru Mudstone[1]	Mudstone, sandstone[1]	1.14 ± 0.02[1]
	146–226[1]		Allaru Mudstone[1], Toolebuc Formation[1]	Mudstone, calcareous mudstone, sandstone[1]	1.14 ± 0.02[1]
	226–390[1]		Wallumbilla Formation[1]	Mudstone, sandstone[1]	1.13 ± 0.05[1]
	390–1500[2, 3]	Millungera Basin	Millungera Basin (Undiff.)[1,2]	Sandstone[1]	6.64 ± 0.18[1]
	1500–5000[3]	Mount Isa Province	Williams Supersuite[3]	Granitoid[4]	3.20 ± 0.73[5]

GSQ Dobbyn 2 data used to extrapolate stratigraphy over a gravity low (50 km north of borehole location)
[1] GSQ Dobbyn 2 (Fitzell *et al.*, 2012)
[2] Korsch *et al.*(2011)
[3] GSQ gravity modelling
[4] Geological Survey of Queensland (2011)
[5] GSQ unpublished database

Depth to inferred geothermal resource

The depth to the 150°C cut-off temperature within Area A is 3239 m, giving an inferred resource between 3239 and 5000 m (150–232°C) within the Williams Supersuite and Soldiers Cap Group (Figure 4-4).

In Area B, the depth to the 150°C cut-off temperature is estimated to be 3098 m. The inferred resource is therefore within the interpreted Williams Supersuite, between 3098 and 5000 m (150–240°C) (Figure 4-5).

Millungera Basin – South

The area (848 km^2) of the inferred geothermal resource for Millungera Basin – South is defined by the interpreted intrusive body directly underlying GSQ Julia Creek 1 (Figure 4-6, Figure 4-7). The intrusive is attributed to the Williams Supersuite and has a low to moderate magnetic response (Figure 4-6; Geological Survey of Queensland, 2011).

Stratigraphic estimations to 5 km depth are highlighted in Table 4-3. GSQ Julia Creek 1 intersected 310 m of Eromanga Basin strata with the measured thermal conductivity values highlighted in Table 4-3. The underlying Millungera Basin is interpreted to be 2500 m thick, based on seismic and magnetotelluric surveys. The haematitic, siliceous quartzite and sandstone intersected in GSQ Julia Creek 1 were used to assign the thermal properties to the entire sequence. Gravity modelling of the underlying intrusive unit suggests an average thickness of 1 km, with the Soldiers Cap Group forming basement to 5 km depth.

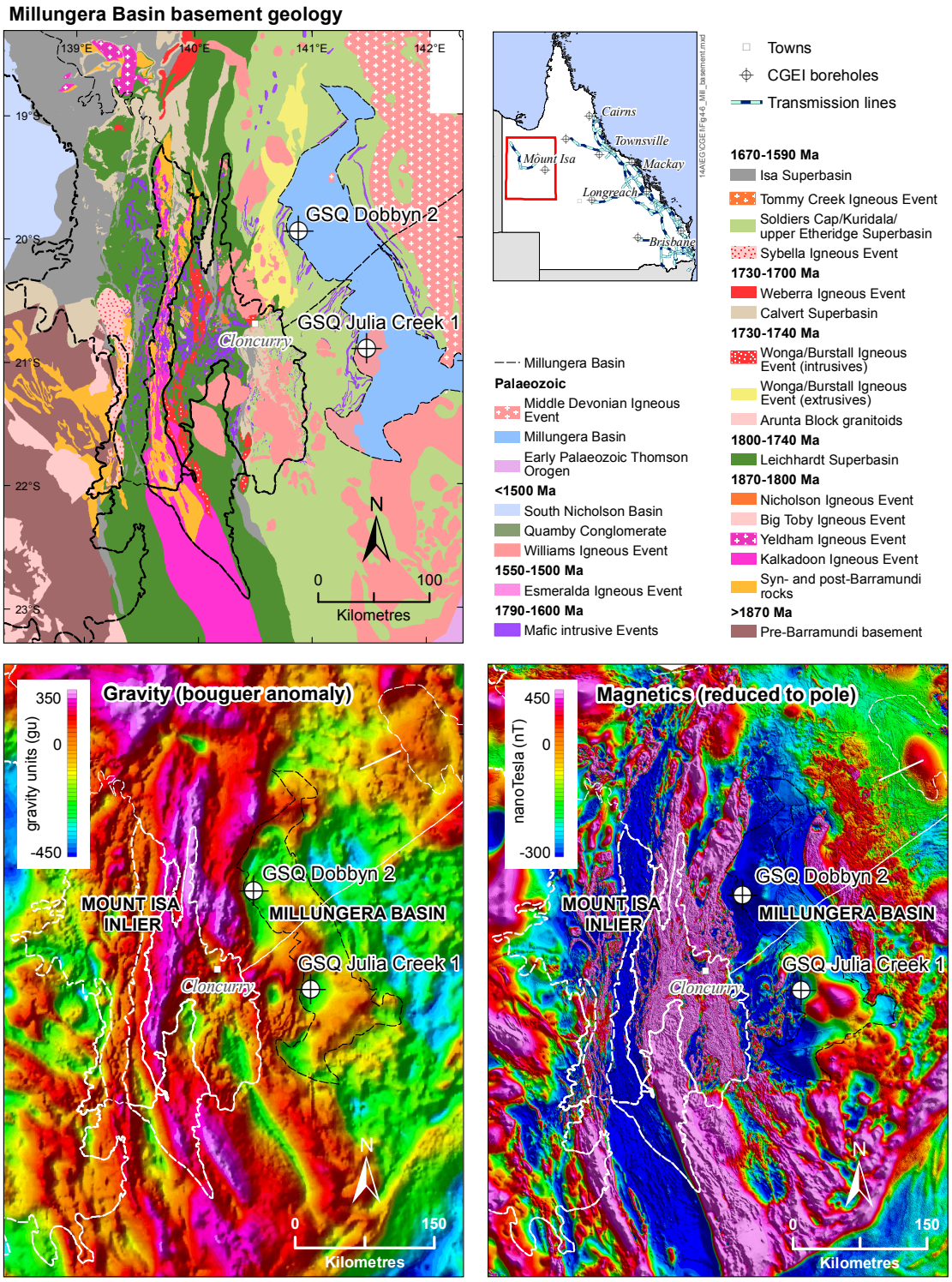

Figure 4-6. Basement geology and geophysics of the Millungera Basin region.

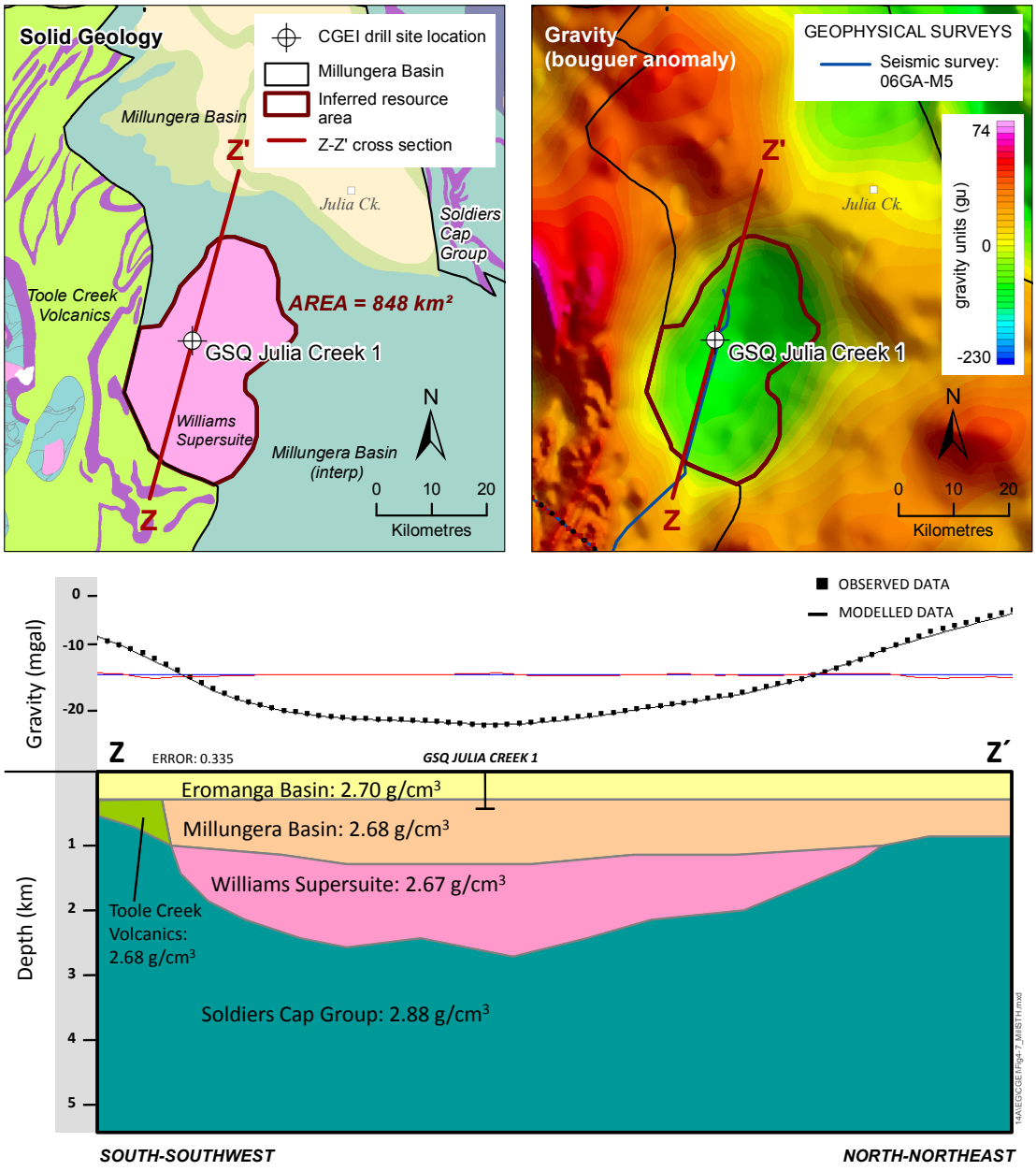

Figure 4-7. Inferred resource area and cross section through the Millungera Basin – South.

Depth to inferred geothermal resource

For Millungera Basin – South, the temperature estimation suggests the 150°C cut-off temperature will be intersected at 3190 m. The inferred resource is therefore between 3190–5000 m (150–238°C) within the Soldiers Cap Group (Figure 4-7).

Stress regime

Structural trends observed in outcrop of the Soldiers Cap Group were used in conjunction with the structural evolution of the Mount Isa Eastern Succession to infer existing fractures which may influence reservoir stimulation. The structural architecture of the Mount Isa Province is complex with dominant faulting reflecting north–south, east–west and northeast–southwest trending compressional and extensional events (Geological Survey of Queensland, 2011). In particular, the steeply dipping north–south trending structures are dominant across the whole Mount Isa Province (Geological

Survey of Queensland, 2011). Additionally, a wrenching phase in the later stages of the Isan Orogeny culminated in the reactivation of east–west trending faults, which cross-cut the Mesoproterozoic Williams Supersuite (Withnall & Hutton, 2013). The orogenic phases of Mount Isa's structural history would have generated a suitable stress vector (SH>Sh>SV) within the Soldiers Cap Group to facilitate stimulation of shallow to horizontal fractures.

Table 4-3. Estimated stratigraphy to 5 km depth beneath Julia Creek 1, Millungera Basin – South, inferred resource area.

Borehole name	Depth interval (m)	Tectonic unit	Formation	Rock type	Thermal conductivity (W/mK)
GSQ Julia Creek 1	120–235[1]	Eromanga Basin	Allaru Mudstone, Toolebuc Formation	Mudstone, sandstone[1]	1.37 ± 0.06[1]
	235–310[1]		Wallumbilla Formation, Hooray Sandstone	Mudstone, sandstone[1]	1.53 ± 0.05[1]
	310–1500[2, 3]	Millungera Basin	Millungera Basin (Undiff.)	Quarztite, sandstone[1]	5.43 ± 0.16[1]
	1500–2500[3]	Mount Isa Province	Williams Super Suite	Granitoid[4]	3.20 ± 0.73[5]
	2500–5000[3]		Soldiers Cap Group (Undiff.)	Metasediments[4]	3.26 ± 0.87[5]

[1] GSQ Julia Creek 1 (Faulkner *et al.*, 2012a)
[2] Korsch *et al.* (2011)
[3] GSQ gravity modelling
[4] Geological Survey of Queensland (2011)
[5] Beardsmore & Cull (2001)

The Eromanga and Carpentaria basins are devoid of major faulting in the region where they overlie the Millungera Basin. This reflects a stabilisation in SH, Sh and SV stress vectors during the Jurassic–Cretaceous.

Currently, the stress regime across northern Australia reflects a substantial horizontal compression (SH) propagating from oblique collision at the northern plate margin (Dehnam *et al.*, 1979). In the Millungera Basin region, the orientation of SH is northeast-southwest (Figure 4-8). Under this stress field, propagation of shallow to horizontal reservoir growth under hydro-fracturing stimulation could be facilitated across the Millungera Basin. However, the complex and steeply dipping crustal architecture within the Soldiers Cap Group, representing multiple phases of extension and compression, is likely to influence the direction of hydro-fracturing at a prospect scale.

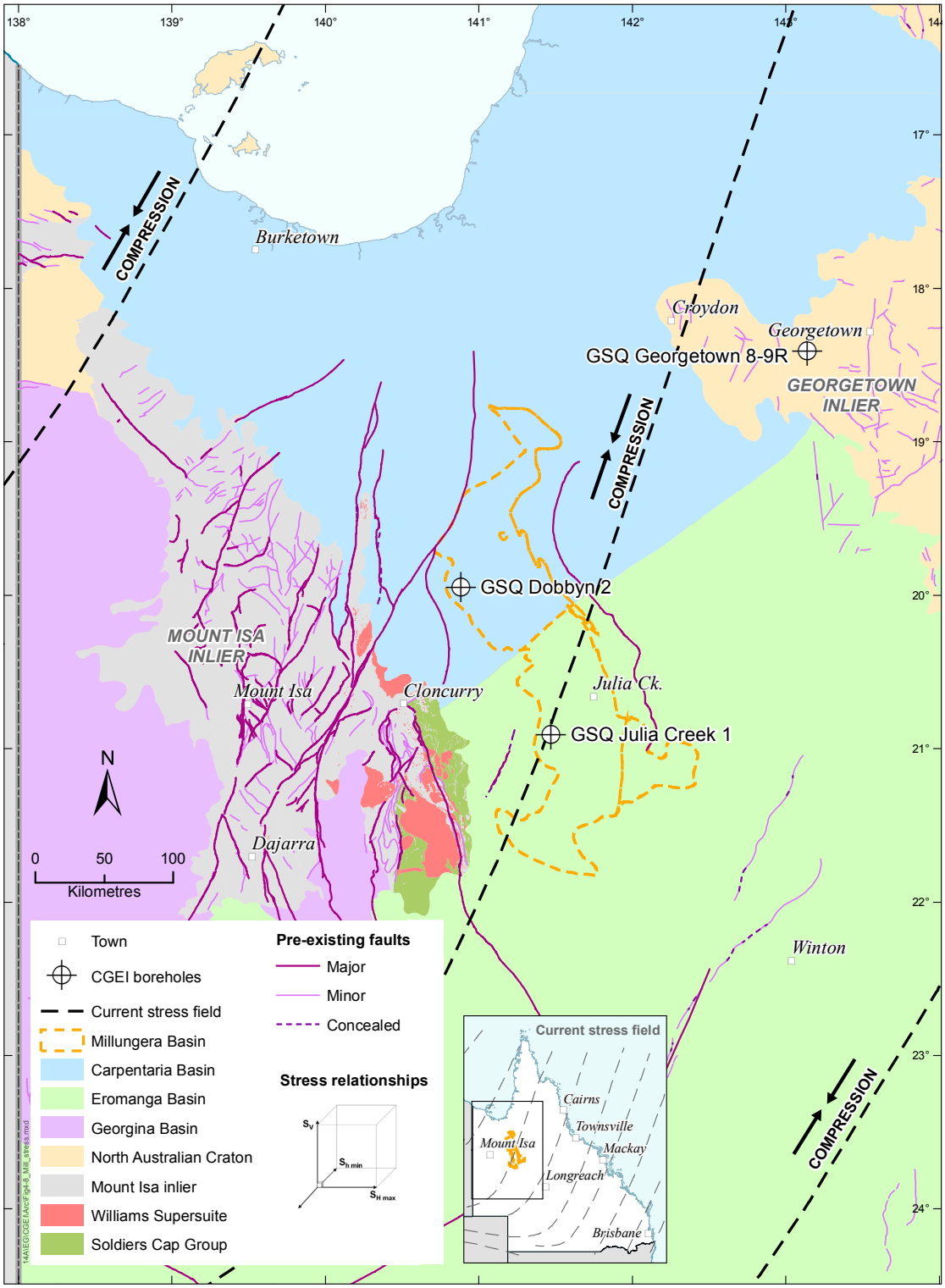

Figure 4-8. Stress regime around the Carpentaria, Eromanga and Millungera basins (adapted from Clark & Leonard, 2003).

4.1.3 Summary

Millungera Basin – North

Heat flow	Insulation	Temp @5km	Stress regime	Prospectivity for EGS

Good
Average
Poor

Millungera Basin – South

Heat flow	Insulation	Temp @5km	Stress regime	Prospectivity for EGS

Good
Average
Poor

4.2 Surat Basin (Roma Shelf)

GSQ Roma 9 was drilled on the Roma Shelf targeting the Roma granites. The Roma Shelf presents a highly prospective region due to the presence of well-defined granites at depth, and sufficient insulation within the Surat Basin. Using the modelled heat flow for GSQ Roma 9-10R (82.5 ± 2.4 mW/m^2), a temperature of 187°C is estimated at 5 km depth, indicating significant potential for a 2621 km^2 inferred resource area

4.2.1 Geological framework

The Roma Shelf is a stable basement platform located to the south of the Denison Trough and west of the Taroom Trough, and is bounded by the Hutton-Wallumbilla Fault and the Merivale and Arbroath faults (Figure 4-9; Exon, 1976). Basement in the Roma Shelf region comprises the **Timbury Hills Formation**, intruded in places by the Roma granites (Figure 4-10; Murray, 1994; Fergusson & Henderson, 2013). The formation consists of steeply dipping metasediments of probable Devonian age. These rocks have undergone folding to produce upright, tight to isoclinal folds. Metamorphism reached at least lower greenschist facies, indicating that it was likely regional, synchronous with folding, and prior to the intrusions of the Roma granites (Murray, 1994). The turbiditic quartzose sandstone and mudstone of the Timbury Hills Formation were deposited in a deep-marine environment (Fergusson & Henderson, 2013) after the sea transgressed over the Thomson Orogen in the Devonian (Murray & Kirkegaard, 1978). From the Brisbane–Eromanga seismic survey, Finlayson (1990) interpreted that the Timbury Hills Formation extends to great depth within the Roma Shelf region.

The **Roma granites** intrude the Timbury Hills Formation, and have been divided into two distinct groups: the more widespread of the two is a likely S-type granite, dated ~355–360 Ma and comprising muscovite-biotite granite, with minor muscovite granite (Murray, 1994). To the east of these S-type granites, two samples have been identified in a probable discreet pluton classified as I-Type (Murray, 1994). Their mineralogy places them on the boundary of the granite and granitoid fields of the Streckeisen (1973) classification. This granite has not yet been dated, so their age relative to the S-type suite is unknown; however, this granite is likely to have been intruded synchronously with the rest of the Roma granites. Murray (1994) suggested that the granites were produced by the melting of a thickened crust following compressional folding and low-grade metamorphism of the Timbury Hills Formation.

The early Permian – late Middle Triassic **Bowen Basin** covers 160 000 km^2 in eastern Queensland (Figure 4-9). Sedimentary thickness varies, and is up to 10 000 m thick in the Taroom and Denison troughs (Day *et al.*, 1983). The basin formed in a backarc setting, during a period of extension in the early Permian, followed by subsidence related to thermal relaxation. This thermal relaxation was followed in the latest early Permian by a major contractional event leading to the development of a foreland basin (Donchak *et al.*, 2013). These tectonic events influenced deposition in the basin, with fluvial and lacustrine sediments and volcaniclastics deposited in a series of half-grabens to the west, and a thick succession of coals and non-marine clastics in the east. During the thermal relaxation, a series of transgressive and regressive events lead to the deposition of marine and deltaic successions. Following the onset of the foreland basin phase, deltaic, fluvial, and shallow-marine environments dominated deposition (Donchak *et al.*, 2013).

In the Roma region, the basin onlaps the southeast dipping Roma Shelf. The Permian–Triassic stratigraphy of the Bowen Basin in the Roma Shelf region of the Bowen Basin is given in Figure 4-11.

The latest Triassic–Cretaceous intracratonic **Surat Basin** covers 300 000 km^2 of central-southern Queensland and central-northern New South Wales (Figure 4-9). The basin is laterally continuous with the Eromanga Basin over the Nebine Ridge to the west and the Clarence–Moreton Basin over the Kumbarilla Ridge in the east. The sedimentary succession of the Surat Basin dips gently into the Mimosa Syncline, with a maximum thickness of 2700 m (Goscombe & Coxhead, 1995). Deposition commenced in the latest Triassic with the onset of a period of passive thermal subsidence of parts of

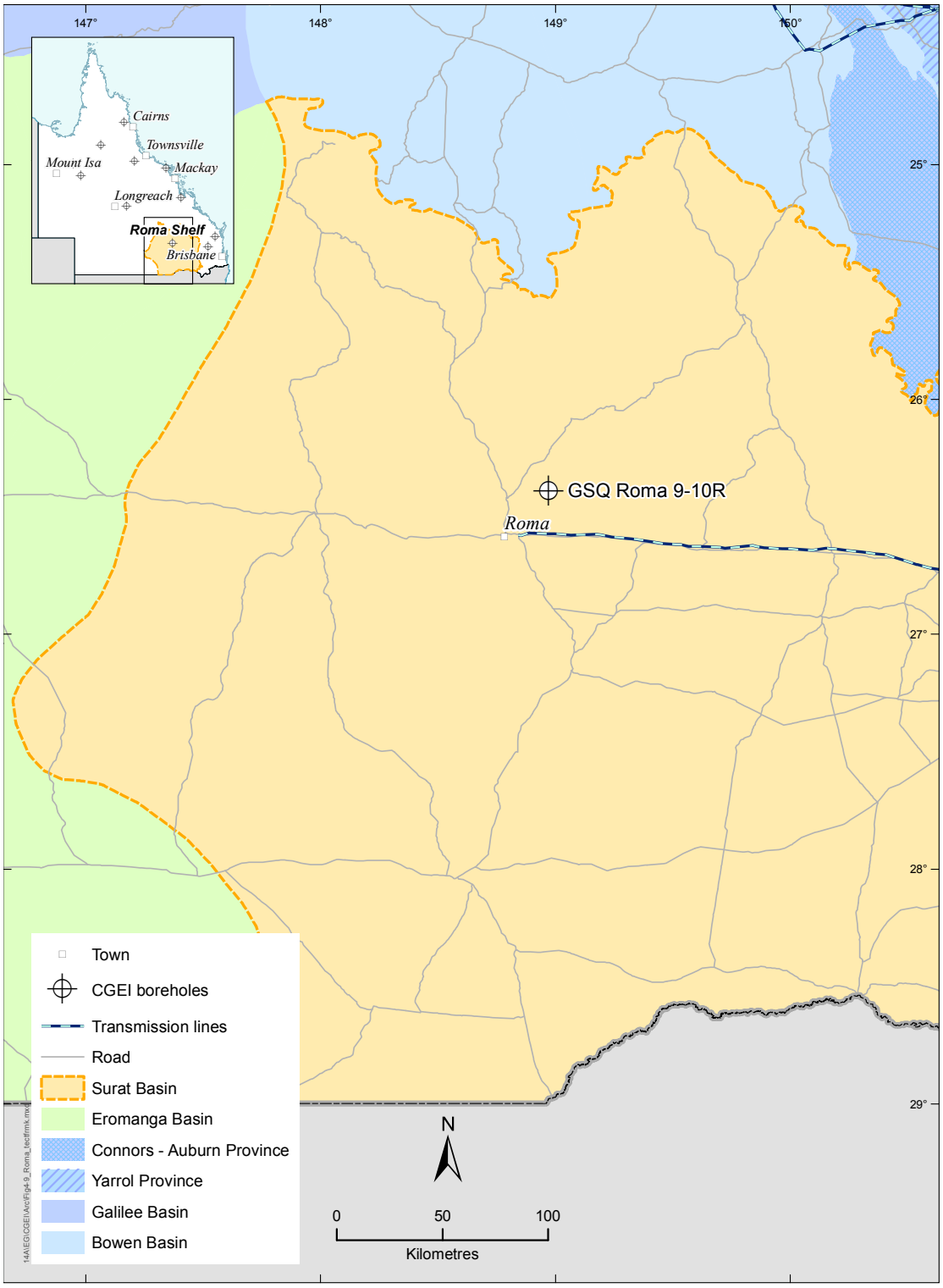

Figure 4-9. Tectonic framework of the Bowen and Surat basins (Queensland).

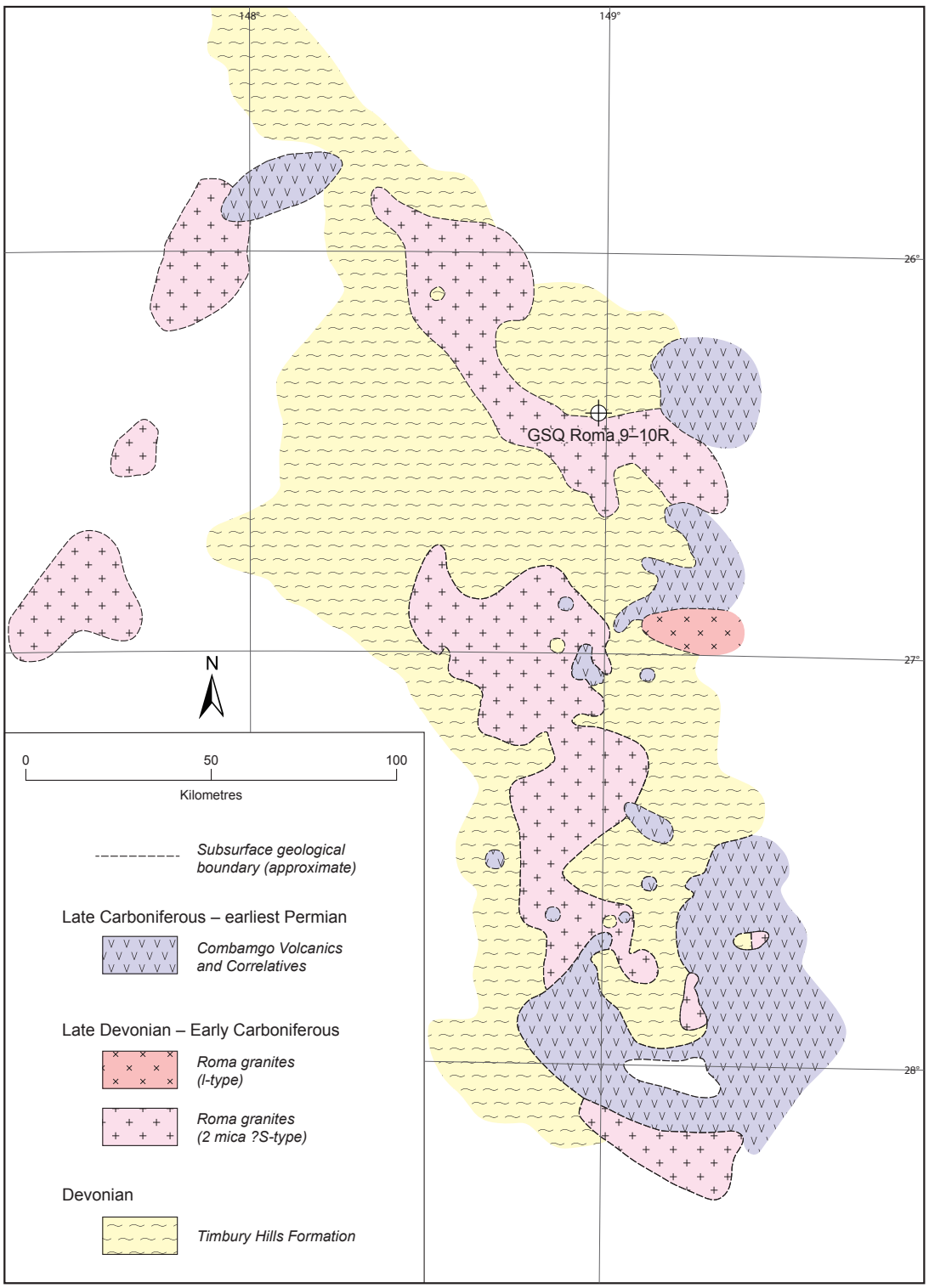

Figure 4-10. Basement geology of the Roma Shelf region (adapted from Murray, 1994).

eastern Australia, but did not become continuous and widespread until the early Jurassic when the Precipice Sandstone was deposited. Environments ranged from fluvial to lacustrine to paludal during the Early Jurassic to earliest Cretaceous. A marine transgression during the Early Cretaceous deposited paralic and marine sediments, followed by a regression producing fluvial, lacustrine, and paludal environments (Geoscience Australia, 2008c; Cook *et al*., 2013). Figure 4-12 shows the stratigraphy of the Surat Basin.

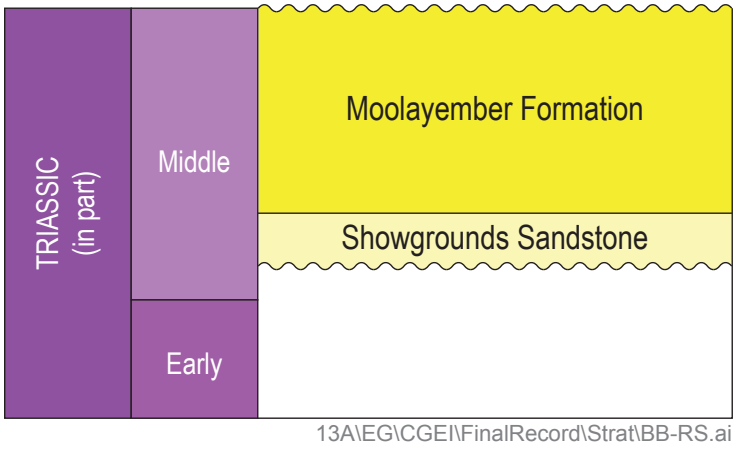

Figure 4-11. Bowen Basin stratigraphy in the Roma Shelf region (adapted from Donchak et al., 2013).

4.2.2 Resource investigation

Potential heat source and insulation

The Roma granites have been identified as a potential geothermal heat source. Recent analysis of granite samples indicated a moderate heat production capability (Siégel *et al*., 2013). Elevated geothermal gradients are indicated across the region from bottom hole temperatures in petroleum wells.

The Surat Basin sequence in GSQ Roma 9-10R has low thermal conductivity (Faulkner *et al*., 2012b). Whilst there are no thermal conductivity data from the rocks below GSQ Roma 9-10R, the coals, mudstones, siltstones, and sandstones of the Surat Basin are likely to provide good insulation. In particular, the Walloon Coal Measures are a highly effective insulator.

Inferred geothermal resource area

The inferred resource area is based on the subsurface extent of the Roma granites, with an area of 2621 km^2, as mapped by Murray (1994) (Figures 4-10, 4-13). GSQ Roma 9-10R was drilled on the northern margin of this inferred resource area.

The stratigraphic estimations to 5 km depth were then used to estimate depth to the 150°C cut-off temperature. Within the inferred resource area, 1058 m of Surat and Bowen basin strata are predicted, based on AAO Pleasant Hills 1 (Wecker, 1972) (Table 4-4). These sedimentary sequences comprise predominantly sandstones, siltstones and mudstones, with coal seams present within the Middle Jurassic Walloon Coal Measures.

The muscovite-biotite S-type Roma granites are predicted to be intersected from 1058 m. Two-dimensional gravity modelling, using a representative density value of 2.58 g/cm^3 for the Roma granites and 2.68 g/cm^3 for the Timbury Hills Formation, highlighted in Figure 4-14, suggests the thickness of the Roma granites ranges from 3 km in the north to 2 km towards the south. However, in order to simplify the geometry of the inferred resource area, an average thickness of ~2 km was used (Table 4-4, Figure 4-14).

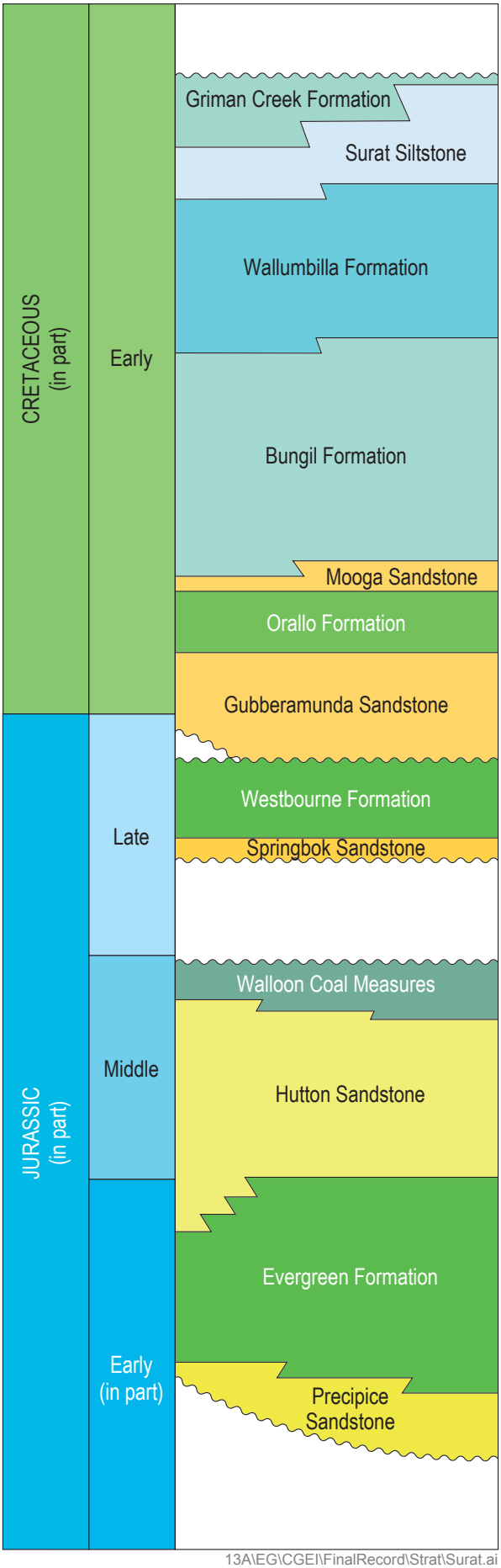

Figure 4-12. Stratigraphy of the Surat Basin in the Roma Shelf region (Cook et al., 2013).

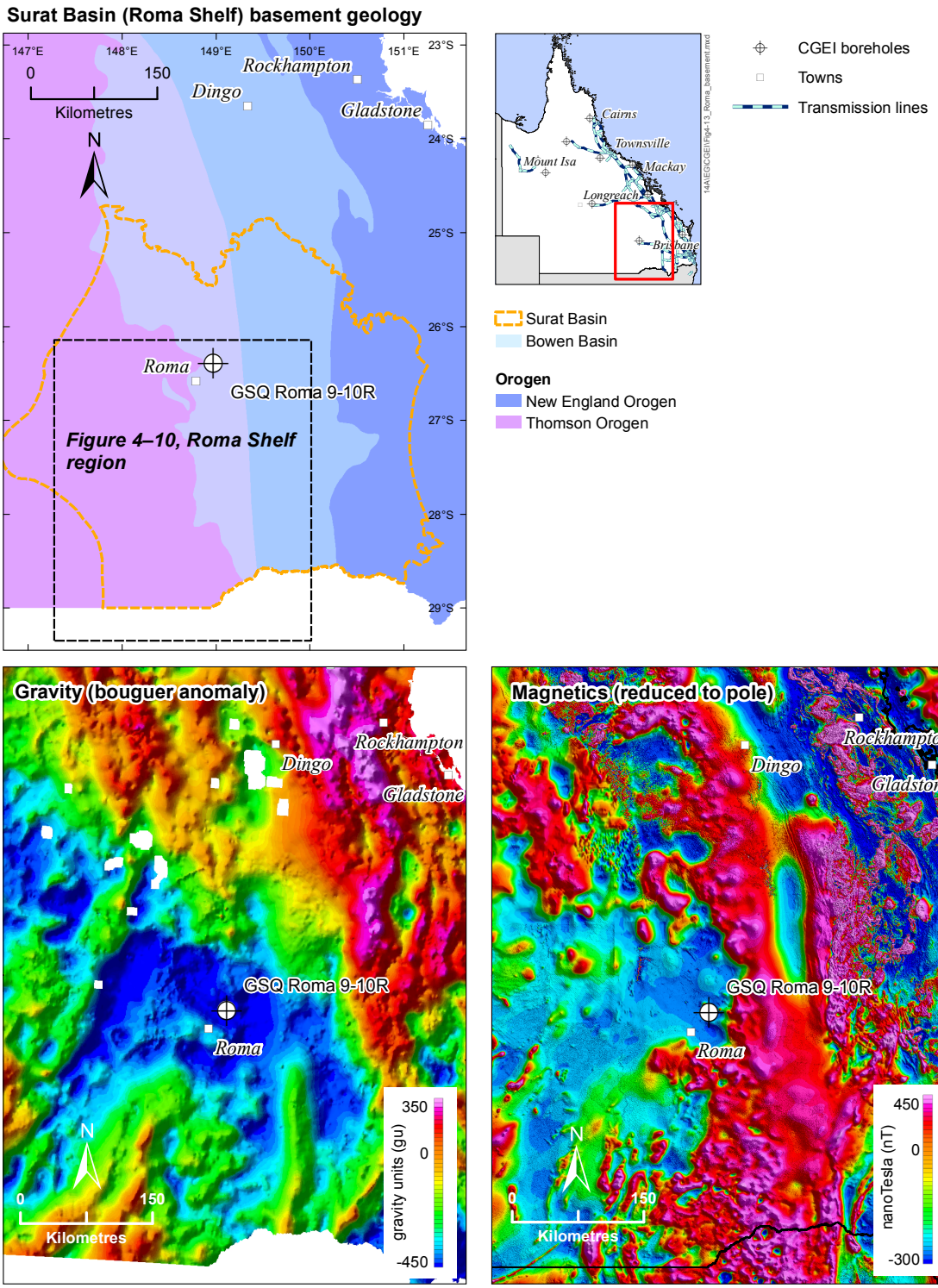

Figure 4-13. Basement geology and geophysics of the Surat Basin region.

Table 4-4. Estimated stratigraphy to 5 km depth beneath GSQ Roma 9-10R (Roma granites).

Borehole name	Depth interval (m)	Tectonic unit	Formation	Rock type	Thermal conductivity (W/mK)
GSQ Roma 9-10R**	106–245[1]	Surat Basin	Orallo Formation[1]	Sandstone, mudstone[1]	2.06 ± 0.08[1]
	245–308[1]		Gubberamunda Sandstone[1]	Sandstone[1]	2.58 ± 0.17[1]
	308–412[2]		Westbourne Formation[2]	Mudstone, sandstone, siltstone[2]	2.02 ± 0.11[1]
	412–457[2]		Springbok Sandstone[2]	Mudstone, sandstone[2]	2.02 ± 0.11[3]
	457–670[2]		Walloon Coal Measures[2]	Sandstone, mudstone, coal[4]	3.18 ± 1.26[3]
	670–750[2]		Eurombah Formation[2]	Sandstone, mudstone, coal[2,4]	1.65 ± 0.03[5]
	750–901[2]		Hutton Sandstone[2]	Sandstone[6]	3.18 ± 1.26[3]
	901–1035[2]		Evergreen Formation[2]	Sandstone[6]	3.18 ± 1.26[3]
	1035–1045[2]		Precipice Sandstone[2]	Sandstone[6]	3.18 ± 1.26[3]
	1045–1058[2]	Bowen Basin	Moolayember Formation[2]	Sandstone[6]	3.18 ± 1.26[3]
	1058–3000[7]	Thomson Orogen (Roma Shelf)	Roma granites[2,8]	Granite[8]	3.23 ± 0.73[3]
	3000–5000[7]		Timbury Hills Formation[7,8]	Metasiltstone[8]	2.82 ± 0.68[3]

[1] GSQ Roma 9-10R (Faulkner *et al.*, 2012b)
[2] AAO Pleasant Hills 1 (Wecker, 1972)
[3] Beardsmore & Cull (2001)
[4] Green (1997)
[5] GSQ St Lawrence 1 (Troup *et al.*, 2012)
[6] Bradshaw *et al.*, (2009)
[7] GSQ unpublished gravity modelling
[8] Murray (1994)

The Timbury Hills Formation comprises quartzose metasiltstones and is interpreted to extend to at least 5 km depth.

Depth to inferred geothermal resource

Using the stratigraphy described above, the 150°C cut-off temperature is estimated to be intersected at 4041 m, indicating an inferred resource between 4041 and 5000 m (150°C–187°C). The resource is anticipated to exist within the Timbury Hills Formation.

Stress regime

Core samples from basement intersections in the Roma Shelf region assigned to the Timbury Hills Formation are steeply dipping, with a well-developed cleavage parallel to bedding (Murray, 1994).

At a regional scale, the overlying Bowen Basin has a north-northwest trending structure, developed from east-northeast compression during the Permian and Triassic (Fielding *et al.*, 1997; Holcombe *et al.*, 1997). This major episode of compression associated with the Hunter–Bowen Orogeny is likely to have generated shallow to horizontal fractures trending towards the south-southwest. The structures of the overlying Surat Basin trend north–south and are strongly influenced by basement structures (Cook *et al.*, 2013).

The current stress regime through the Roma Shelf region is northeast–southwest compression (Clark & Leonard, 2003) (Figure 4-15). Whilst this regime is preferable for reservoir stimulation, the steeply dipping bedding and cleavage of the Timbury Hills Formation may induce vertical fracture growth and is likely to influence reservoir stimulation.

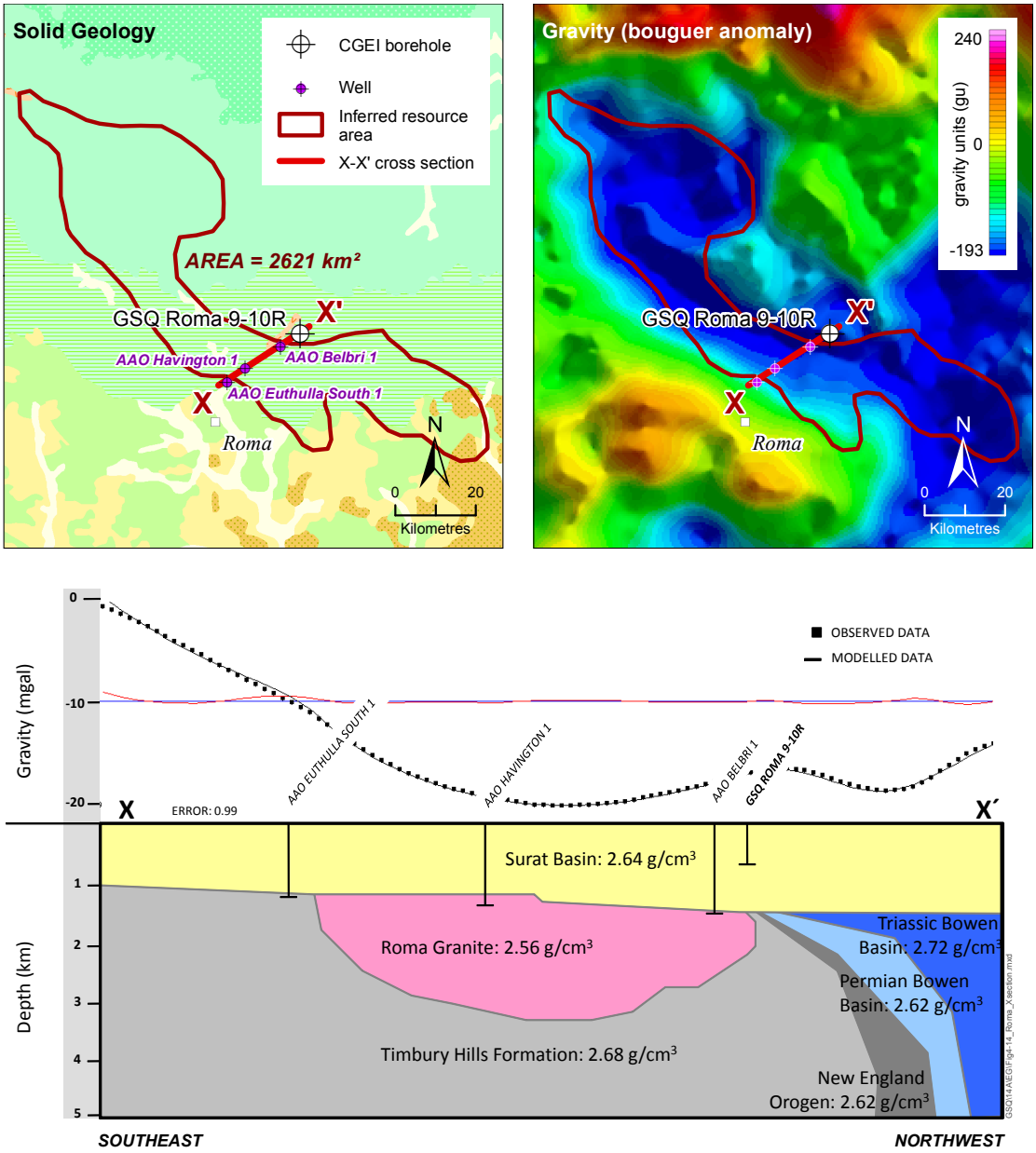

Figure 4-14. Inferred resource area and cross section through GSQ Roma 9-10R, within the Roma Shelf.

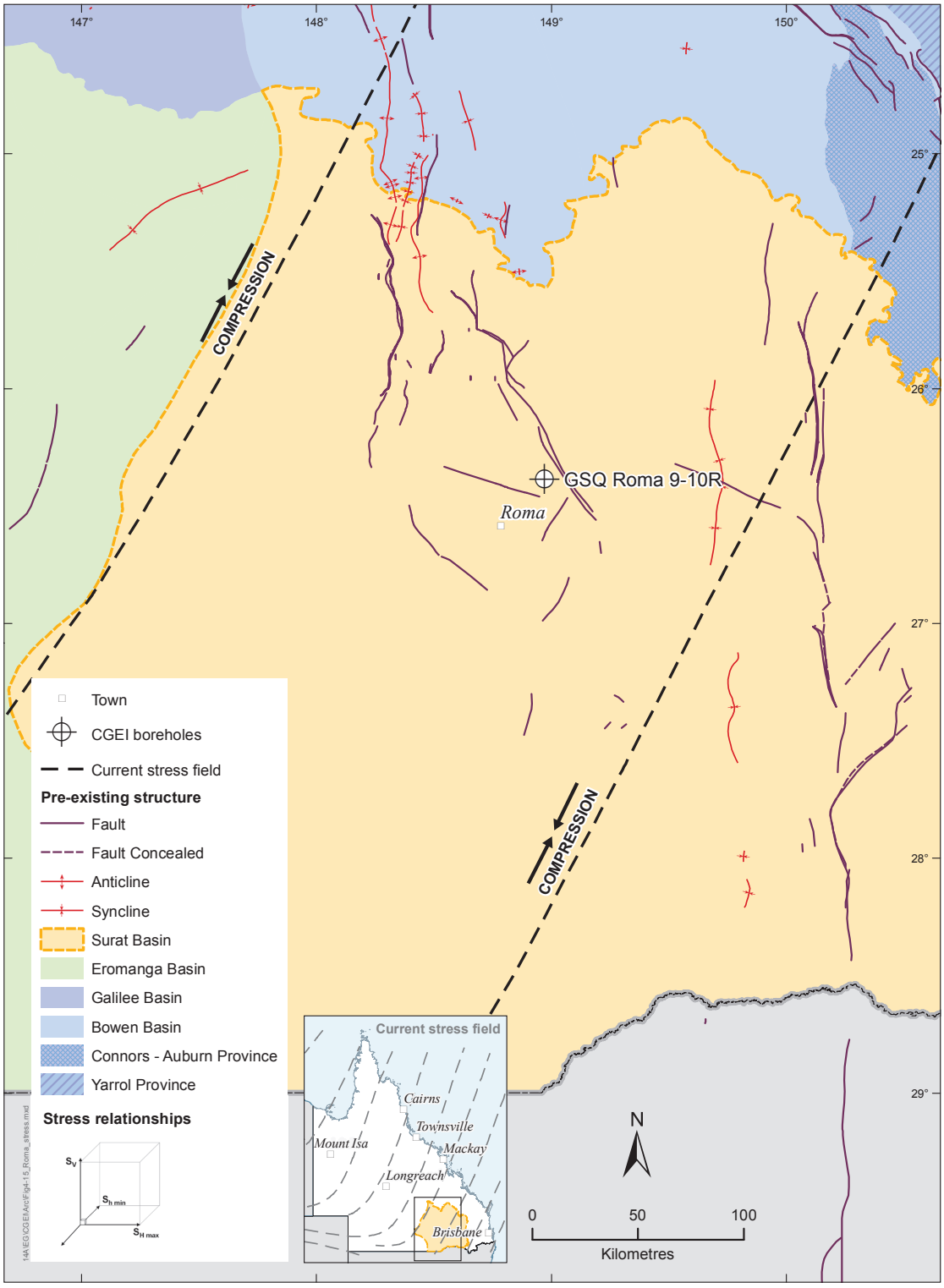

Figure 4-15. Stress regime around the Bowen and Surat basins (adapted from Clark & Leonard, 2003).

4.2.3 Summary

Heat flow	Insulation	Temp @5km	Stress regime	Prospectivity for EGS

Good
Average
Poor

4.3 Hillsborough Basin

GSQ Bowen 1 was drilled in the southern end of the Hillsborough Basin, for which high heat flow was modelled (71.0 ± 2.3 mW/m^2). The sedimentary strata of the Hillsborough Basin and units of the underlying Campwyn Volcanics provide reasonable insulation, and the targeted heat source is residual heat from past tectonic and volcanic activity. A preliminary resource assessment has indicated significant potential for a 456 km^2 inferred resource area within the Hillsborough Basin at 3880–5000 m depth.

4.3.1 Geological framework

The Campwyn Subprovince, the northern expression of the Yarrol Province, is mainly represented by the late Devonian – early Carboniferous **Campwyn Volcanics** and early Carboniferous **Edgecumbe beds** (Figure 4-16). These two units are broadly correlative (Paine, 1972). The Campwyn Volcanics primarily comprise felsic to intermediate volcanic flows and pyroclastics, and shallow marine to fresh-water sedimentary sequences. Bryan *et al.* (2003) defined a mafic lower association overlain by a silicic upper association. The Edgecumbe beds consist of felsic to intermediate lava and tuff, with shale, sandstone, and limestone, and were deposited in similar environments. The beds are vertical to very steeply dipping towards the east-northeast (Clarke *et al.*, 1971). The Campwyn Volcanics crop out along the southeastern margin of the Hillsborough Basin (Paine, 1967), and the Edgecumbe beds crop out along its northeastern side.

The Early Cretaceous **Whitsunday Volcanic Province** is faulted against the eastern edge of the **Campwyn Subprovince** (Figure 4-16). The province is considered to be the northern extension of the Whitsunday Silicic Large Igneous Province (SLIP), which extends over 2500 km along the east coast of Australia (Bryan *et al.*, 2000; Ewart *et al.*, 1992). The Whitsunday SLIP represents a major regional-scale thermal event related to the breakup of eastern continental Gondwana, and the formation of the eastern Australian passive margin during the Late Cretaceous to Cenozoic.

The **Hillsborough Basin** covers an area of 2700 km^2 on the central Queensland coast, north of Mackay (Figure 4-16), with the majority of the basin lying offshore (Bradshaw *et al.*, 2009). The basin is a narrow, linear, fault-bounded Cenozoic graben, which developed during a phase of extension associated with the opening of the Tasman and Coral seas, beginning in the Late Cretaceous (Day *et al.*, 1983). The Hillsborough Basin is one of four structural blocks in the Proserpine area; the others include the Midgeton Block to the west and possibly southeast of the basin, the Airlie Block in the northeast, and the Whitsunday Block (Whitsunday Volcanic Province) in the east. The basin contains the Paleogene Cape Hillsborough beds (Figure 4-17), a succession of sandstone, mudstone, carbonaceous shale, and minor coal. From seismic survey data, the beds are inferred to be up to 2100 m thick onshore (Ampol Exploration (QLD), 1965), thinning towards the southern onshore boundary (Paine, 1972). The northeastern margin of the basin is defined by a fault system that was active during deposition, resulting in the thickest sequence developing in this region. Seismic and gravity surveys show that the basin infill is repeatedly faulted, and the southwestern flank of the graben is interpreted as a series of small step faults (Paine, 1972).

4.3.2 Resource investigation

Potential heat source and insulation

Residual heat from recent tectonism and high heat producing volcanic rocks may form viable geothermal targets in the Hillsborough Basin. These heat sources, insulated by the thick sedimentary sequences of the Cape Hillsborough beds, may contribute to the slightly elevated heat flow modelled for GSQ Bowen 1.

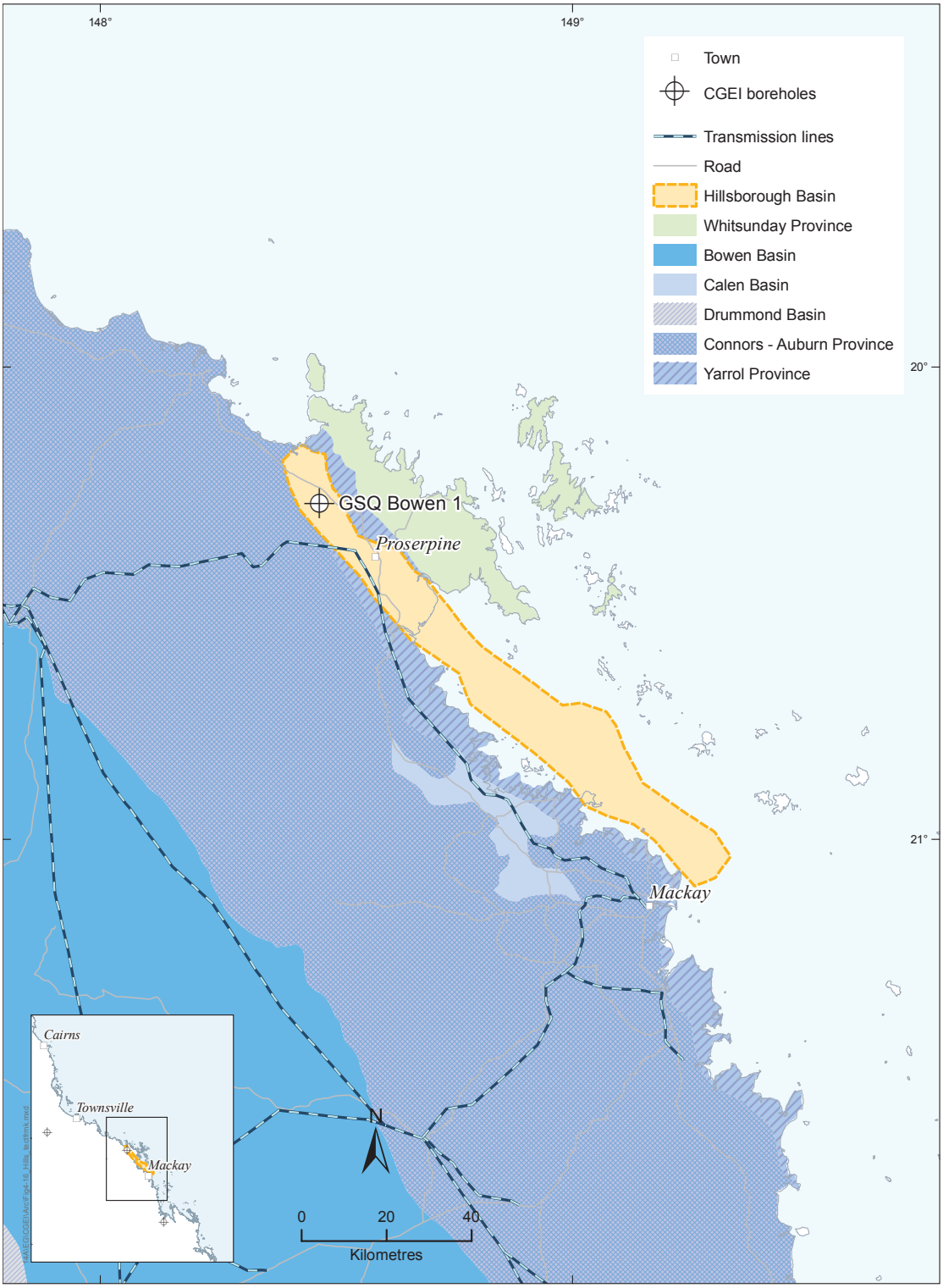

Figure 4-16. Tectonic framework of the Hillsborough Basin region.

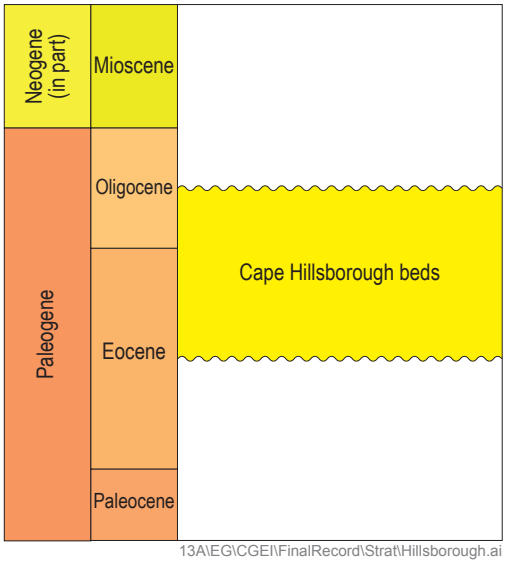

Figure 4-17. Stratigraphy of the Hillsborough Basin (adapted from Bradshaw et al., 2009).

The Whitsunday Volcanic Province is dominated by rhyolitic ignimbrites, which have similar enrichment of U, Th and K to high heat producing granitoids (Bryan, Queensland University of Technology, unpublished data). The Whitsunday SLIP may have high heat production due to the long-lived igneous activity and enrichment in heat producing elements in late stage magmas.

There are also several intrusions to the west of the Hillsborough Basin that show a high response on the radiometric ternary image indicating enrichment in all three radioactive elements: U, Th and K (Figure 4-18).

The thermal conductivity of rocks of the Cape Hillsborough beds is low, ranging from 0.47–2.46 W/mK. There is a relatively high proportion of carbonaceous mudstone and coal within the basin; the low thermal conductivity of these rock types and the overall thickness of the basin sequence suggests a reasonable insulating capacity.

Inferred geothermal resource area

The inferred resource area (456 km^2) is defined by the igneous basement underlying the entire onshore component of the Hillsborough Basin (Figure 4-19).

In order to estimate temperatures at 5 km depth, the stratigraphic succession in AEL Proserpine 1 was used in conjunction with the regional geological framework described by Bryan *et al*. (2000) and Day *et al*. (1983) to predict stratigraphy and rock types below the depth penetrated by GSQ Bowen 1 (Table 4-5).

The Cape Hillsborough beds, intersected in AEQ Proserpine 1 (Ampol Exploration (QLD), 1965), and AEL HB 1C (Gorton, 2010), are fine- to coarse-grained sandstone, siltstone and mudstone (carbonaceous in places). Maximum onshore thickness of the Cape Hillsborough beds is 2100 m, but in the vicinity of GSQ Bowen 1, the beds are estimated to be 1300 m thick (Ampol Exploration (QLD), 1965).

Basement under the Hillsborough Basin in the vicinity of GSQ Bowen 1 is interpreted to be the Campwyn Volcanics (Figure 4-20). The Bryan *et al*. (2003) subdivision has been used as the basis for assigning the thermal properties required for temperature modelling (Table 4-5). Bryan *et al*. (2003) suggested a minimum thickness of 1000 m from outcrop for each association of the volcanics, whilst Day *et al*. (1983) suggested a thickness of 3000–8000 m for the entire unit. As a result, a thickness of 2200 m was estimated for the Upper silicic and 1500 m for the Lower mafic associations (Table 4-5).

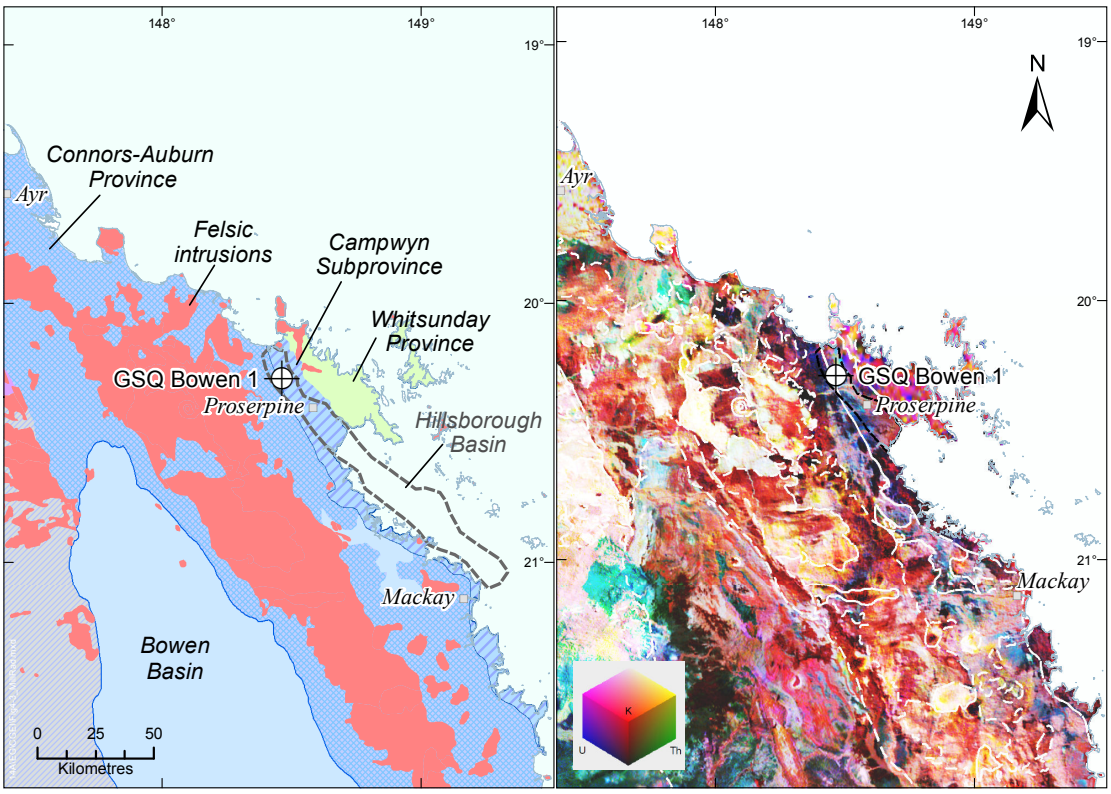

Figure 4-18. Radiometric ternary image of the Hillsborough Basin region.

Depth to inferred geothermal resource

Based on the estimated thermal properties of this stratigraphy and the determined heat flow for the borehole, the 150°C isotherm is expected at 3880 m, indicating the inferred resource is between 3880 and 5000 m within the Campwyn Volcanics.

Stress regime

The Campwyn Subprovince developed as a volcanic arc overlying a subduction zone and represents the east–west amalgamation of volcanic terranes (Yarrol Project Team, 1997, 2003; Donchak *et al*., 2013). Subsequent phases of compression and extension relating to the onset of the Hunter–Bowen Orogeny and extensional recalibration is likely to have produced steep to vertical, approximately north–south-trending fractures.

By the early Cretaceous, the stress regime was predominantly extensional, with northwest–southeast rifting culminating in the initiation of the Hillsborough Basin. The orientation of fracture networks associated with this event is likely to be steep to vertical with a northwest–southeast strike. Consequently, existing fractures that may be present within the reservoir are anticipated to be steep to vertical, north–south striking.

Currently, collision along the north Australian margin has propagated a compressional stress regime within the Hillsborough Basin, with the maximum horizontal component (SH) at a northeast orientation (Figure 4-21). This existing stress regime could facilitate shallow to horizontal fracture stimulation. However, existing steep to vertical dipping fractures are likely to influence the direction of new fracture growth during reservoir stimulation.

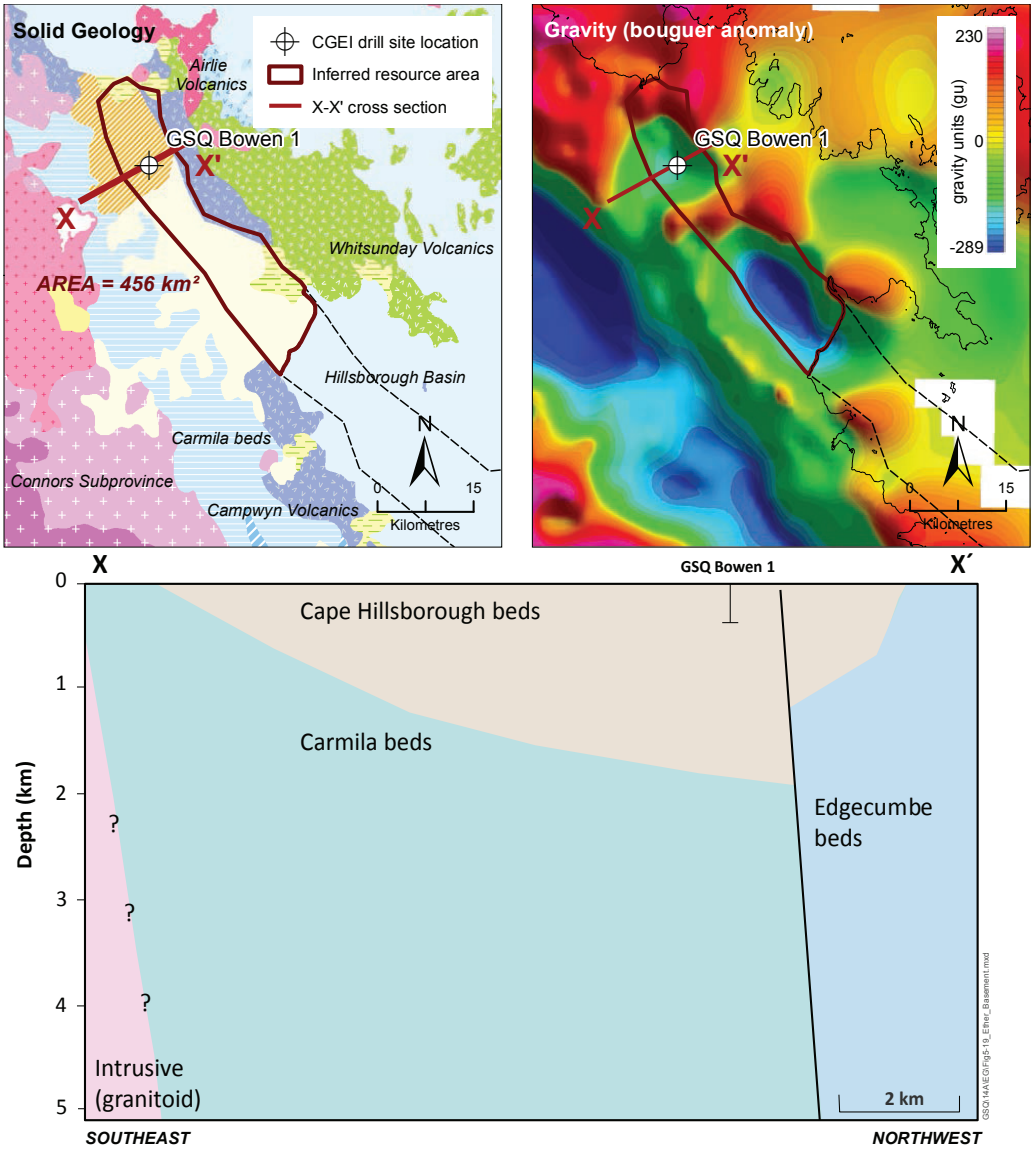

Figure 4-19. Inferred resource area and cross section through GSQ Bowen 1, within the onshore Hillsborough Basin.

Table 4-5. Estimated stratigraphy to 5 km depth beneath GSQ Bowen 1, Hillsborough Basin.

Borehole name	Depth interval (m)	Tectonic unit	Formation	Rock type	Thermal conductivity (W/mK)
GSQ Bowen 1	89–164[1]	Hillsborough Basin	Cape Hillsborough beds[1]	Mudstone, siltstone, sandstone, coal[1]	1.80 ± 0.07[1]
	164–274[1]			Mudstone, sandstone, siltstone[1]	2.45 ± 0.15[1]
	274–320[1]			Sandstone, mudstone, siltstone[1]	2.13 ± 0.14[1]
	320–1300[2]			Sandstone, mudstone, siltstone[1]	1.93 ± 0.11[1]
	1300–3500[3,4,5]	Campwyn Subprovince	Campwyn Volcanics – upper silicic[4]	Sandstone[3]	3.18 ± 1.26[6]
	3500–5000[3,4,5]		Campwyn Volcanics – lower mafic[4]	Basalt[3]	1.74 ± 0.36[6]

[1] GSQ Bowen 1 (O'Connor *et al.*, 2012)
[2] Ampol Exploration (QLD) (1965)
[3] GSQ interpretation
[4] Bryan *et al.* (2003)
[5] Day *et al.* (1983)
[6] Beardsmore & Cull (2001)

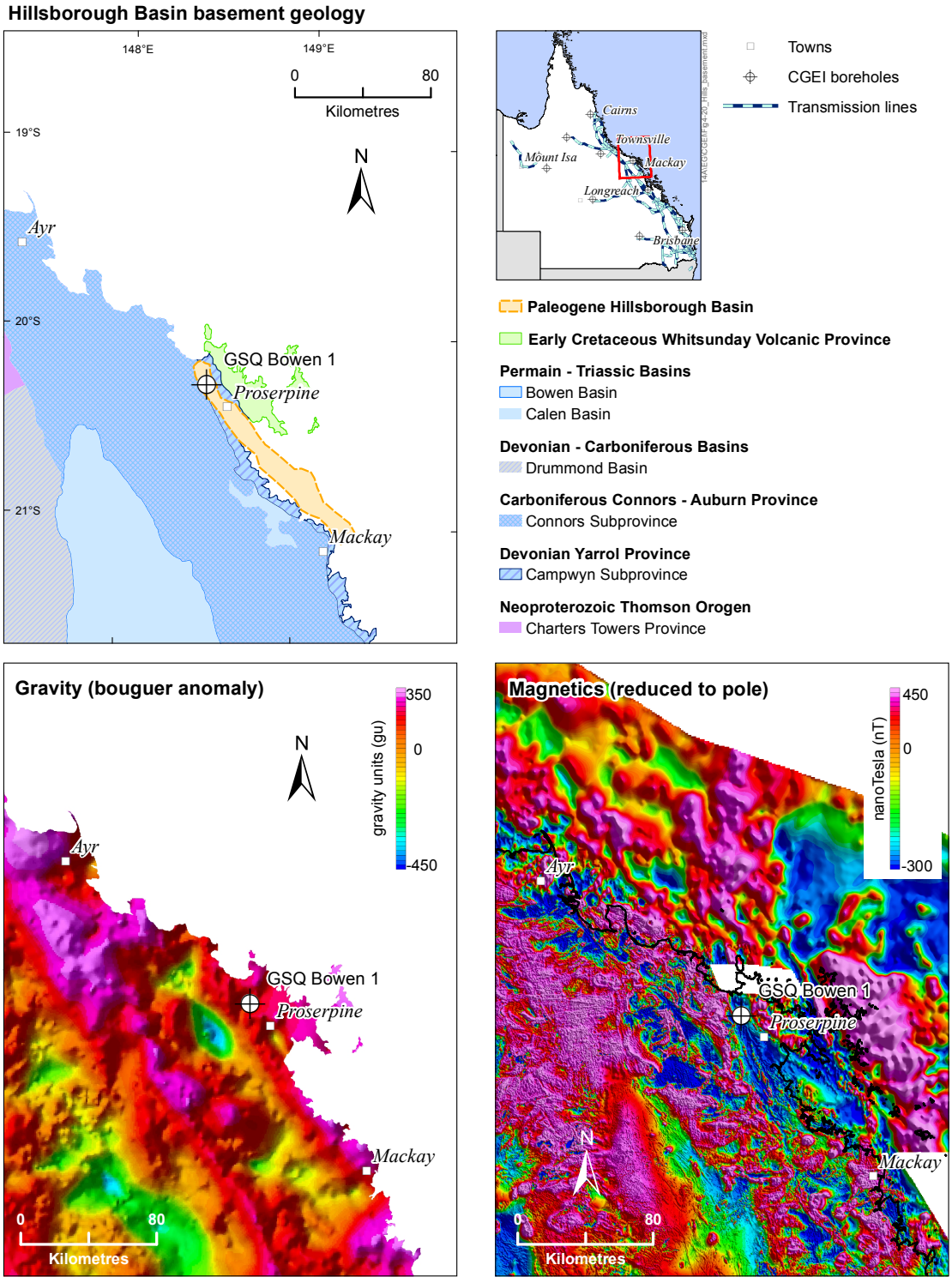

Figure 4-20. Basement geology and geophysics of the Hillsborough Basin region.

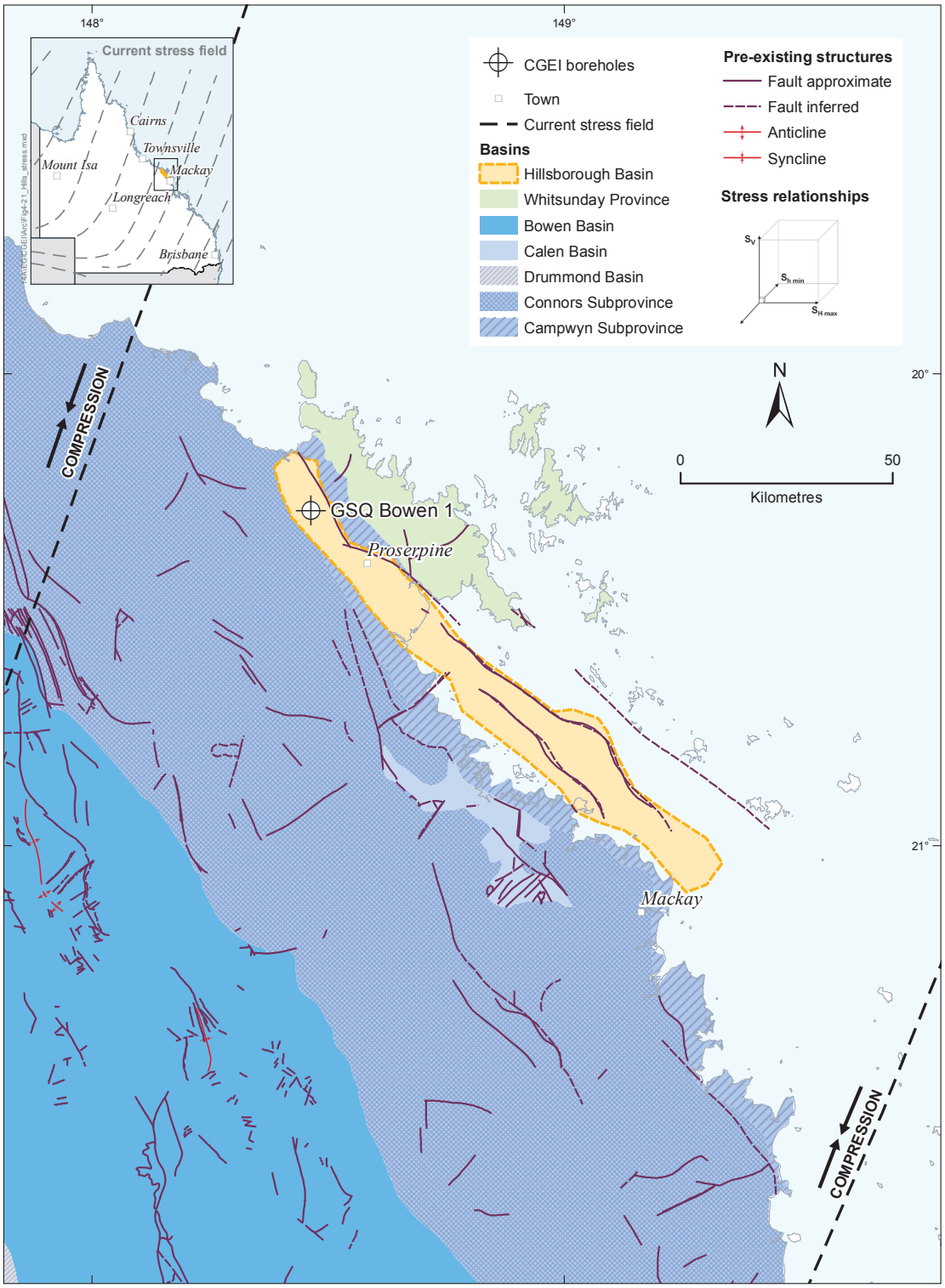

Figure 4-21. Stress regime around the Hillsborough Basin (adapted from Clark & Leonard, 2003).

4.3.3 Summary

Heat flow	Insulation	Temp @5km	Stress regime	Prospectivity for EGS

Good
Average
Poor

4.4 Nambour-Maryborough basins

GSQ Maryborough 16 was drilled in the Nambour Basin, targeting heat from intrusives and residual heat from tectonism and volcanism. The thermal data collected from GSQ Maryborough 16 was extrapolated to the north, where the thicker strata of the Maryborough Basin greatly increases the prospectivity for a geothermal resource. Despite the only marginally higher than average heat flow (67.0 ± 2.9 mW/m^2), the predicted temperature estimated at 5 km for the Maryborough Basin was greater than 200°C. Thus, a preliminary resource assessment has indicated a significant inferred resource area within the Maryborough Basin, over an area of 1465 km^2, between 3357 m and 5000 m depth.

4.4.1 Geological framework

The early Permian to Middle Triassic **Gympie Province** (Figure 4-22) consists of the Gympie Group and Brooweena Formation, which were deposited in a shallow to deep marine environment. The Permian Gympie Group records the evolution of an oceanic volcanic arc and includes basaltic to andesitic and epiclastic flows, limestones, and turbididic sequences. The Gympie Group strata strike north-northwest to northeasterly, with moderate to steep dips and regional fold axes following a similar trend (Cranfield, 1994). The margins of the group are poorly defined although the group is interpreted to underlie the Brooweena Formation in the Gigoomgan area. The Early to Middle Triassic Brooweena Formation is the uppermost unit of the Gympie Province. The formation outcrops extensively to the west of the Nambour-Maryborough basins, and has been mapped and described in detail (Cranfield, 1994).

The **Nambour Basin** is a latest Triassic to Middle Jurassic intracratonic basin that covers 7000 km^2 onshore and 2500 km^2 offshore (Figure 4-22) (McKellar, 1993; Turner *et al.*, 2009; Geoscience Australia, 2008b). The basin is located to the east of the Paleozoic D'Aguilar Block in the north, and the Beenleigh Block in the south. In the south, the basin overlies Paleozoic basement and, in the north, it underlies part of the Maryborough Basin.

Uplift at the end of the Triassic exposed the craton to erosion and sediments were deposited into basins and structural depressions. Throughout the basin, strata are subhorizontal with broad, open, north-northwest trending folds plunging gently to the southeast (Cook *et al.*, 2013). The basin was thought to have a sedimentary thickness of 600 m; however, WPO Cribb Island 1 and WPL (Wellington Point) 1 near Brisbane intersected basement at 166 and 1127 m respectively, suggesting asymmetrical sediment deposition over an irregular erosive surface. The northern part of the basin comprises the Duckinwilla Group, previously included in the Maryborough Basin (Day *et al.*, 1983). This group consists of the Myrtle Creek Sandstone and the overlying Tiaro Coal Measures.

The Early Cretaceous **Maryborough Basin** (Figure 4-22) developed in two main stages—transtensional rifting followed by thermal subsidence. A period of substantial rift-related volcanic activity resulted in the initiation of the basin with the deposition of the Grahams Creek Formation, which unconformably overlies Nambour Basin in the north, and also the metasedimentary sequences of the Gympie Province. This formation is overlain by shallow-marine and fluvio-deltaic sequences of the Maryborough Formation and the Burrum Coal Measures (Cook *et al.*, 2013) (Figure 4-23). The basin covers an area of 9100 km^2 onshore and 15 500 km^2 offshore, with a maximum thickness of 6500 m (Cook *et al.*, 2013). In the north, a series of broad, open folds, produced by deformation in the mid-Cretaceous to Paleogene, trend north-northwest. In the south, deformation was more intense, producing faults and tight isoclinal folds.

Basement to the Maryborough–Nambour basins has been intruded by Late Triassic and Late Jurassic – Cretaceous intrusives. In the vicinity of GSQ Maryborough 16, the **Mount Urah** and **Mount Bauple** intrusives have been postulated to extend under cover. Mount Urah varies in composition between hornblende-biotite granodiorite and pyroxene-hornblende microdiorite, and Mount Bauple comprises biotite quartz syenite (Geoscience Australia, 2012a).

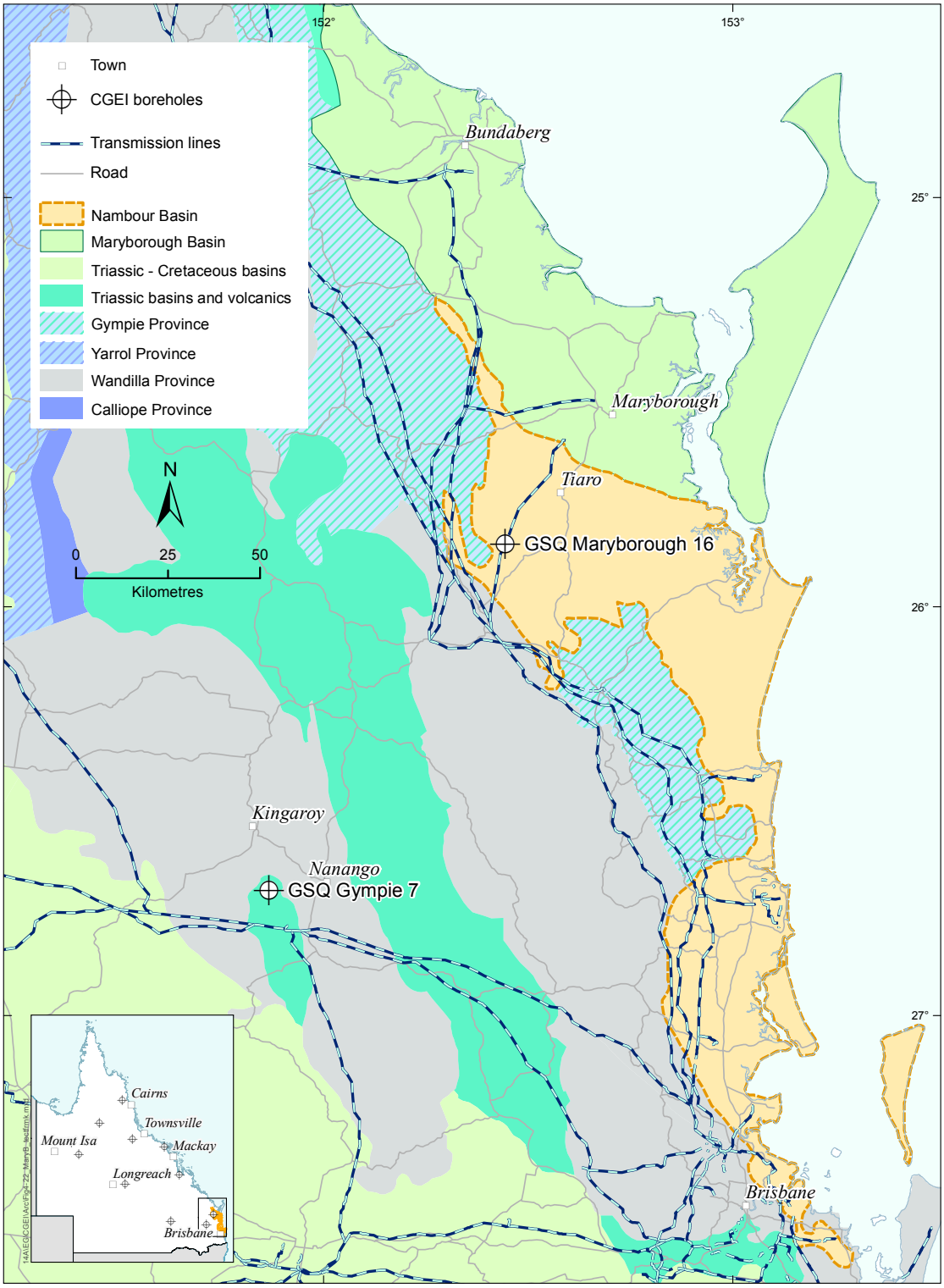

Figure 4-22. Tectonic framework of the Nambour-Maryborough basins region.

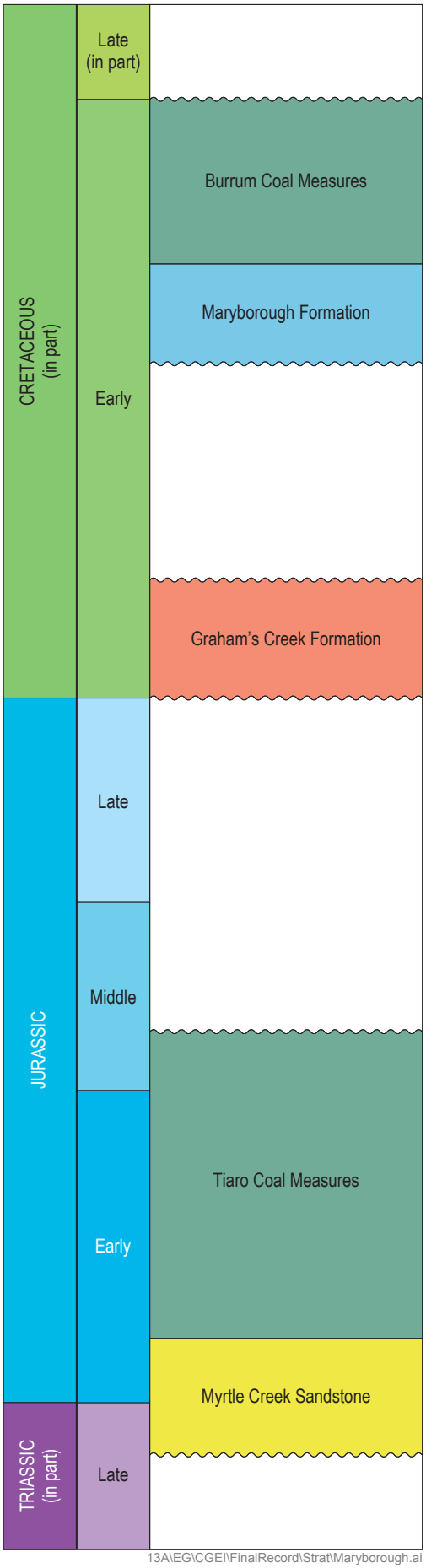

Figure 4-23. Stratigraphy of the Nambour-Maryborough basins (adapted from Bradshaw et al., 2009).

4.4.2 Resource investigation

Potential heat source and insulation

GSQ Maryborough 16 was drilled into the Tiaro Coal Measures in the northern Nambour Basin. The thermal data gathered from this borehole was then used to assess the geothermal prospectivity of the Maryborough Basin, which overlies the Nambour Basin, as the insulation provided by the Burrum Coal Measures greatly increases the prospectivity.

The Mount Urah and Mount Bauple intrusions are postulated to extend under the sedimentary cover of the Maryborough Basin, and could provide a heat source at depth. A lack of heat production values for these intrusives makes it difficult to quantify this potential. However, on radiometric ternary images, both intrusions show a high response for radioactive U, Th and K, which under insulation may retain sufficient heat to form a viable resource (Figure 4-24).

The high thermal regime in the Cretaceous probably continued into the Cenozoic, as evident from the wide spread episodic volcanism and tectonic activity throughout the Nambour-Maryborough basins region (Robertson, 1990). A residual heat component from these tectonic processes, insulated by the thick sedimentary sequences of both basins, could also form a geothermal resource.

The thermal insulation of the Nambour and Maryborough basins is excellent, comprising siltstones, sandstones, volcanics and coal measures. In particular the insulating capacity of the Tiaro Coal Measures (Nambour Basin) and the Burrum Coal Measures (Maryborough Basin) would be sufficient to retain high temperatures at depth just from the average crustal heat flow.

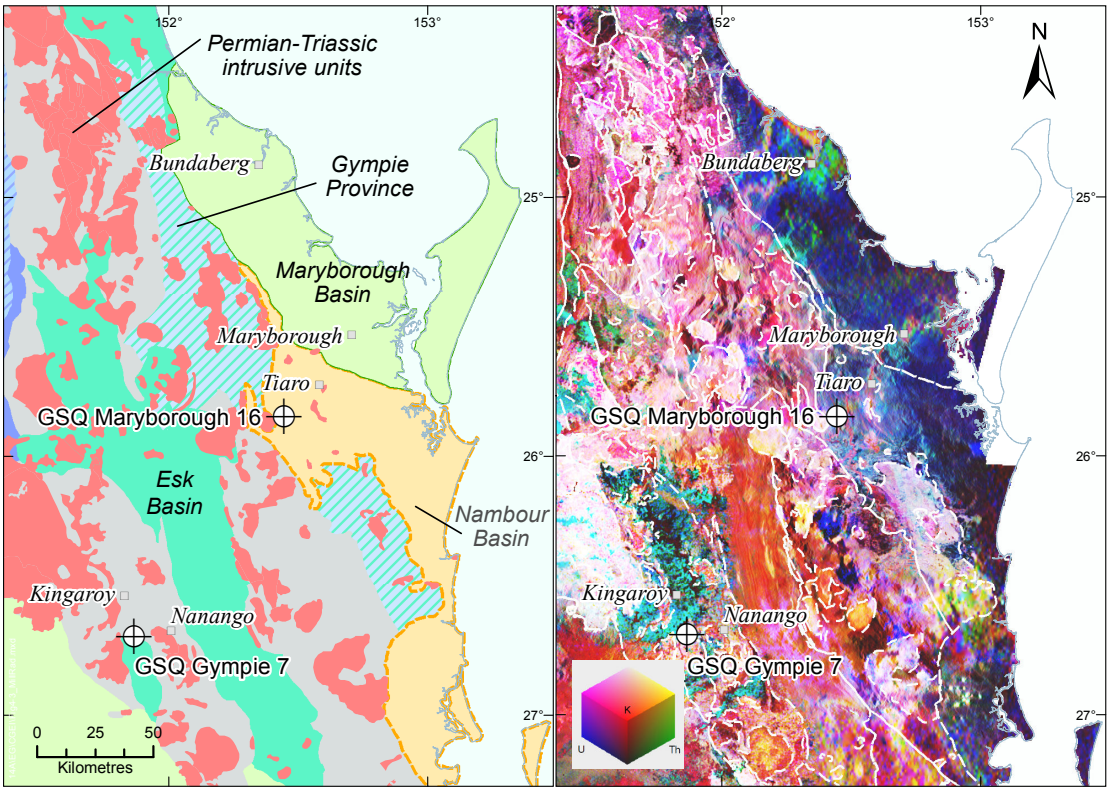

Figure 4-24. Radiometric ternary image of the Nambour-Maryborough basins region.

Inferred geothermal resource area

The inferred resource area is defined based on the average 600 m thickness of the Burrum Coal Measures. An area of 1465 km² is interpreted based on adjacent drilling intersections (Figure 4-25).

GSQ Maryborough 16 was drilled into the Tiaro Coal Measures at the northern end of the Nambour Basin. The thermal data collected was then used to estimate temperatures to 5 km depth below the Maryborough Basin, where the Burrum Coal Measures would significantly increase insulation and geothermal prospectivity. Consequently, adjacent drilling information and regional geological information (Cranfield, 1994; Denaro *et al*., 2007) were used to estimate stratigraphy and rock types within the inferred resource area (Table 4-6).

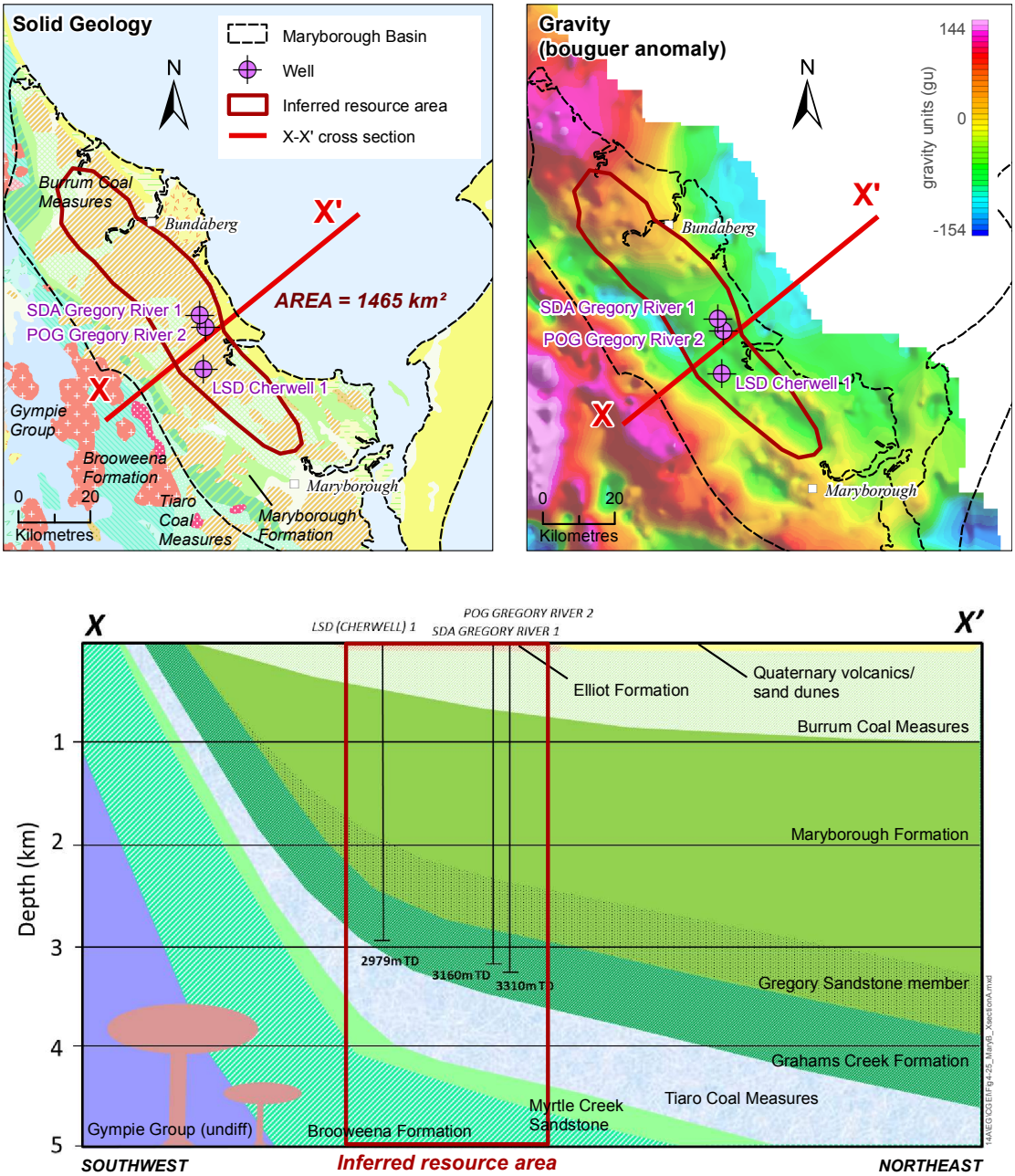

Figure 4-25. Inferred resource area and cross section within the onshore Maryborough Basin.

Table 4-6. Estimated stratigraphy to 5 km depth beneath Maryborough Basin (inferred resource area).

Borehole name	Depth interval (m)	Tectonic unit	Formation	Rock type	Thermal conductivity (W/mK)
GSQ Maryborough 16**	0–600[1]	Maryborough Basin	Burrum Coal Measures[1]	Mudstone[1]	2.00 ± 0.15[2]
	600–1500[3]		Maryborough Formation[3]	Mudstone[3]	1.88 ± 0.54[4]
	1500–2000[5]		Gregory Sandstone member[5]	Sandstone[1,5,7]	3.18 ± 1.26[4]
	2000–3200[6]		Grahams Creek Formation[6]	Andesite[8]	1.65 ± 0.33[9]
	3200–4000[6]	Nambour Basin	Tiaro Coal Measures[6]	Siltstone/coal[2]	2.00 ± 0.15[2]
	4000–4600[7]		Myrtle Creek Sandstone[7]	Sandstone[9]	3.18 ± 1.26[4]
	4600–5000[8,9]	Gympie Province	Brooweena Formation[9]	Siltstone[9]	2.82 ± 0.68[4]

** GSQ Maryborough 16 data used to extrapolate stratigraphy to 5 km within the Maryborough Basin (located 70 km north of borehole location)
[1] LSD Cherwell 1 (Siller, 1965)
[2] GSQ Maryborough 16 (Sargent *et al.*, 2012a)
[3] MAP Burrum 1 (Enter & Grant, 2007a); MAP Burrum 2 (Enter & Grant, 2007b)
[4] Beardsmore & Cull (2001)
[5] SDA Gregory River 1 (Shell Development, 1967); POG Gregory River 2 (Derrington, 1981)
[6] Ellis (1968)
[7] Cranfield (1994)
[8] Denaro *et al.* (2007)
[9] Magellan Petroleum Australia Limited (1992)

The petroleum wells SDA Gregory River 1 (Shell Development, 1967) and POG Gregory River 2 (Derrington, 1981) were used to interpret stratigraphy to 5 km. The Burrum Coal Measures of the Maryborough Basin are estimated to be about 600 m thick, and comprise sandstone and siltstone, with minor shale and coal. Underlying these coal measures is 1400 m of the Maryborough Formation, comprising mudstone, shale, siltstone, and sandstone—estimated from MAP Burrum 1 (Enter & Grant, 2007a) and MAP Burrum 2 (Enter & Grant, 2007b). Within the Maryborough Formation, the basal 500 m has been assigned to the Gregory Sandstone member to represent a higher thermal conductivity. The lowermost unit of the Maryborough Basin is the Grahams Creek Formation, which contains up to 1200 m of volcanics and volcaniclastic sequences (Cranfield, 1994).

The Tiaro Coal Measures of the Nambour Basin consist predominantly of sandstone, siltstone, shale and coal, with an estimated thickness of 800 m (Cranfield, 1994). The underlying Myrtle Creek Sandstone comprises quartzose to sublabile sandstone, with siltstone and shale, and is about 650 m thick (Cranfield, 1994).

The Brooweena Formation of the Gympie Province is interpreted to unconformably underlie the Myrtle Creek Sandstone and form basement to the Nambour Basin (Figure 4-26). The exact thickness of this formation is unknown but has been predicted from 4600 to 5000m.

Depth to inferred geothermal resource

Estimations using this stratigraphy indicate that the 150°C cut-off temperature can be expected at 3357 m. This suggests an inferred geothermal resource exists in the 3357–5000 m interval, in the Brooweena Formation, Myrtle Creek Sandstone and Tiaro Coal Measures.

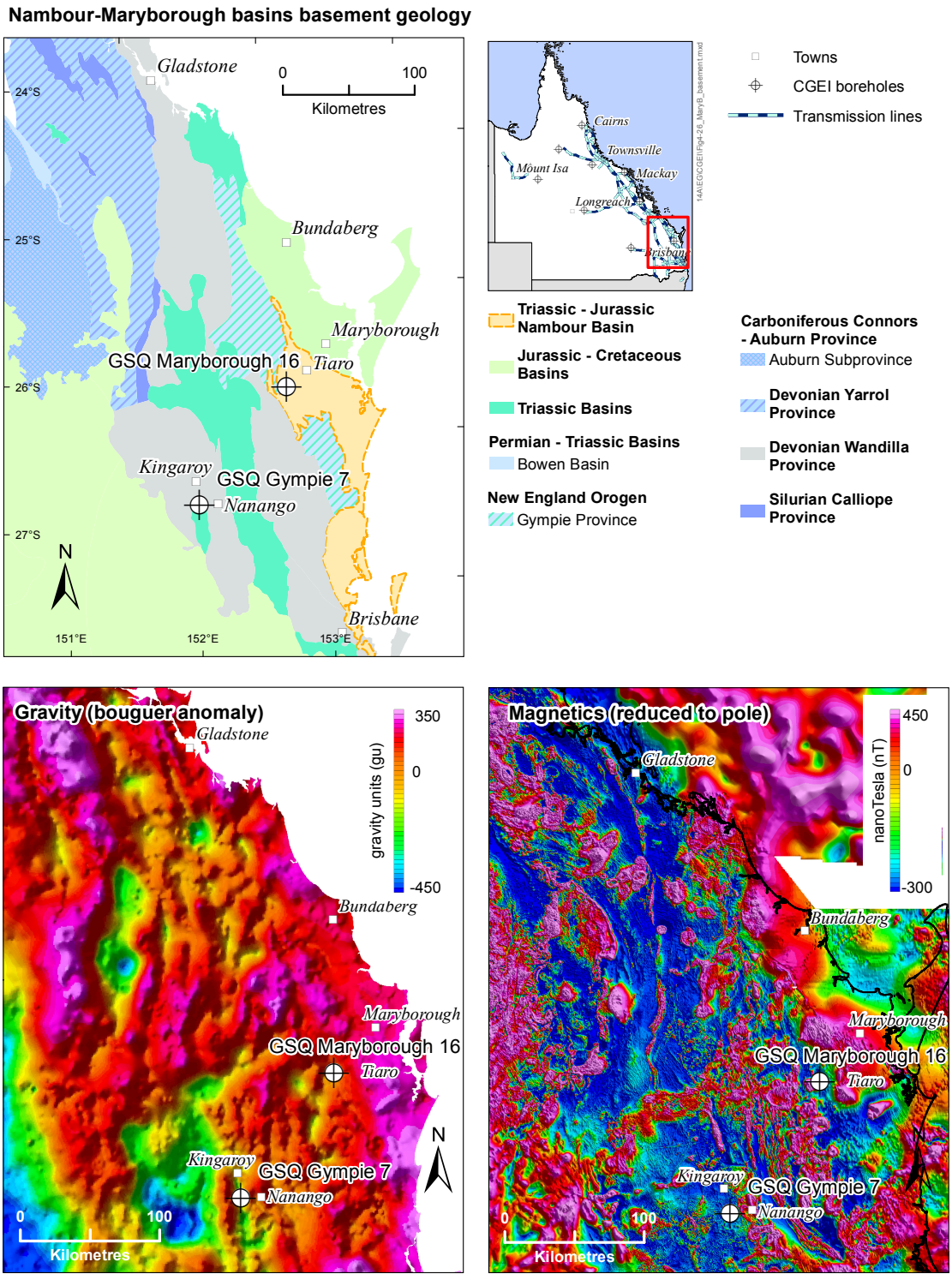

Figure 4-26. Basement geology and geophysics of the Nambour-Maryborough basins region.

Stress regime

The tectonic history of the New England Orogen (encompassing the Gympie Province) and the overlying Nambour-Maryborough basins was used to infer existing fractures that may influence reservoir stimulation.

The Gympie Province represents an accreted oceanic island arc and is intensely deformed, with fold axes trending north-northwest and northeast (Donchak *et al.*, 2013; Cranfield, 1992). Whilst this compressional event is likely to have propagated shallow to horizontal fractures trending south-southeast and southeast these fractures may have rotated by further strike slip displacement in the Triassic (Holcombe, 1997a,b).

The Cretaceous marked the onset of rifting, initiating the Maryborough Basin within a northwest–southeast extensional stress field, and is likely to have produced steeply dipping fractures.

The Nambour-Maryborough basins region is currently subjected to a northeast–southwest compressional stress regime (Clark & Leonard, 2003) (Figure 4-27), which could be optimal for reservoir stimulation in a horizontal direction. However, steeply dipping fractures associated with accretion and rifting may propagate fractures towards the vertical orientation.

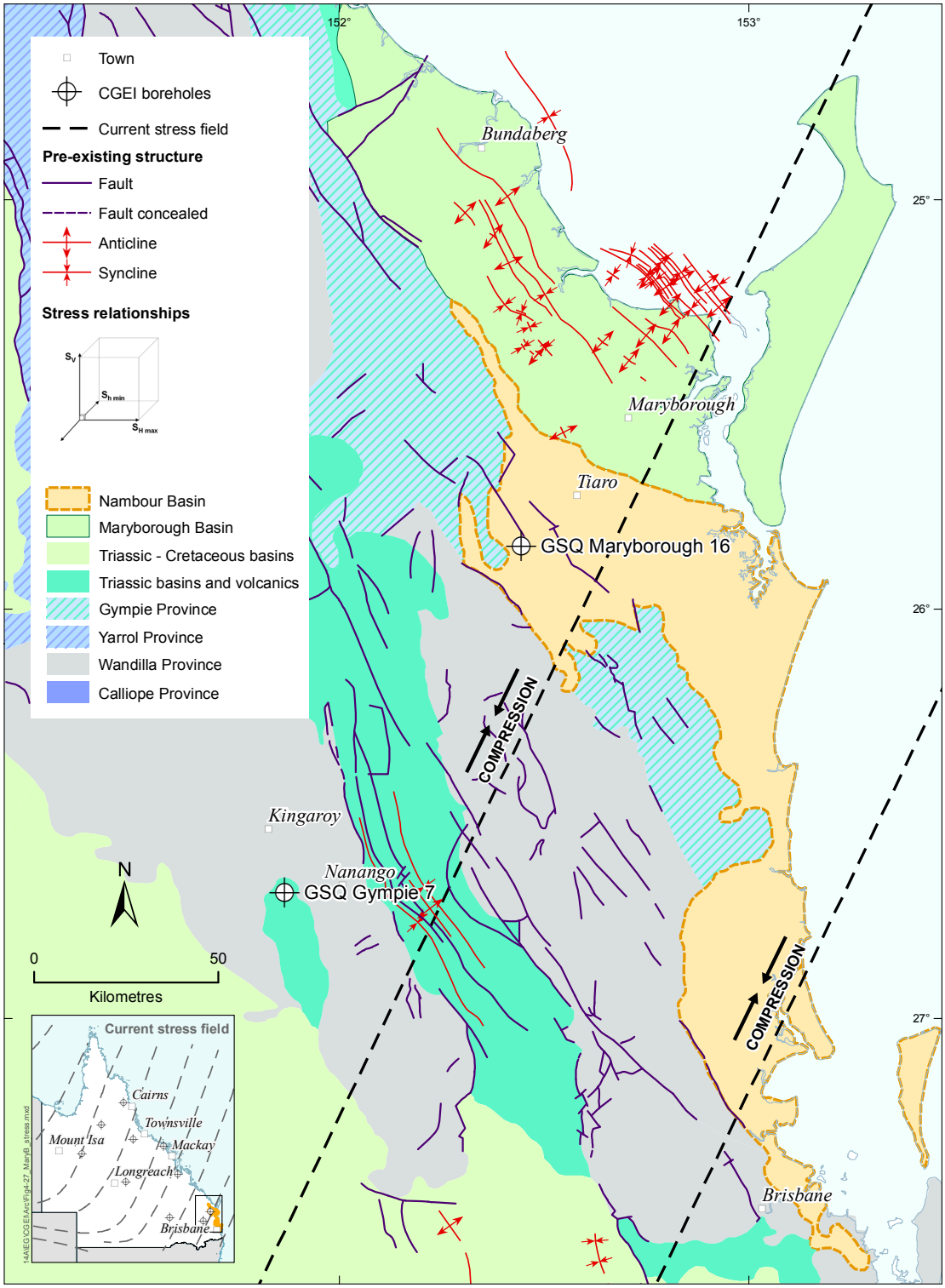

Figure 4-27. Stress regime around the Nambour-Maryborough basins (adapted from Clark & Leonard, 2003).

4.4.3 Summary

Heat flow	Insulation	Temp @5km	Stress regime	Prospectivity for EGS

Good
Average
Poor

5. Low prospectivity regions

5.1 Styx Basin

In the Styx Basin region, the Back Creek Group and intrusives of the Connors Arch are the targeted heat source in GSQ St Lawrence 1. The coal measures of the overlying Styx Basin provide good insulation, but despite this only an average heat flow was modelled (64.5 ± 1.1 mW/m^2). Further modelling indicated the depth to the 150°C cut-off temperature was 4235 m, which is marginal for creating a sufficient reservoir thickness. In addition, the temperature difference between 4235 and 5000m is insignificant, limiting the viability of the target as a geothermal energy resource.

5.1.1 Geological framework

Basement to the Styx Basin consists of the Early Permian Carmila beds, which comprise siltstone and mudstone, volcanolithic sandstone and conglomerate, minor altered basalt, and local rhyolitic to dacitic volcanic rocks (Withnall *et al.*, 2009).

In the Strathmuir Synclinorium, near the eastern margin of the Bowen Basin (Figure 5-1), the Carmila beds are conformably overlain by the Early to Middle Permian **Back Creek Group** (Figure 5-1). The intensity of folding in the Strathmuir Synclinorium increases to the east, towards the Gogango Thrust Zone, with folding during the middle or late Permian (Day *et al.*, 1983). The Back Creek Group consists dominantly of massive cleaved mudstone and lithic sandstone, deposited within a predominantly shallow marine environment (Withnall *et al.*, 2009). The Back Creek Group exhibits a 'hot' signature on the ternary radiometric image, indicating that the group may be a suitable heat source.

The **Styx Basin** is a small elongate intracratonic half-graben, covering an area of approximately 300 km^2 onshore and 500 km^2 offshore on the central Queensland coast (Figure 5-1; Benstead, 1976; Cook *et al.*, 2013). The basin onlaps the Back Creek Group, and formed due to subsidence along the Strathmuir Synclinorium (Cook *et al.*, 2013; Pinder, 2007). The Styx Coal Measures, the only formation present in the basin (Figure 5-2; Benstead, 1976; Cook *et al.*, 2013), are an Early Cretaceous succession of sandstone, mudstone coal and conglomerate, with sporadic marine incursions (Malone, 1970). Numerous coal seams are present, which differ in thickness and lateral extent.

The Styx Coal Measures onlap the underlying Permian strata in the west, and are faulted against them in the east. The basin plunges gently to the north, with strata generally dipping to the east. Its sedimentary succession is known from drilling to be at least 552 m thick (ARM Styx River 1; Pinder, 2007), but geophysical data suggest the thickness could be up to 900 m in the north of the basin (Benstead, 1976).

5.1.2 Resource investigation

Potential heat source and insulation

In the Styx Basin region, the Back Creek Group gives a high response on radiometric ternary images, indicating enrichment in all three radioactive elements (Figure 5-3). Also, the Carboniferous granitoids of the Connors Arch are predominantly felsic, and some also exhibit high responses on the ternary radiometric image. Whilst heat production values for several granitic intrusions of the Connors Arch were low to moderate (1–3 μW/m^3), they may still form a heat source at depth under sufficient insulation.

The coal seams of the Styx Coal Measures have vitrinite reflectance (RV max) values between 0.86 and 0.99 per cent (Troup *et al*., 2012), which correspond to a maximum palaeo-geothermal gradient of 69°C/km, significantly higher than the current geothermal gradient (35°C/km). This suggests the basin was subjected to a high thermal regime in the past.

The Styx Coal Measures have thermal conductivity values between 0.33 and 2.59 W/mK, and are considered good insulators (Troup *et al*., 2012). The presence of coal within the basin also greatly contributes to the insulation.

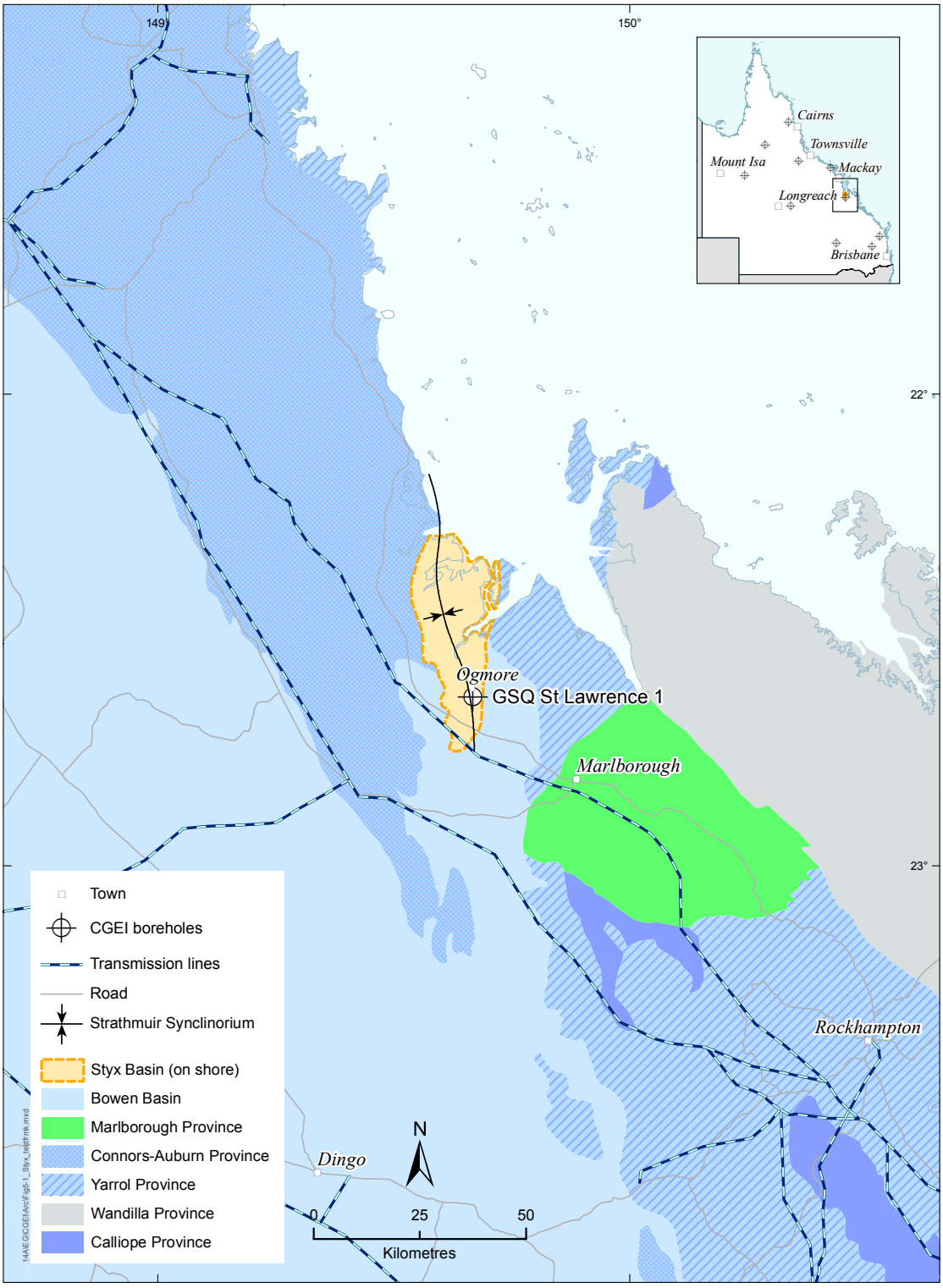

Figure 5-1. Tectonic framework of the Styx Basin region.

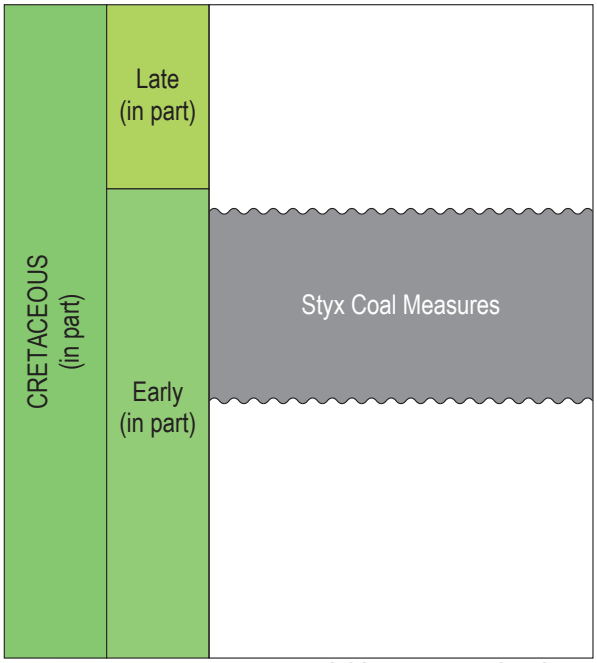

Figure 5-2. Stratigraphy of the Styx Basin (adapted from Bradshaw et al., 2009).

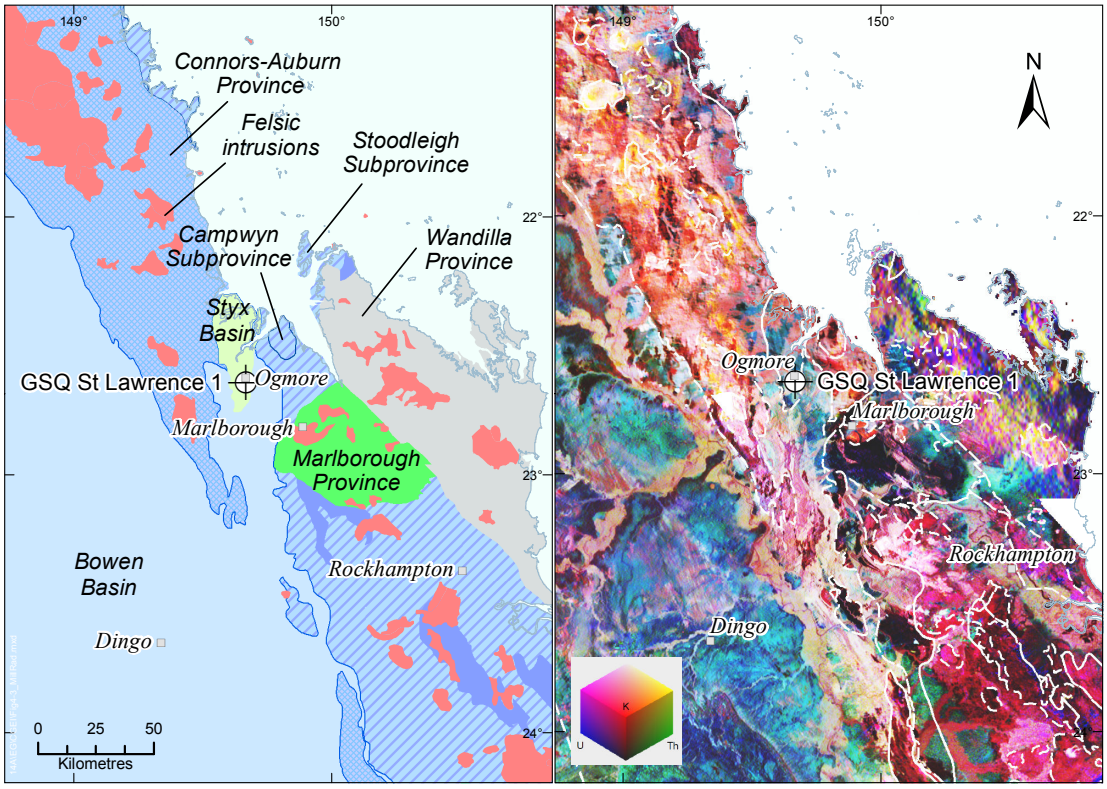

Figure 5-3. Radiometric ternary image of the Styx Basin region.

Target area

GSQ St Lawrence 1 was drilled in the southern end of the Styx Basin. Existing drilling and regional geology described by Withnall *et al.* (2009) was used to estimate the stratigraphy to 5 km depth (Table 5-1).

Table 5-1. Estimated stratigraphy to 5 km depth beneath GSQ St Lawrence 1, Styx Basin.

Borehole name	Depth interval (m)	Tectonic unit	Formation	Rock type	Weighted mean conductivity (W/mK)
GSQ St Lawrence 1	90–264[1]	Styx Basin	Styx Coal Measures[1]	Sandstone, mudstone, coal[1]	1.65 ± 0.03[1]
	264–310[1]		Styx Coal Measures[1]	Sandstone, mudstone, coal[1]	1.08 ± 0.03[1]
	310–1580[1,2]	Bowen Basin	Back Creek Group [1,2]	Mudstone[1,2]	1.73 ± 0.19[1]
	1580–3080[2]		Back Creek Group (Undiff.)[2]	Sandstone[2]	3.18 ± 1.26[3]
	3080–5000[4]	Connors–Auburn Province	Carmila beds[4]	Sandstone[4]	3.18 ± 1.26[3]

[1] GSQ St Lawrence 1 (Troup *et al.*, 2012)
[2] Malone (1970)
[3] Beardsmore & Cull (2001)
[4] Withnall *et al.* (2009)

GSQ St Lawrence 1 intersected 310 m of the Styx Coal Measures, comprising sandstone, mudstone and coal. This unit was underlain by the Back Creek Group.

The Back Creek Group underlying the Styx Basin comprises cleaved sandstone, mudstone, siltstone and minor limestone (Withnall *et al.*, 2009). The thickness of the Back Creek Group differs, ranging from 300 m to greater than 2000 m (Withnall *et al.*, 2009 and Malone, 1970, respectively). The Back Creek Group has been informally divided into lower sandstone and upper mudstone units as the basis for assigning bulk thermal conductivity values to this highly heterogeneous group (Table 5-1). Due to the structural complexity and stratigraphic repetition observed by Malone (1970) in Gogango Thrust Zone (Sliwa *et al.*, 2008), a thickness of 2770 m was estimated.

Basement to the Styx Basin in the vicinity of GSQ St Lawrence 1 includes the Back Creek Group and Carmila beds (Figure 5-4). The Carmila beds, which conformably underlie the Back Creek Group, have been described as siltstone, mudstone, volcanolithic sandstone and conglomerate, minor altered basalt and local rhyolitic to dacitic volcanic rocks (Withnall *et al.*, 2009). There is no estimate for the unit thickness, and as a result, in the vicinity of GSQ St Lawrence 1, the Carmila beds have been arbitrarily estimated to be present between 3080 and 5000 m.

Based on this stratigraphy, temperature estimation suggests the 150°C cut-off temperature occurs at 4235 m. However the Styx Basin has been classified as a low prospectivity region due to insufficient reservoir thickness and insignificant temperature difference between the cut-off temperature depth and 5000 m.

Stress regime

The structural characterisation of the Gogango Thrust Zone was used to estimate the orientation of existing fractures, which may influence reservoir stimulation in the Styx Basin area. Sliwa *et al.* (2008) identified moderate to tight upright folds and east over west thrust faults across the zone. Consequently,

the fractures within the Back Creek Group and Carmila beds are inferred to be shallow to horizontal and trending north–south, based on work by Anderson (1951).

The current stress regime is also compressional with an approximate northeast–southwest stress field, and is considered favourable for inducing shallow to horizontal fractures during hydro-fracturing stimulation (Figure 5-5).

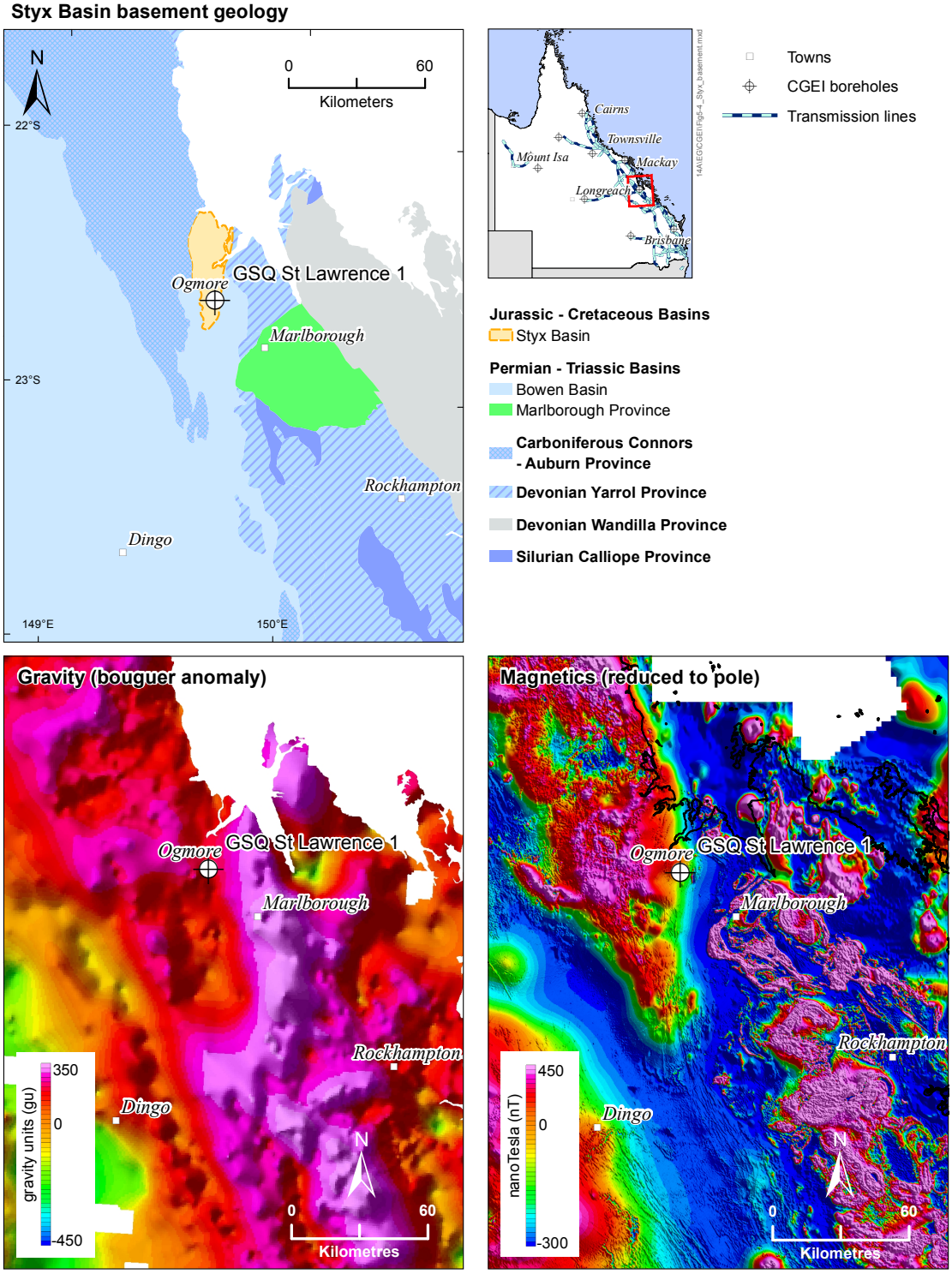

Figure 5-4. Basement geology and geophysics of the Styx Basin region.

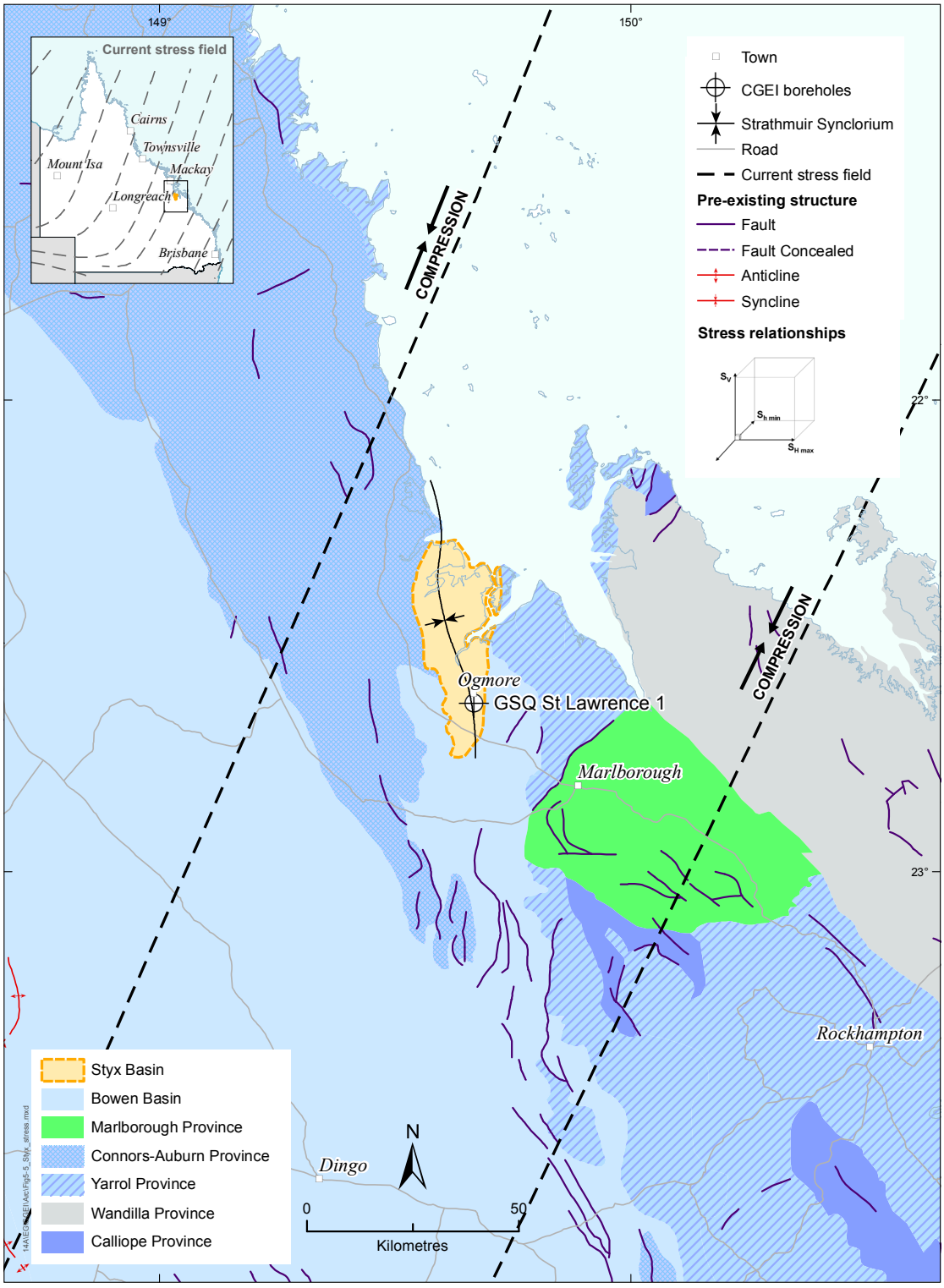

Figure 5-5. Stress regime around the Styx and Bowen basins (adapted from Clark & Leonard, 2003).

5.1.3 Summary

Heat flow	Insulation	Temp @5km	Stress regime	Prospectivity for EGS

Good
Average
Poor

5.2 Eromanga and Galilee basins

The targeted heat source for GSQ Longreach 2 is an inferred granite intruding basement under the Galilee Basin. The modelled heat flow is 60.0 ± 2.5 mW/m^2—approximately the mean crustal heat flow of the Australian continent—indicating the lack of a viable heat source. The depth to the 150°C cut-off temperature is 5407 m, further indicating the limited potential for EGS development, despite the good insulation provided by the Eromanga and Galilee basins.

5.2.1 Geological framework

In the vicinity of GSQ Longreach 2, basement comprises the Neoproterozoic–Ordovician **Thomson Orogen** (Figure 5-6)—an extensive, dominantly subsurface package of igneous and siliciclastic sedimentary rocks, with minor carbonate rocks. In central Queensland, basement cores that intersected the orogen contain low-grade metamorphosed interbedded quartz-rich sandstones and mudstones (Fergusson & Henderson, 2013). Widespread phases of igneous activity are also evident from both intrusive and extrusive units intersected in boreholes in the vicinity of GSQ Longreach 2 (Purdy & Brown, 2011).

The mid-Carboniferous to late Middle Triassic **Galilee Basin** occupies ~250 000 km^2 in central Queensland (Scott *et al.*, 1995; Fergusson & Henderson, 2013) and is almost entirely unconformably overlain by the Eromanga Basin. It connects with the Bowen Basin across the Springsure Shelf and Nebine Ridge, and lies adjacent to the Cooper Basin, separated by the Canaway Ridge (Hoffman, 1989). The Galilee Basin overlies the Drummond and Adavale basins, and in places directly overlies basement—the Thomson Orogen. Sedimentary sequences up to 3000 m were deposited in three primary depocentres: the Lovelle Depression in the northwest, the Koburra Trough in the northeast, and the Powell depression in the south (Bradshaw *et al.*, 2009). This geothermal assessment focusses on the area between the Koburra Trough and the Maneroo Platform (Figure 5-6). Basin development initiated in the late Carboniferous – early Permian, when crustal extension reactivated older faults in the underlying basins (Bradshaw *et al.*, 2009). A fluvial environment dominated initial deposition in the Koburra Trough, until fluvial and lacustrine sedimentation extended to other depocentres, along with volcaniclastics and tuffs produced during explosive volcanism. Towards the end of the Early Permian, east–west compression caused uplift and erosion across the basin. During the late Permian to Middle Triassic, thermal subsidence and foreland loading lead to the deposition of fluvio-deltaic, paralic, and paludal sequences (Hawkins & Green, 1993). Deposition of fluvial and lacustrine sediments continued until the Middle Triassic when east–west compression during the Hunter–Bowen Orogeny terminated sedimentation in the basin (Bradshaw *et al.*, 2009). The stratigraphy of the Galilee Basin in the Koburra Trough is summarised in Figure 5-7.

The **Eromanga Basin** covers more than 600 000 km^2 of Queensland (Figure 5-6) (Bradshaw *et al.*, 2009), overlying the Galilee and Cooper basins, and directly overlying basement—the Thomson Orogen —on the Maneroo Platform. Its structure and depositional history have been described in detail in Section 4.1.1, and the stratigraphy of the basin is shown in Figure 5-8.

5.2.2 Resource investigation

Potential heat source and insulation

GSQ Longreach 2 targeted a gravity low inferred to be a granitoid intruding basement under the Galilee Basin. This gravity low coincides with high fluoride anomalies, suggesting fluid interactions with granitic basement (Evans, 1996). There are known granitic intrusions across the northeastern Galilee Basin, but their heat producing capacity is poorly understood. Petroleum well data indicate elevated geothermal gradients and, across the extent of the Galilee Basin, there are a variety of possible sources of heat production. The water bore Coreena-23 (Radke *et al.*, 2000), close to GSQ Longreach 2, has an elevated geothermal gradient of approximately 60°C/km (Figure 5-9).

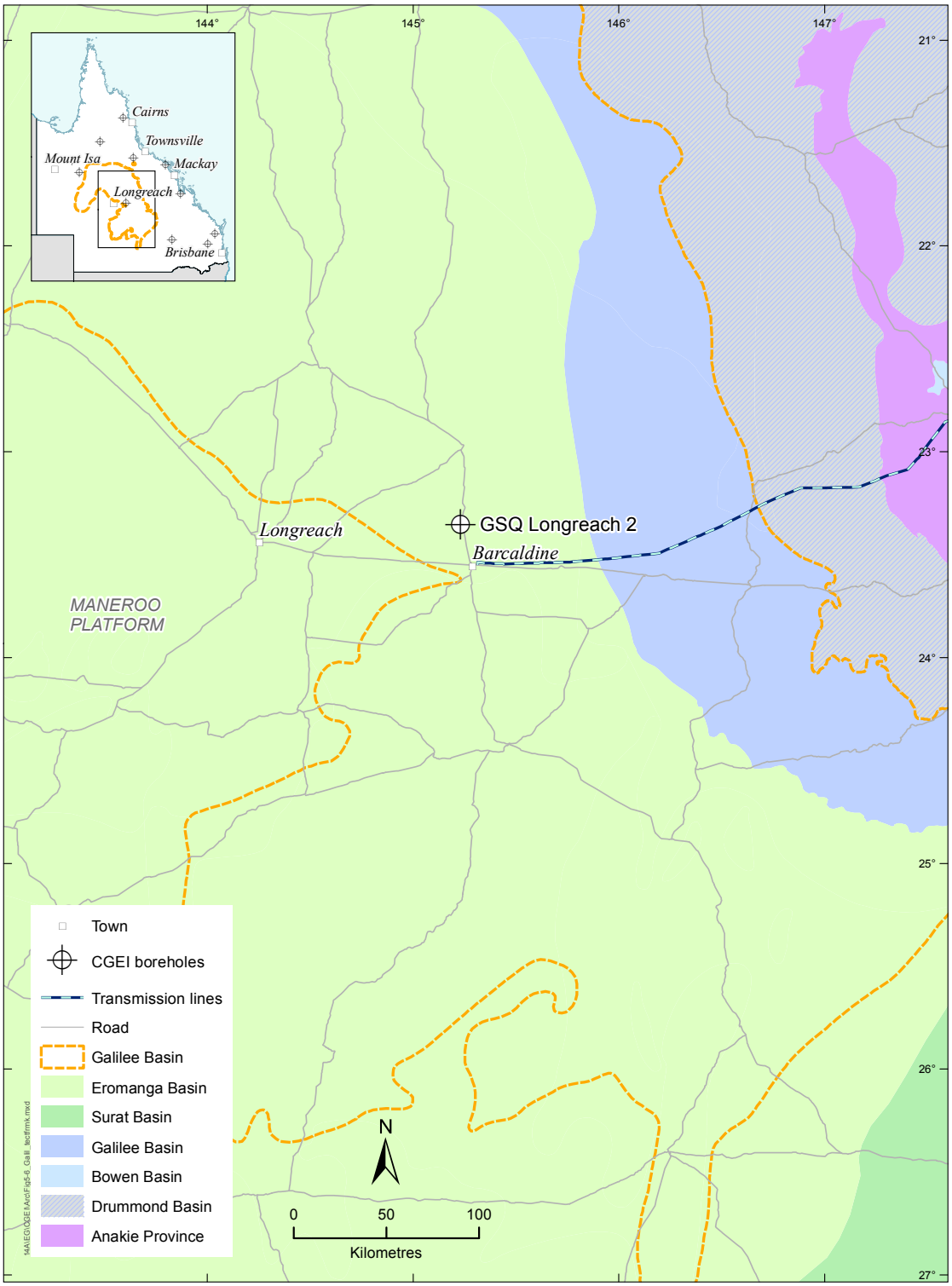

Figure 5-6. Tectonic framework of the Galilee Basin region.

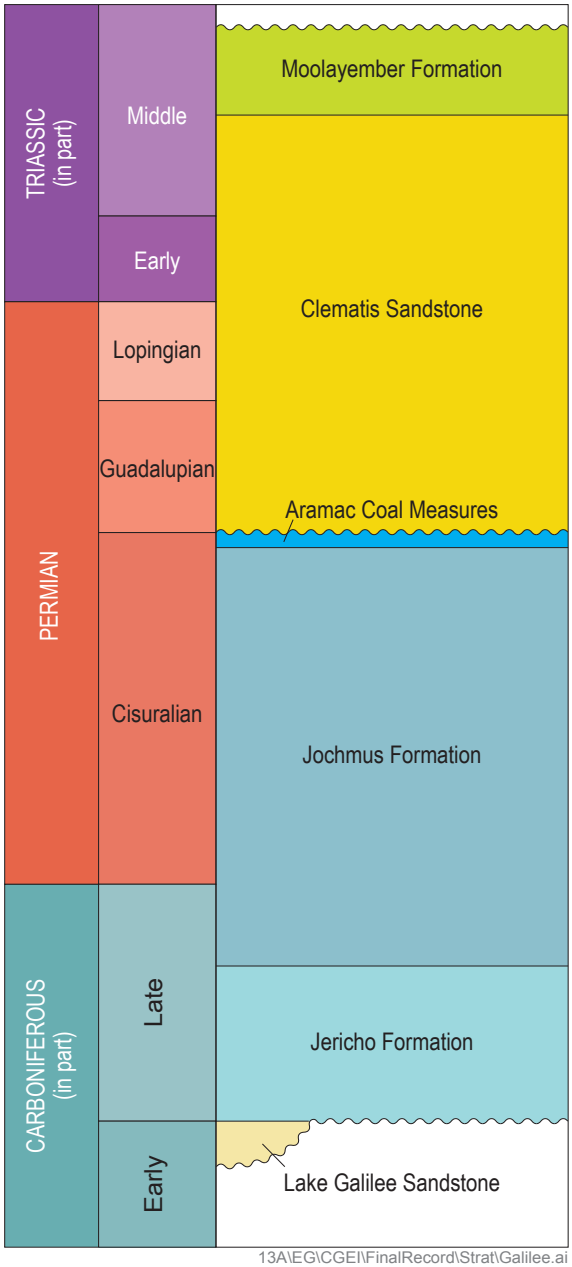

Figure 5-7. Stratigraphy of the Galilee Basin (adapted from Bradshaw et al., 2009; Fergusson & Henderson, 2013).

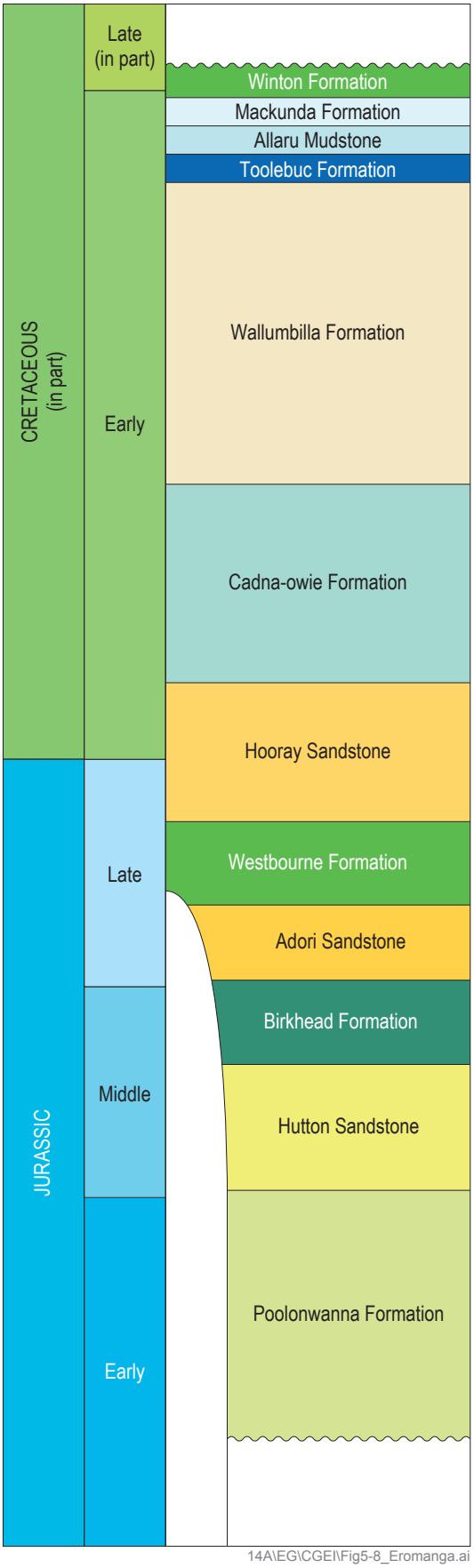

Figure 5-8. Stratigraphy of the Eromanga Basin (adapted from Bradshaw et al., 2009; Fergusson & Henderson, 2013).

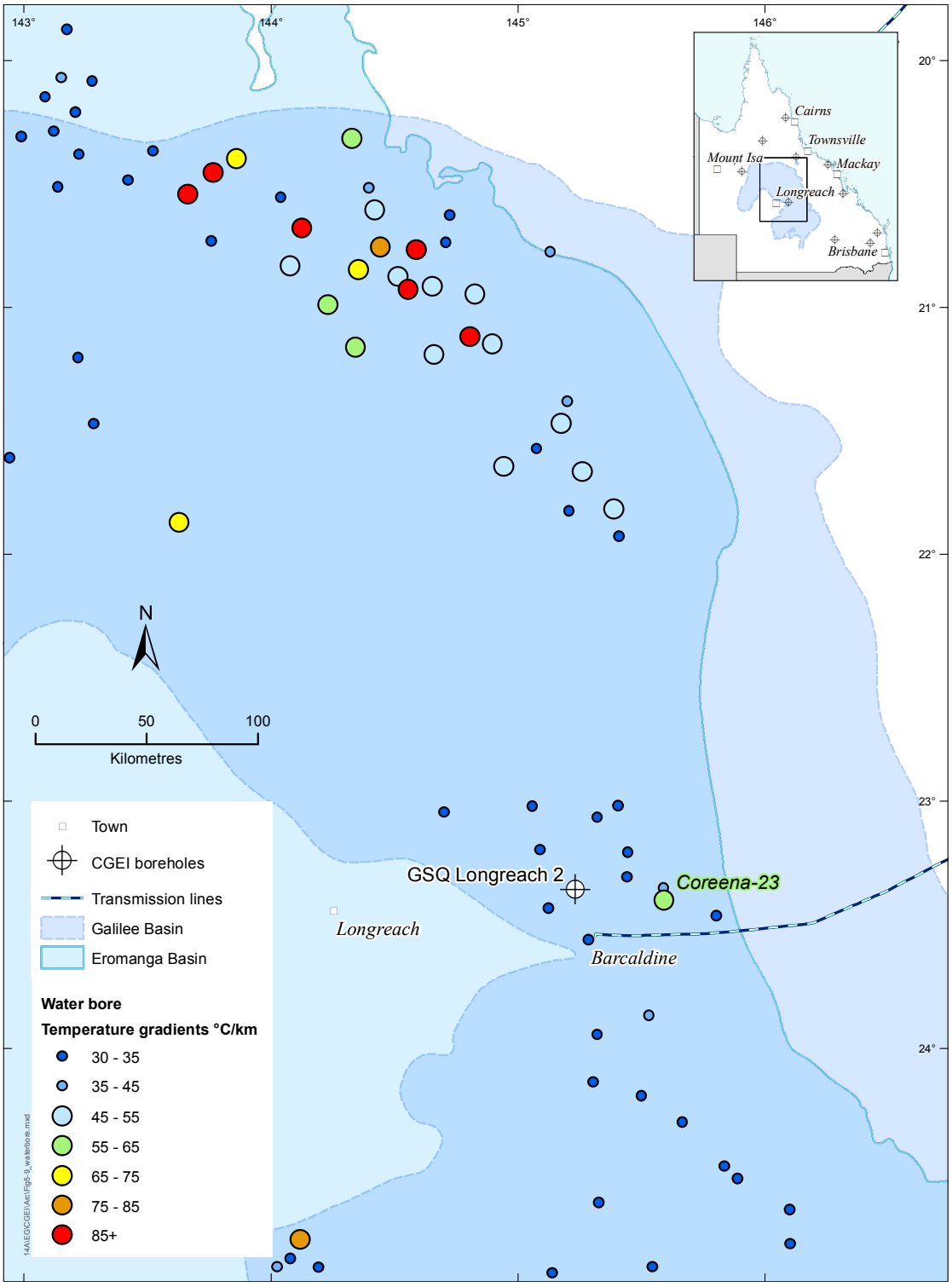

Figure 5-9. Water bore temperatures in the vicinity of GSQ Longreach 2.

For GSQ Longreach 2, a heat flow of 60.0 ± 2.5 mW/m^2 was modelled—comparable to the average crustal value, suggesting there is no anomalous heat in the area. All water bores within 150 km of the drill site have gradients of less than 45°C/km. However, the temperature data from water bores indicate that the geothermal energy potential may increase significantly towards the northeastern region of the Galilee Basin (Figure 5-9).

The Eromanga Basin strata intersected in GSQ Longreach 2 had thermal conductivity values between 1.13 and 2.57 W/mK, and are considered as having good insulating properties.

Target area

The resource area is approximated by the gravity low attributed to an inferred granitoid in basement. Basement depths and rock types vary greatly in the vicinity of the Maneroo Platform, introducing uncertainty in estimating stratigraphy to 5 km.

Data from surrounding petroleum wells were compiled to map basement rock types. The wells, PPL Glenaras 1, BEA Coreena 1 and LOL Saltern Creek 1, were used to approximate the stratigraphy and rock types to 5 km below GSQ Longreach 2 (Table 5-2).

Table 5-2. Estimated stratigraphy to 5 km depth beneath GSQ Longreach 2, Galilee Basin.

Borehole name	Depth interval (m)	Tectonic unit	Formation	Rock type	Thermal conductivity (W/mK)
GSQ Longreach 2	83–292[1]	Eromanga Basin	Allaru Mudstone, Toolebuc Formation, Wallumbilla Formation[1]	Mudstone, sandstone[1]	1.37 ± 0.06[1]
	292–312[1]		Hooray Sandstone[1]	Sandstone, mudstone[1]	2.02 ± 0.11[1]
	312–340[1,2]		Westbourne Formation[1,2]	Mudstone, sandstone[1,2]	1.94 ± 0.15[1]
	340–512[3]		Adori Sandstone, Birkhead Formation, Hutton Sandstone[3],	Sandstone[3]	3.18 ± 1.26[4]
	512–690[6]	Galilee Basin	Bandanna Formation, Colinlea Sandstone[6]	Sandstone[3]	3.18 ± 1.26[4]
	690–865[3]		Aramac Coal Measures[6]	Siltstone[3]	2.82 ± 0.68[4]
	865–1307[3]		Jochmus Formation[6]	Sandstone[3]	3.18 ± 1.26[4]
	1307–1407[3]		Jericho Formation[6]	Siltstone[3]	2.82 ± 0.68[4]
	1407–3000[2,5,6,7]	Thomson Orogen	Thomson Orogen (undiff.) [2,5,6,7]	Metasediments[2,5,7]	3.18 ± 1.26[4]
	3000–5000[8]		Interpreted intrusive[8]	Granitoid (intermediate)[8]	3.23 ± 0.73[4]

[1] GSQ Longreach 2 (Brown et *al.*, 2012a)
[2] LOL Marchmont 1 (Longreach Oil, 1990)
[3] Bradshaw *et al.* (2009)
[4] Beardsmore & Cull (2001)
[5] AGL Glenaras 1 (McDonagh, 1967)
[6] BEA Coreena 1 (Leslie Warren, 1970)
[7] LOL Saltern Creek 1 (Longreach Oil, 1964)
[8] GSQ gravity modelling

The Eromanga Basin succession, predominantly comprised of sandstone, siltstone and mudstone, is predicted to extend to 512 m depth, estimated from GSQ Longreach 2 and LOL Marchmont 1.

The Galilee Basin predominantly comprises sandstone and siltstone with minor coal (Bradshaw *et al.*, 2009), and is likely to be present between 512 to 1407 m based on Leslie Warren (1970).

In the vicinity of GSQ Longreach 2, metasediments attributed to the undifferentiated Thomson Orogen are postulated to constitute basement (Figure 5-10). Based on stratigraphic correlation with the adjacent petroleum wells (PPL Glenaras 1, BEA Coreena 1 and LOL Saltern Creek 1), and the location of the Longreach basement high, it is anticipated that basement under GSQ Longreach 2 would be intersected at approximately 1407 m depth. There is a high degree of difference in basement composition intersected in the petroleum wells adjacent to GSQ Longreach 2. Rock types intersected have been categorised as felsic volcanics, felsic intrusives, and metasedimentary sequences.

The gravity response suggests an intermediate intrusive unit may be present from 3000–5000 m.

On the basis of this stratigraphy, the 150°C cut-off temperature is intersected at a depth of 5407 m, indicating limited potential for geothermal energy development.

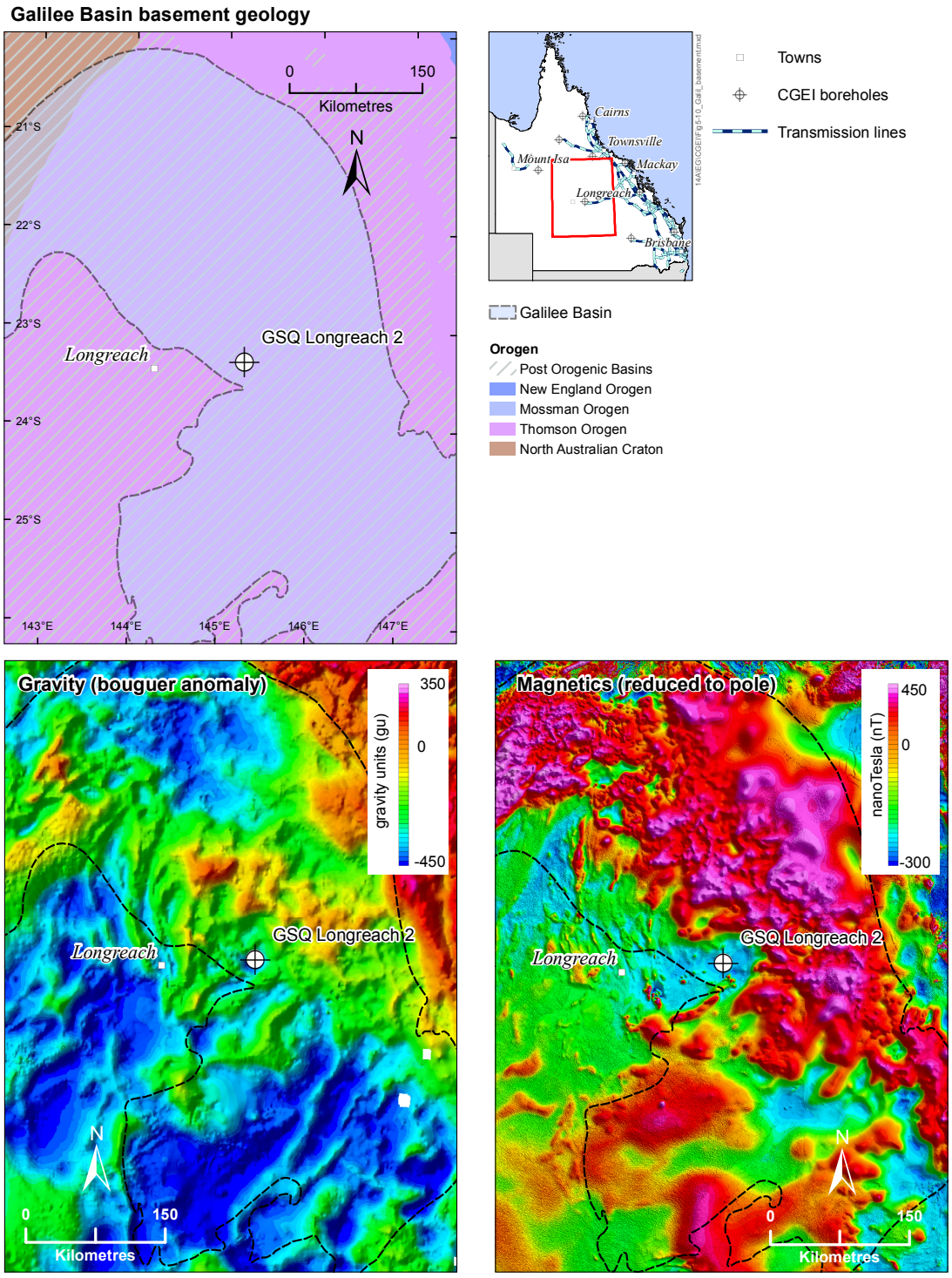

Figure 5-10. Basement geology and geophysics of the Galilee Basin region.

Stress regime

Due to the variety of basement rock types, and the limited data on structure available, it is futile to estimate the crustal framework that exists in the vicinity of GSQ Longreach 2.

Currently, a northeast–southwest compressional stress regime is dominant in this region, which is anticipated to be optimal for generating fracture growth in a shallow to horizontal direction (Figure 5-11). However, limited understanding of the orientation of the existing basement structures may inhibit efficient reservoir stimulation at the prospect scale.

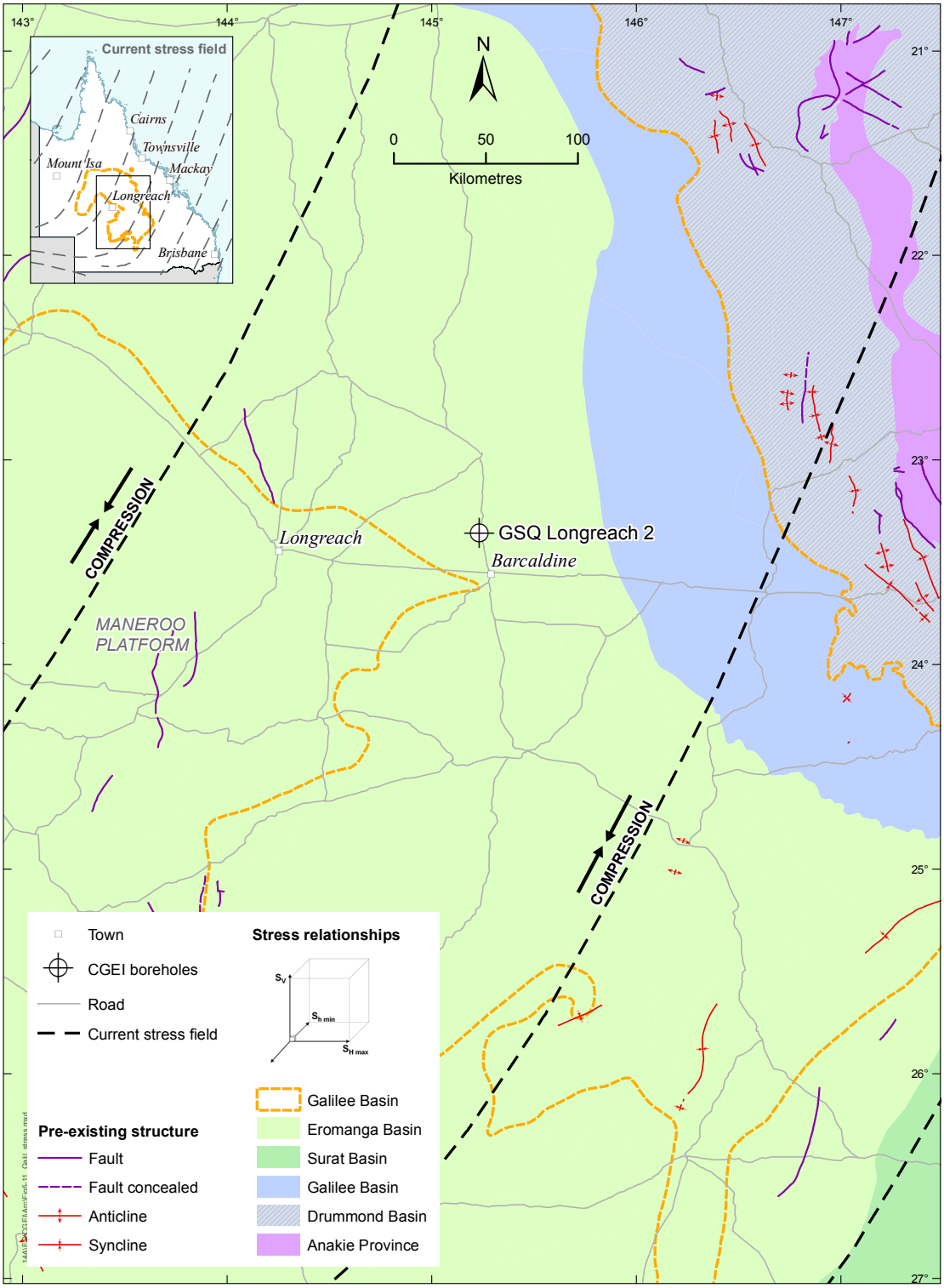

Figure 5-11. Stress regime around the Eromanga and Galilee basins (adapted from Clark & Leonard, 2003).

5.2.3 Summary

Heat flow	Insulation	Temp @5km	Stress regime	Prospectivity for EGS

Good
Average
Poor

5.3 Hodgkinson Province

GSQ Mossman 2-3R was drilled in the Hodgkinson Province targeting the Whypalla Supersuite. The intrusives of the supersuite have high heat production, which contributed to the slightly elevated heat flow modelled for the site (77.0 ± 0.9 mW/m^2). However, the metasediments of the Hodgkinson Formation have high thermal conductivity, thus high temperatures are unlikely to be retained at depth. The 150°C isotherm is predicted at 5462 m, limiting the potential for EGS development.

5.3.1 Geological framework

The **Hodgkinson Province** is a major constituent of the Mossman Orogen and forms the most northern expression of the Tasmanides (Glen, 2005). The 2007 deep crustal seismic survey line 07GA-A01 shows the Hodgkinson Province overlies a significant section of continental crust comprising the Greenvale Seismic Province (a presumed Thomson Orogen correlative), over the Agwamin Seismic Province (Korsch *et al.*, 2011), as well as segments of the Etheridge Province and basal Abingdon Seismic Province (Figure 5-12).

The Hodgkinson Province consists of two formations: the Silurian–Devonian limestone rich Chillagoe Formation in the west, overlain by the more regionally extensive Hodgkinson Formation further to the east. The Hodgkinson Formation is dominated by mainly steeply dipping sequences of variably metamorphosed sandstone, siltstone and mudstone.

The Hodgkinson Formation has been intruded by voluminous granitic rocks of the **Whypalla Supersuite**, attributed to the Carboniferous–Permian Kennedy Igneous Association (Henderson *et al.*, 2013). Granites of this supersuite are dated between 265 and 285 Ma (mid-Permian) and are considered highly fractionated S-type granites (Champion & Bultitude, 2013). Calculated heat production values range from 3.5 to 5 μW/m^3, indicating moderate to high concentrations of radioactive U, Th and K (Geological Survey of Queensland, unpublished data). These granites are interpreted as the conceptual heat source for GSQ Mossman 2-3R.

5.3.2 Resource investigation

Potential heat source and insulation

The targeted heat source is the Whypalla Supersuite, which outcrops in the vicinity of GSQ Mossman 2-3R. The associated intrusions have high heat production (3.5–5 μW/m^3), and the ternary radiometric image also highlights the high concentrations of radioactive elements in these intrusions (Figure 5-13).

Mulligan *et al.* (2003) highlighted a general thinning of the crust towards Queensland's northeastern margin, supported by further work by Fishwick *et al.* (2008), Farrington *et al.* (2010), and Kennett *et al.* (2011). Underneath the Hodgkinson Province, the Moho is at 30–35 km depth, similar to that under the Cooper and Otway basins' geothermal fields (Figure 5-14). Whilst the geothermal potential of the Cooper Basin has been attributed to high heat-producing granites underlying thick sedimentary sequences, a mantle source has also been postulated as a contributing factor to elevated temperatures at depth (Huddlestone-Holmes & Gerner, 2012). Consequently, a mantle component may also be a potential heat source contributing to the high heat flow (77.0 ± 0.3 mW/m^2) modelled in the Hodgkinson Province (Brown *et al.*, 2012b), but further investigation is required to quantify this contribution.

The insulation capacity of the Hodgkinson Formation is estimated from thermal conductivity analysis from GSQ Mossman 3R (Brown *et al.*, 2012b). Thermal conductivity values representing siliceous to lithic sublabile metasedimentary sequences intersected in GSQ Mossman 2-3R were between 3.5 and 4.5 W/mK, probably owing to the high degree of alteration of the rocks. These values indicate poor to moderate insulation of any potential heat sources.

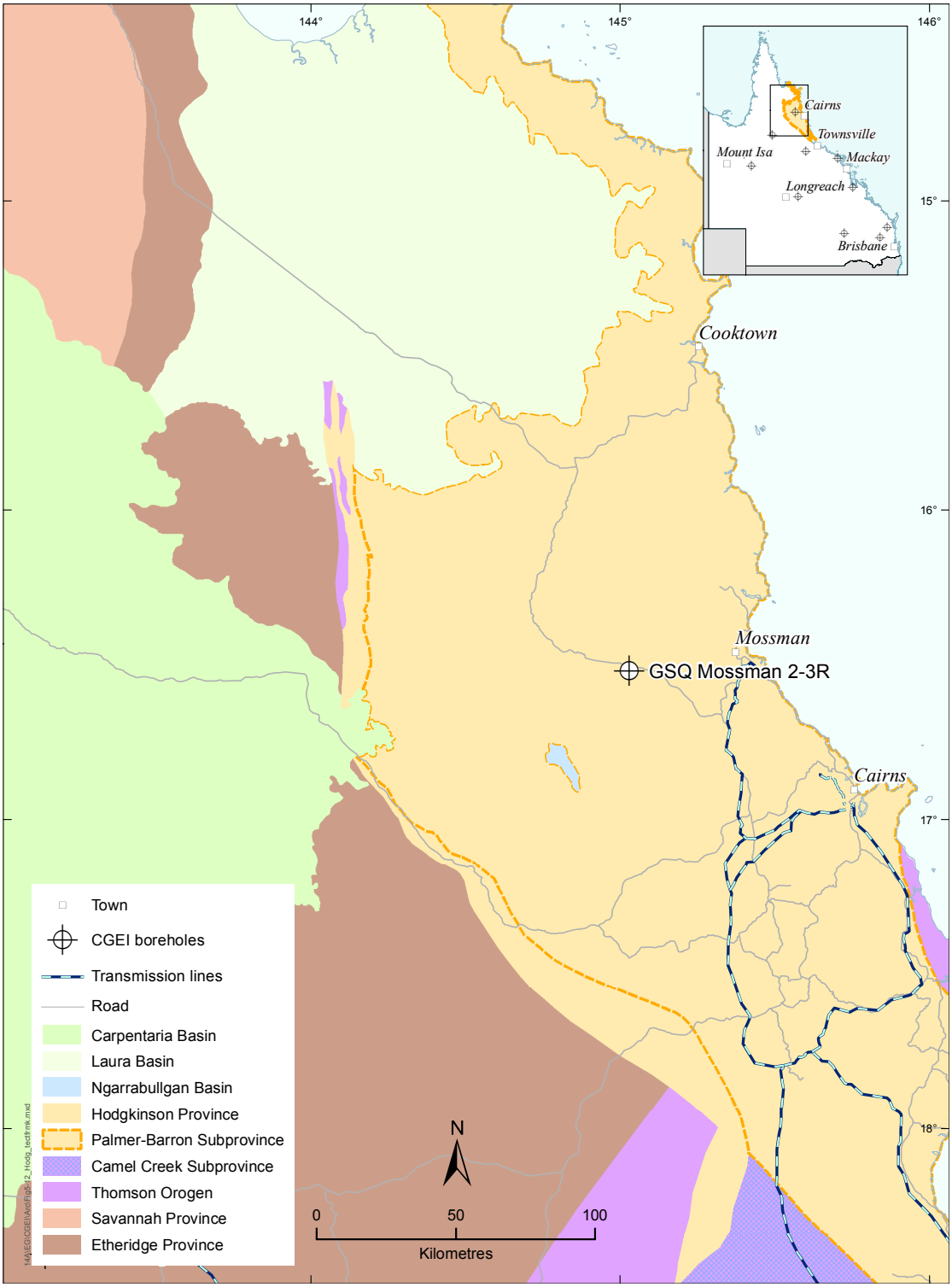

Figure 5-12. Tectonic framework of the Hodgkinson Province region.

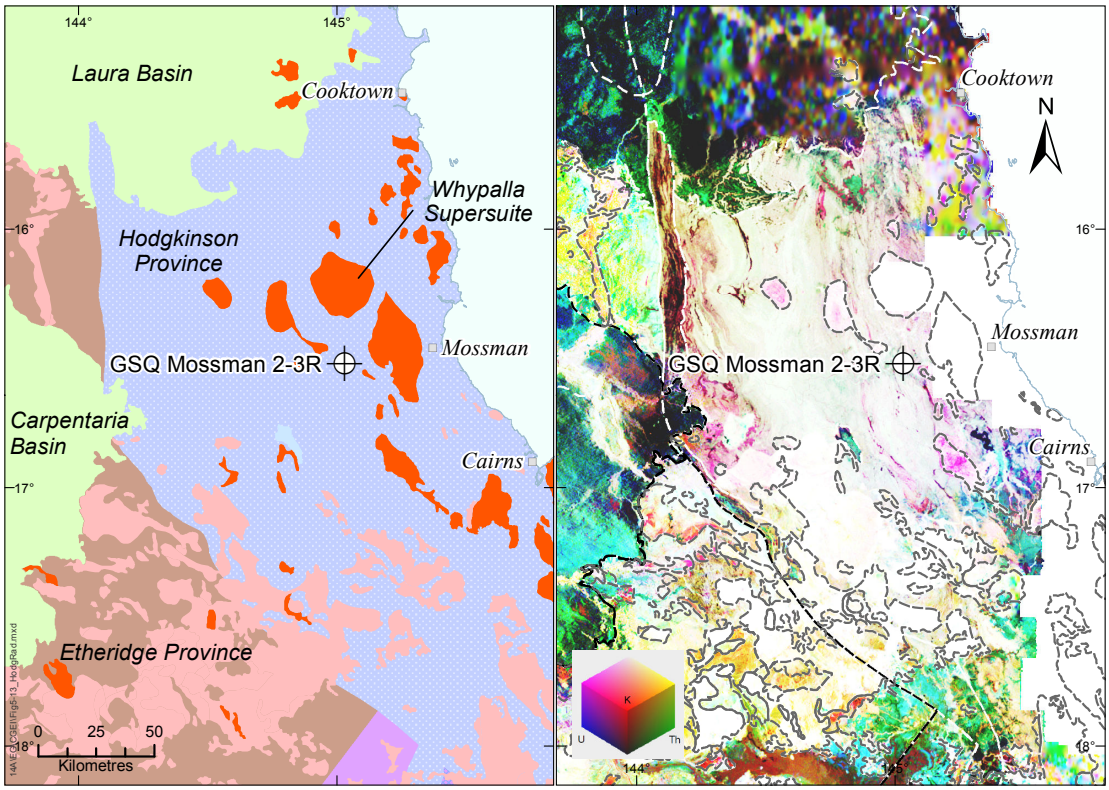

Figure 5-13. Radiometric ternary image of the Hodgkinson Province region.

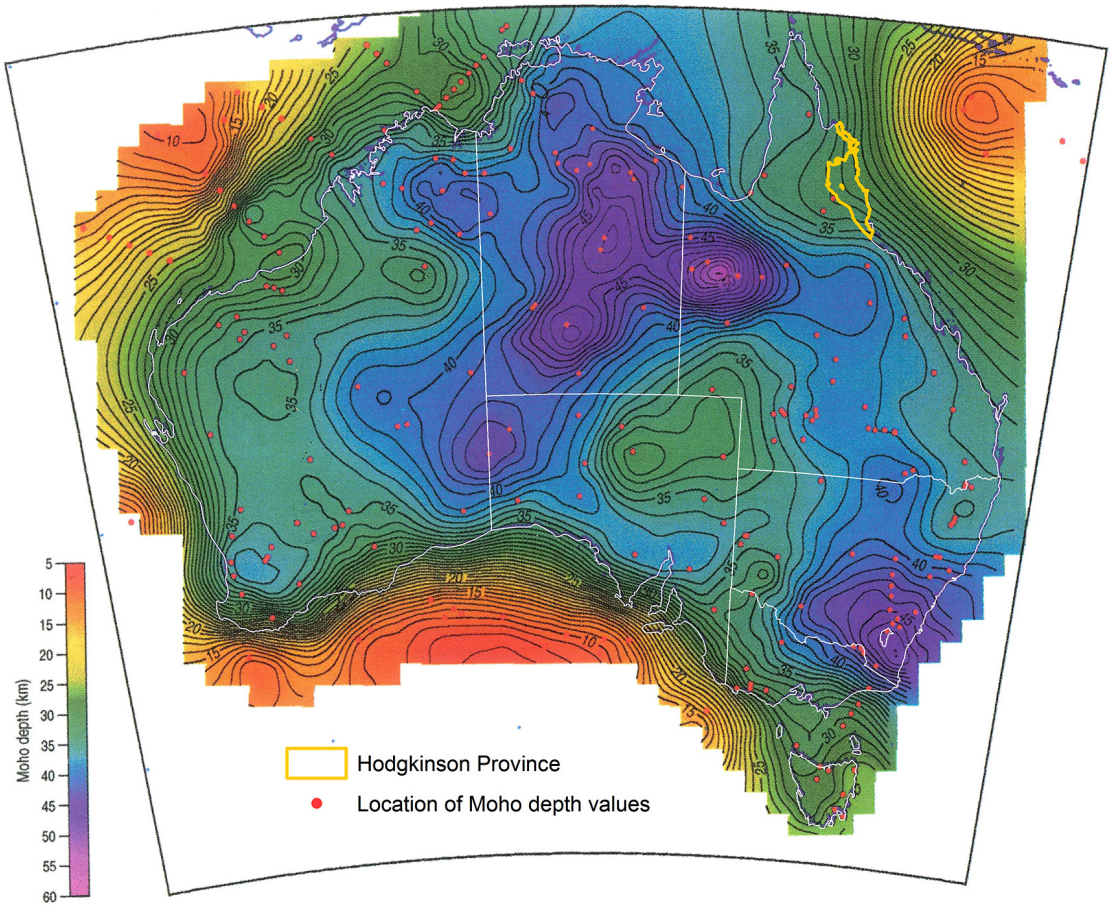

Figure 5-14. Crustal thickness of the Australian Continent (Mulligan et al., 2003).

Target area

GSQ Mossman 2-3R was drilled into the Hodgkinson Formation. In order to estimate temperatures at 5 km depth, regional geological information from Korsch *et al.* (2012), Henderson *et al.* (2013) and Amos & De Keyser (1964) was used to predict stratigraphy and rock types below the depth penetrated by GSQ Mossman 2-3R (Table 5-3).

Table 5-3. Estimated stratigraphy to 5 km depth beneath GSQ Mossman 2-3R, Hodgkinson Province.

Borehole name	Depth interval (m)	Tectonic unit	Formation	Rock type	Thermal conductivity (W/mK)
GSQ Mossman 2-3R	62–103[1]	Hodgkinson Province	Hodgkinson Formation[1,2]	Sandstone, siltstone[1]	4.54 ± 0.15[1]
	103–189[1]			Sandstone, siltstone[1]	3.79 ± 0.06[1]
	189–265[1]			Sandstone, mudstone[1]	3.89 ± 0.07[1]
	265–5000[1,2]			Greywacke[3]	4.04 ± 0.05[4]

[1] GSQ Mossman 2-3R (Brown *et al.*, 2012b)
[2] Henderson *et al.* (2013)
[3] Amos & de Keyser(1964)
[4] Beardsmore & Cull (2001)

Under GSQ Mossman 2-3R, the Hodgkinson Formation is predicted to extend to at least 5 km depth (Bultitude *et al.*, 1993; Figure 5-15, Table 5-3) as repeating turbididic sequences (Henderson *et al.*, 2013). Consequently, the core intersected in GSQ Mossman 2-3R (Brown *et al.*, 2012b) was used to estimate the composition of the entire Hodgkinson Formation.

Temperature estimation based on this predicted stratigraphy suggests the cut-off temperature (150°C) would be intersected at a depth of 5462 m. This estimate indicates that the Hodgkinson Province is not prospective for the development of EGS.

Stress regime

Field observations of the Hodgkinson Formation (Brown *et al.*, 2012b) were used in conjunction with the structural evolution of the province to infer existing fractures, which may influence reservoir stimulation.

The Hodgkinson Province developed as a north–south-trending basin with structures generally trending north to northwest. Four generations of folding are evident across the province, including tight to isoclinal folds with north-northwest trending axial planes (Henderson *et al.*, 2013; Bain & Draper, 1997). Consequently in outcrop, the Hodgkinson Formation is a steeply dipping unit with prominent axial-plane, slaty cleavage, which has overprinted bedding.

Currently, the stress regime is compressional and orientated approximately northeast–southwest (Figure 5-16). This stress regime would facilitate the shallow to horizontal fracture networks considered optimal for reservoir stimulation. However, steeply dipping cleavage developed within the Hodgkinson Formation is likely to propagate fracture growth in the vertical direction during reservoir stimulation.

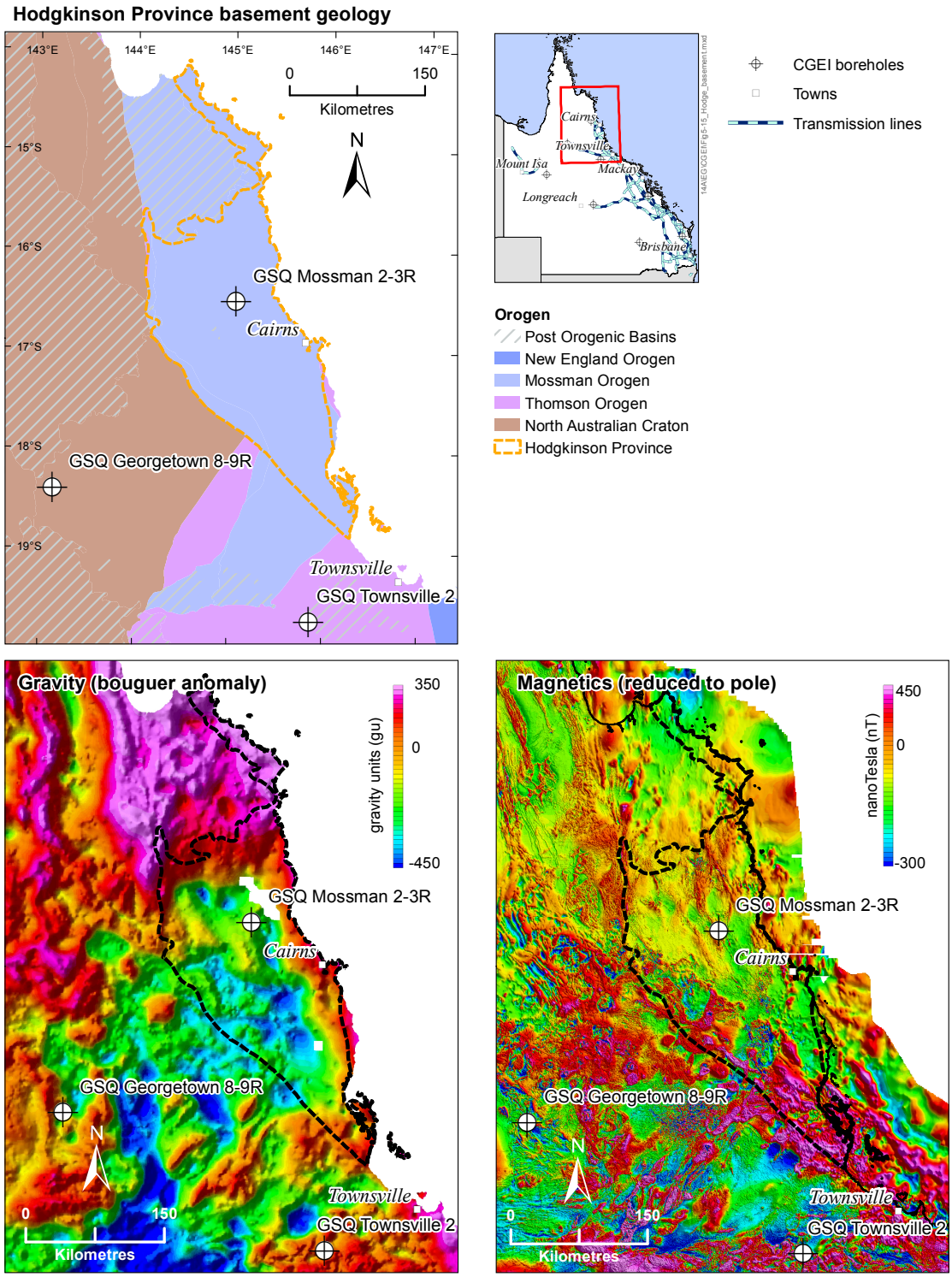

Figure 5-15. Basement geology and geophysics of the Hodgkinson Province region.

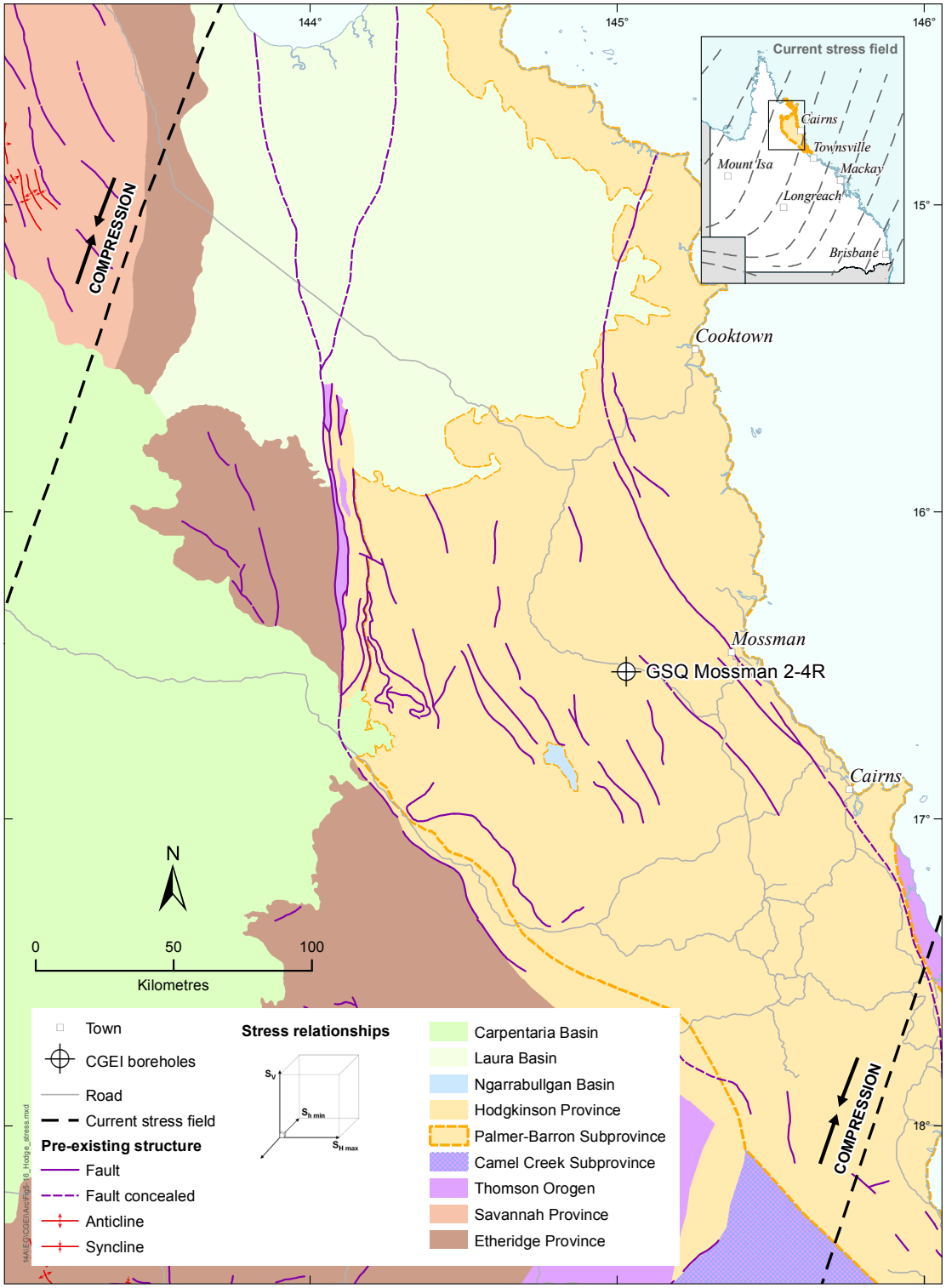

Figure 5-16. Stress regime around the Hodgkinson Province (adapted from Clark & Leonard, 2003)

5.3.3 Summary

Heat flow	Insulation	Temp @5km	Stress regime	Prospectivity for EGS

Good
Average
Poor

5.4 Etheridge Province

The targeted heat source for GSQ Georgetown 8-9R is an inferred intrusive body, potentially related to the nearby radioactive Forsayth Supersuite. The target area has experienced a long history of elevated thermal regimes through regional metamorphism, intrusive emplacement and Cenozoic volcanism. However, due to the high thermal conductivity of the metasediments of the Etheridge Province, high temperatures are unlikely at depth. Modelling produced an anomalously low heat flow of 48.5 ± 2.3 mW/m^2 and a predicted cut-off temperature (150°C) at 7574 m depth. This modelling indicates that this part of the Etheridge Province is not prospective for EGS development.

5.4.1 Geological framework

The **Etheridge Group** outcrops over approximately half of the Etheridge Province in the central and southern parts of the Proterozoic Georgetown inlier in northern Queensland (Figure 5-17). Withnall (1996) and Withnall *et al.* (1997) suggested that the Etheridge Group was deposited on a shelf or in an epicontinental sea. Metabasalts and metadolerite sills in the lower part of the Etheridge Group are geochemically similar to modern ocean-floor or island-arc tholeiites and, except for their low potassium, are also similar to some continental tholeiites. Withnall (1985) suggested that their emplacement could be related to extension of ductile late Paleoproterozoic crust, and the subsequent formation of an epicontinental sea in which the Etheridge Group was deposited. The Etheridge Group is multiply deformed with deformation complexity and metamorphic grade both increasing to the east. The regional metamorphic grades range from lower greenschist facies in the southwest to granulite in the northeast.

The Robertson River Subgroup of the lower Etheridge Group is estimated to be between 1000–2000 m thick and comprises the Daniel Creek Formation, Dead Horse metabasalts, Corbett Formation and the Lane Creek Formation. The overlying Townley Formation consists of 40–1500 m of light grey siltstone, mudstone and sandstone. The overlying Heliman Formation is comprised of sericitic siltstone and 'lithic-quartz' sandstone, with prominent beds of very dark-grey siliceous 'flinty' siltstone and quartzose sandstone (Withnall & Mackenzie, 1980). It is this flint that distinguishes the Heliman Formation from adjacent formations.

The Etheridge Group was intruded by a variety of Mesoproterozoic granitoids, including the Forsayth Supersuite. The supersuite comprises mostly grey, porphyritic, biotite–muscovite granites, and was emplaced through a northwest–southeast shortening and low pressure - high temperature metamorphism at 1560–1550 Ma (Withnall & Hutton, 2013).

5.4.2 Resource investigation

Potential heat source and insulation

The targeted heat source is an intrusive body, inferred from a gravity low beneath GSQ Georgetown 8-9R. Whilst there is no outcrop of the inferred heat source, the nearby units of the Forsayth Supersuite are mostly medium to high heat producing granites (Figure 5-18). However, gravity modelling suggests this intrusive unit to be intermediate in composition and ~2km thick, whereas the Forsayth Supersuite, which outcrops adjacent to GSQ Georgetown 8-9R, is felsic (Bain & Draper, 1997). Granites intruding the Etheridge Group were interpreted from seismic line 07-GA-IG2 at a depth of approximately 2 km (Korsch *et al.*, 2009). This intrusive coincides with a gravity low directly underlying GSQ Georgetown 8-9R (Figure 5-19). The low heat flow modelled for GSQ Georgetown 8-9R also suggests that any granites in the vicinity are unlikely to be high heat producing.

The formations intersected in GSQ Georgetown 8-9R have high thermal conductivity, prohibiting sufficient insulation of a viable geothermal resource. This low insulating capacity has been attributed to the high degree of metamorphism and siliceous alteration observed in core (Maxwell *et al.*, 2012).

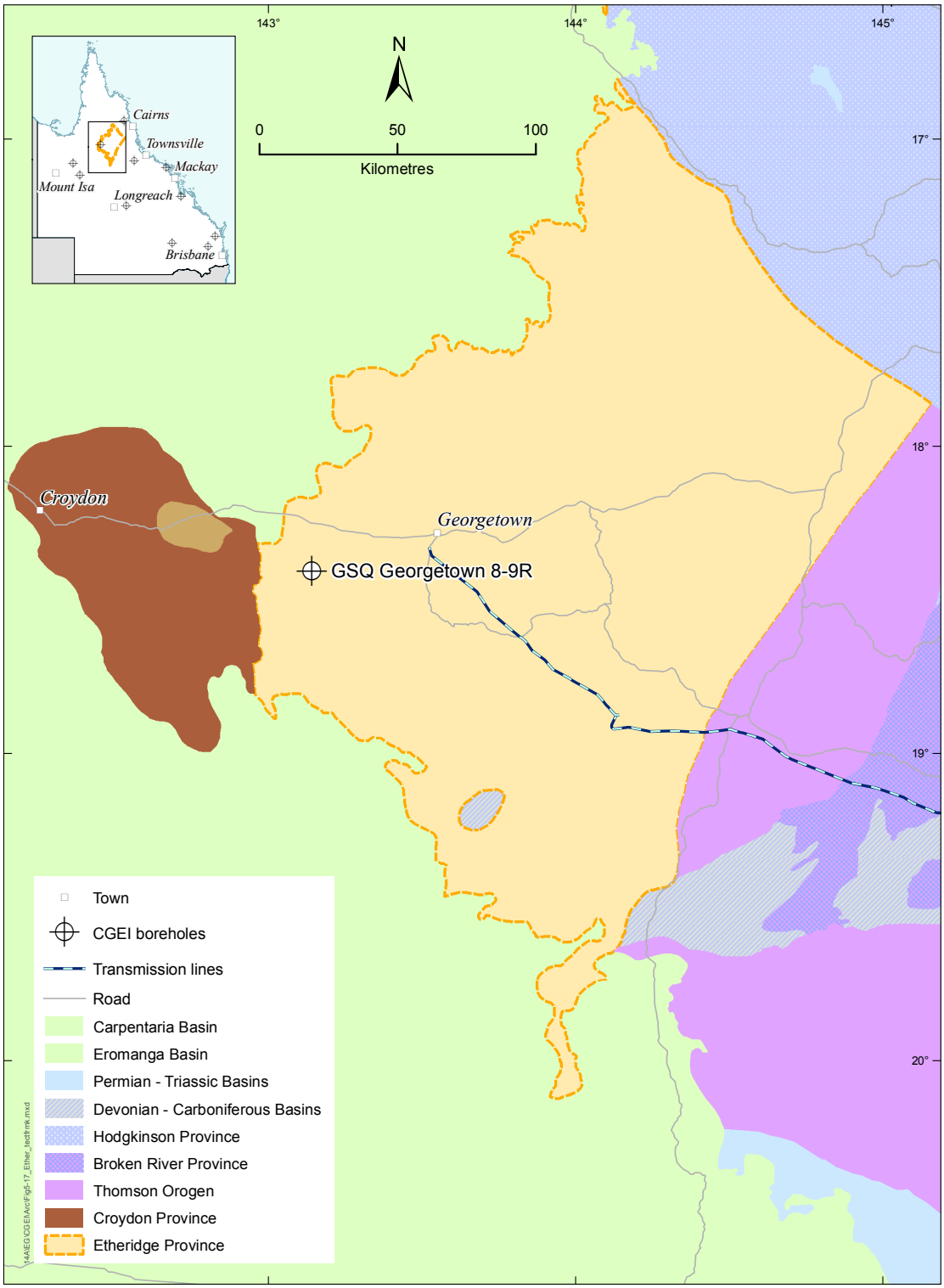

Figure 5-17. Tectonic framework of the Etheridge Province region.

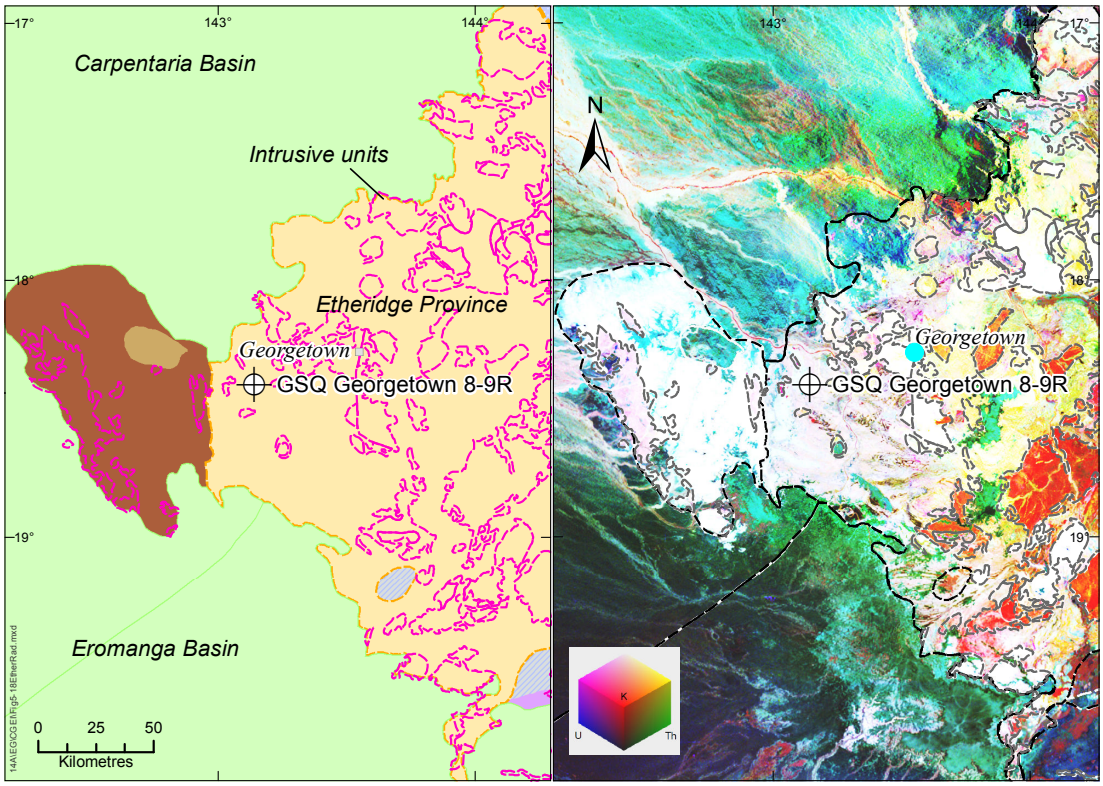

Figure 5-18. Radiometric ternary image of the Etheridge Province region.

Target area

GSQ Georgetown 8-9R was spudded into the Heliman Formation of the upper Etheridge Group, towards the western edge of the Georgetown inlier. Thickness estimations for the Etheridge Province are poorly constrained with much variation noted in the outcrop. Consequently, in order to estimate temperatures at 5 km, regional geology (Withnall & Hutton, 2013; Withnall & Mackenzie, 1980) and seismic interpretation (Korsch *et al*., 2012) were used to predict stratigraphy and rock types below the depth penetrated by GSQ Georgetown 8-9R (Table 5-4). Thermal conductivity values from GSQ Georgetown 8-9R were used to estimate the thermal properties for the entire Etheridge Province. A combined thickness of 1000 m was assigned to the Heliman and Townley formations. The Robertson River Subgroup is interpreted between 1000–2000 m. An intermediate intrusive is interpreted between 2000–4000 m, underlain by 1000 m of undifferentiated Robertson River Subgroup or Bernecker Creek Formation comprising metasediments (Withnall & McKenzie, 1980).

The cut-off temperature (150°C) is estimated at 7574 m depth. This demonstrates the limited potential of the Etheridge Province for EGS development.

Stress regime

The structural evolution of the Etheridge Province was used to infer existing fractures that may influence reservoir stimulation.

The Etheridge Province has a complex structural history resulting in lineaments and faults of various orientations (Withnall & Hutton, 2013; Withnall *et al*., 2009). Consequently, it is futile to infer existing structures at depth; however, steeply dipping structures cross-cutting steeply dipping strata is likely.

The current stress regime is dominated by maximum horizontal compression in a northeast–southwest direction; however complex basement structures are likely and could potentially direct reservoir growth towards the vertical plane, limiting reservoir stimulation (Figure 5-20).

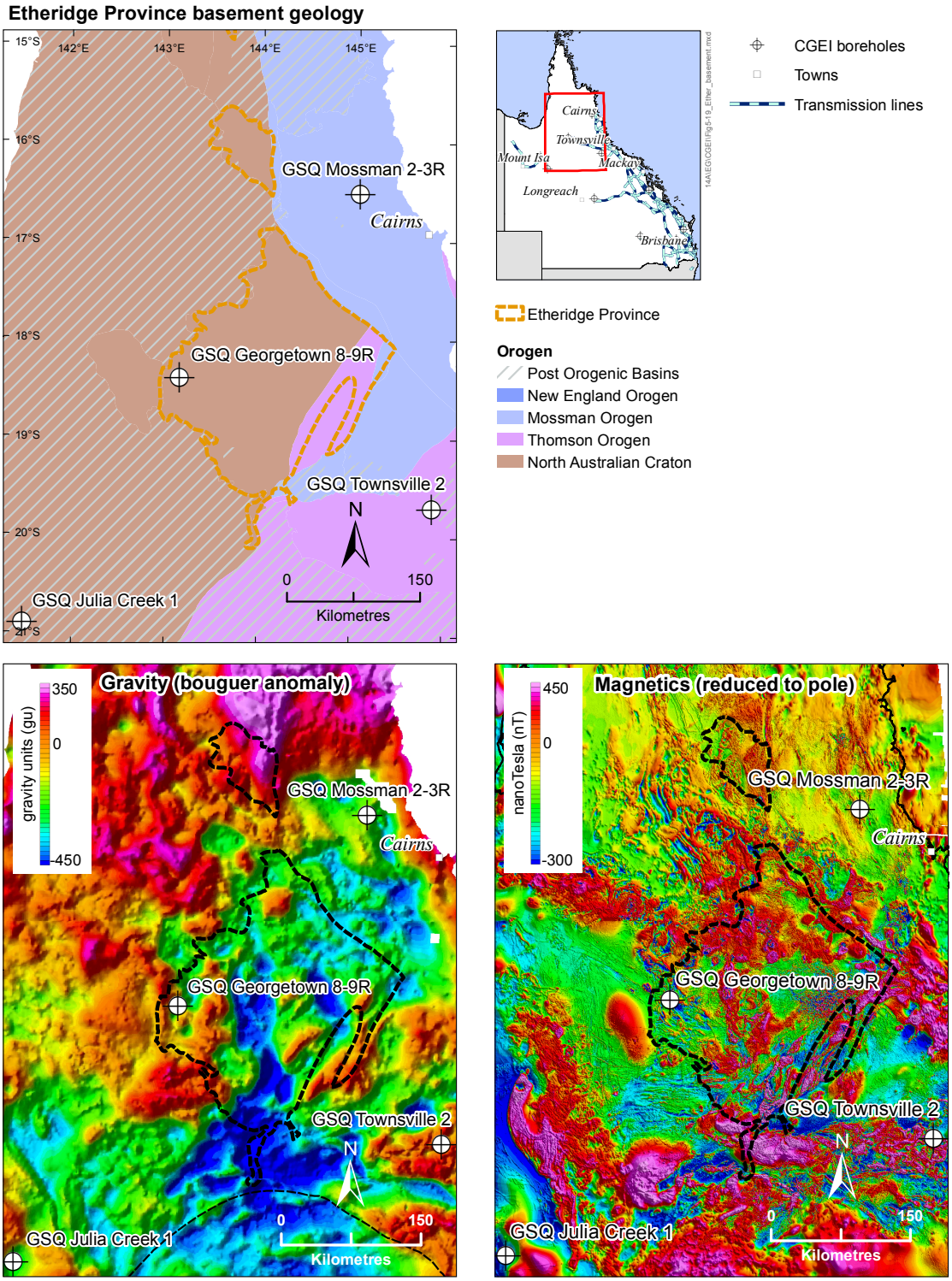

Figure 5-19. Basement geology and geophysics of the Etheridge Province region.

Table 5-4. Estimated stratigraphy to 5 km depth beneath GSQ Georgetown 8-9R, Etheridge Province.

Borehole name	Depth interval (m)	Tectonic unit	Formation	Rock type	Weighted mean conductivity (W/mK)
GSQ Georgetown 8-9R	43–97[1]	Etheridge Province	Heliman Formation[1]	Sandstone, mudstone, siltstone[1]	3.67 ± 0.17[1]
	97–154[1]			Sandstone, siltstone, mudstone[1]	2.33 ± 0.26[1]
	154–209[1]			Sandstone, siltstone[1]	4.07 ± 0.19[1]
	209–284[1]			Sandstone, siltstone, mudstone[1]	4.21 ± 0.58[1]
	284–320[1]			Sandstone, siltstone[1]	3.94 ± 0.12[1]
	320–600[2]			Metasediments[3]	3.70 ± 0.13[1]
	600–1000[2]		Heliman/Townley Formation[1,2]	Metasediments[3]	3.70 ± 0.13[1]
	1000–2000[5]		Robertson River Subgroup[2]	Metasediments[3]	3.70 ± 0.13[1]
	2000–4000[4]	Forsayth Batholith	Interpreted intrusive[4]	Granitoid[4]	3.23 ± 0.73[6]
	4000–5000[5]	Etheridge Province	Robertson River Subgroup or Bernecker Creek Formation[2]	Metasediments[3]	3.70 ± 0.13[1]

[1] GSQ Georgetown 8-9R (Maxwell *et al.*, 2012)
[2] Withnall & Mackenzie (1980)
[3] Withnall *et al.* (2002)
[4] GSQ gravity modelling
[5] Bain & Draper (1997)
[6] Beardsmore & Cull (2001)

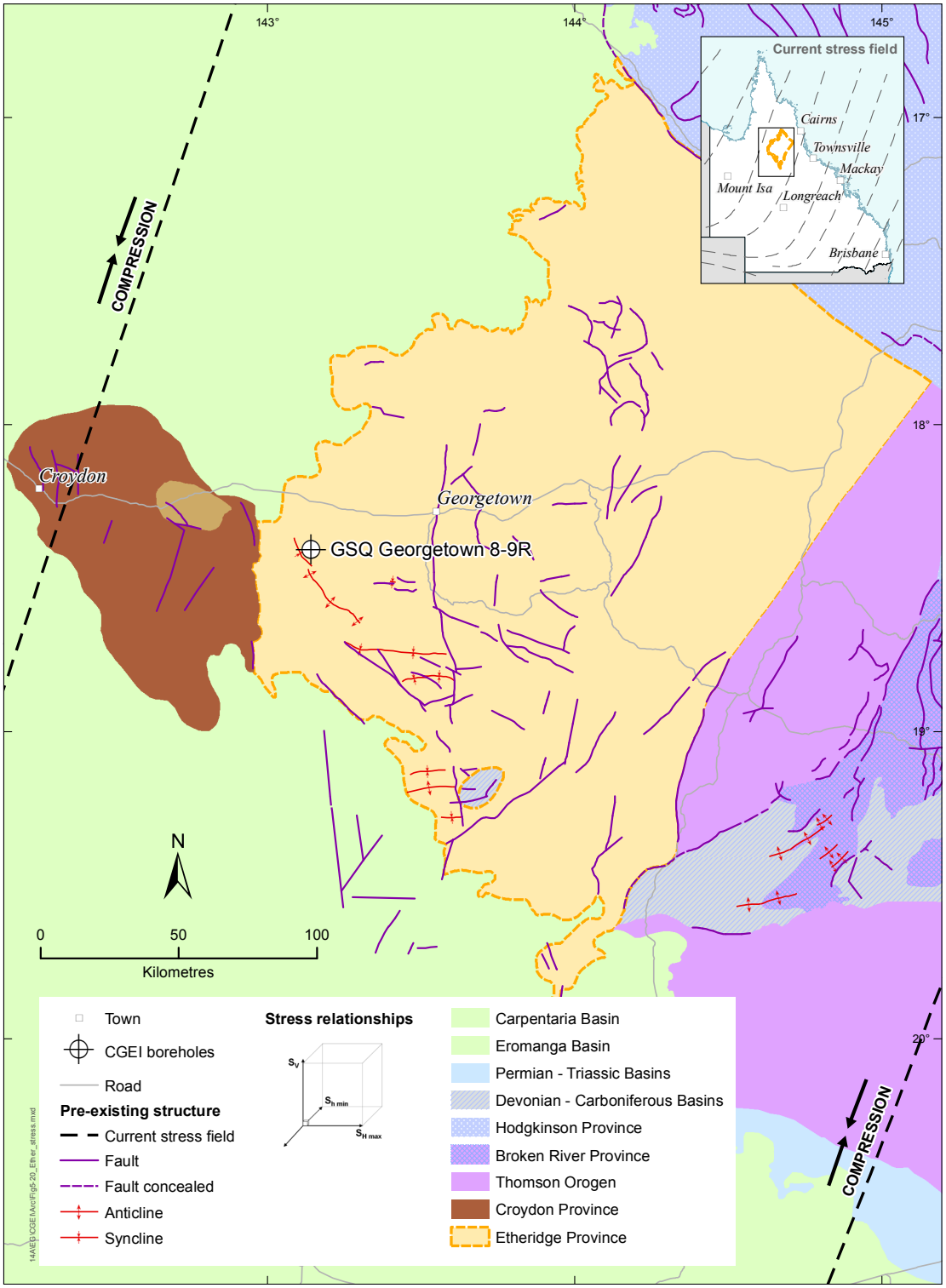

Figure 5-20. Stress regime around the Etheridge Province (adapted from Clark & Leonard, 2003).

5.4.3 Summary

Heat flow	Insulation	Temp @5km	Stress regime	Prospectivity for EGS

Good
Average
Poor

5.5 Tarong Basin

GSQ Gympie 7 was drilled in the Tarong Basin, targeting the underlying Boondooma Igneous Complex. The Tarong beds provide excellent insulation, and the moderate heat production value of the Boondooma Igneous Complex was identified to potentially provide a good heat source. However, modelling indicates the heat flow of GSQ Gympie 7 to be 37.5 ± 1.4 mW/m^2. This is anomalously low relative to the mean crustal heat flow of the Australian continent. The current heat flow may be masked by the coal sequence, as drilling did not intersect the entirety of the sequence. The cut-off temperature (150°C) is predicted to be intersected at 8063 m, limiting the Tarong Basin's prospectivity as an EGS target.

5.5.1 Geological framework

The Wandilla Province is a complex accretionary package represented in the study area by rocks of the Yarraman Subprovince (Figure 5-21) (Donchak *et al.*, 2013). In the Yarraman Subprovince, the rocks are dominated by the Devonian–Carboniferous **Maronghi Creek beds**. This unit comprises predominantly fine-grained sedimentary sequences and mafic sea floor lavas deposited in deep- to marginal-marine environments, before being accreted onto the eastern margin of the Australian Craton as a subduction complex (Cranfield *et al.*, 2001). The beds of this unit strike north–south, and dip steeply to the east and west. The unit outcrops extensively to the east of the Tarong Basin, and has been described in detail by Willey (1998), Cranfield (1999), Cranfield *et al.* (2001), and Tang (2003).

The Yarraman Subprovince is extensively intruded by Permian–Triassic granitoids and mafic intrusions, including the **Boondooma Igneous Complex** (Donchak *et al.*, 2013), the emplacement of which was partly controlled by old crustal weaknesses (Cranfield *et al.*, 2001). The complex comprises felsic to intermediate plutons, which outcrop to the west of the Tarong Basin, and has been subjected to deep weathering.

The Late Triassic **Tarong Basin** is a small, narrow, intermontane basin in southeast Queensland (Figure 5-21). The basin is north-northwest–south-southeast trending (Bradshaw *et al.*, 2009; Cranfield *et al.*, 2001), and unconformably overlies the Yarraman Subprovince. The basin contains a single unit, the Tarong beds, comprising a sequence of sandstone, siltstone, mudstone and coal (Figure 5-22). Whilst no drilling has intersected the entire basin, Pegrem (1995) estimated a preserved thickness of 450 m. Three alluvial fans have been identified in the north, south, and centre of the basin, with coal accumulations in the areas between. The beds are partially faulted by predominantly right-lateral strike-slip faults, likely related to the reactivation of basement structures (Bradshaw *et al.*, 2009). The basin is thought to have developed as a result of dextral transtension, with the Tarong beds deposited in an alluvial valley setting (Garces & Flood, 1984). The Tarong Basin is overlain by Cenozoic sediments and volcanics.

5.5.2 Resource investigation

Potential heat source and insulation

The targeted heat source in the Tarong Basin region is the Boondooma Igneous Complex, which outcrops to the west (Figure 5-23). Radiometric ternary imaging shows moderate to high concentrations of U, Th and K in these rocks (Figure 5-24), and heat production values derived from whole rock geochemical analysis are between 0.33 and 3.90 μW/m^3. However, the anomalously low heat flow modelled for GSQ Gympie 7 suggests that although these intrusions were identified in outcrop as potential sources of heat, they are insufficient to elevate the heat flow of the basin.

The thermal conductivity of the Tarong beds is variable, but the thick coal seams with low thermal conductivity (approximately 0.24 W/mK) suggest a reasonable insulation capacity.

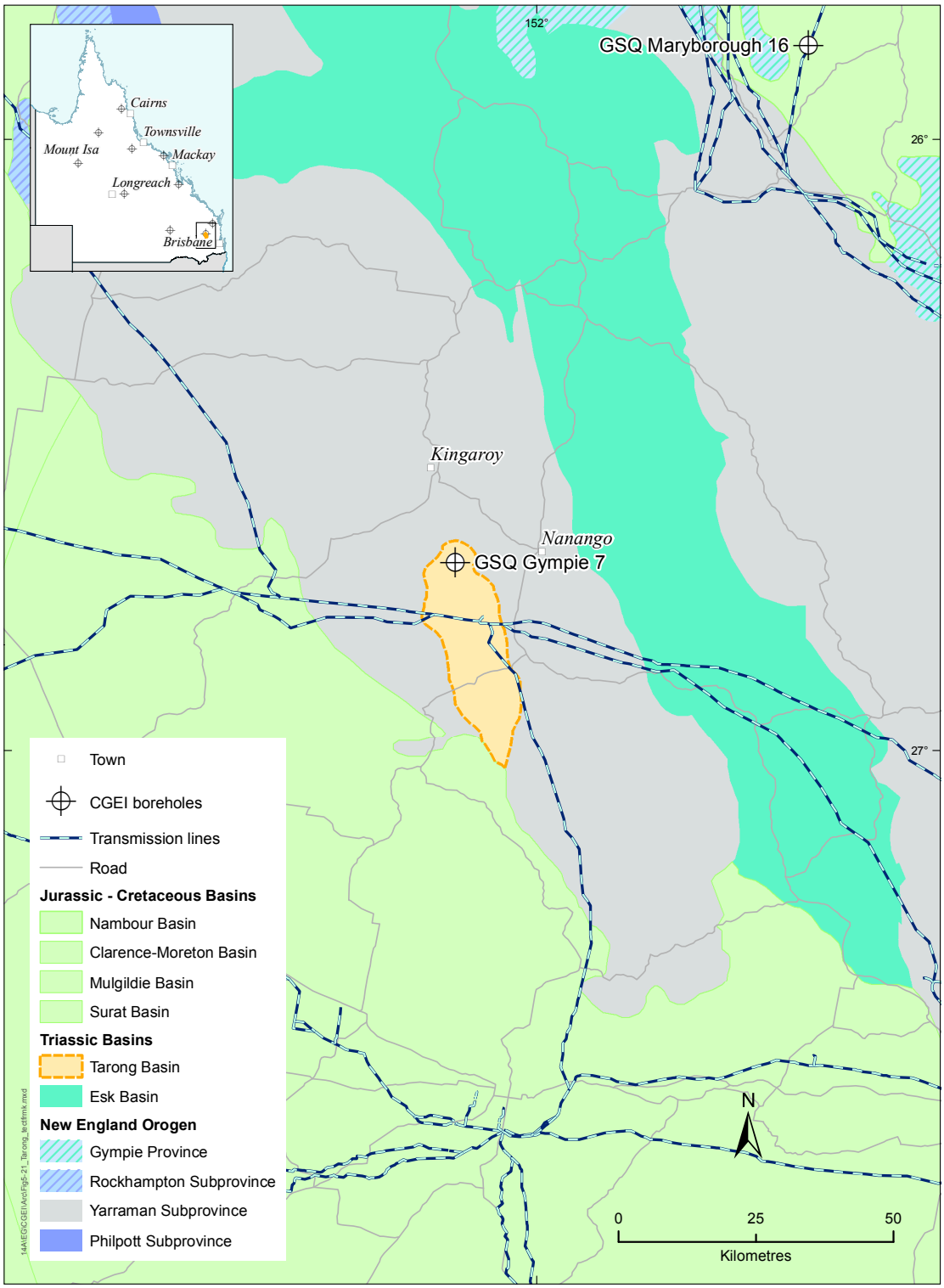

Figure 5-21. Tectonic framework of the Tarong Basin region.

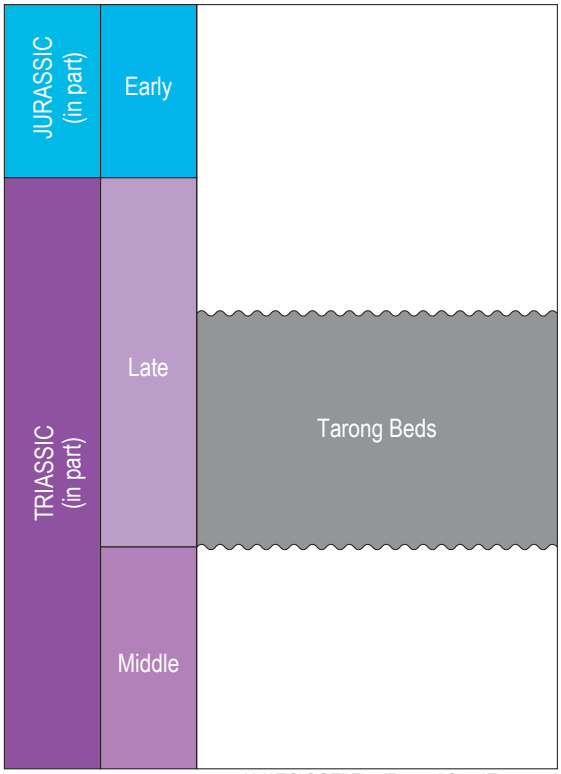

Figure 5-22. Stratigraphy of the Tarong Basin (adapted from Bradshaw et al., 2009).

Target area

In order to estimate temperatures to 5 km depth, regional geological information (Pegrem, 1995; Day *et al*., 1983; Geoscience Australia, 2012b; Cranfield, 1999; Cranfield *et al*., 2001) was used to estimate stratigraphy and rock types below the depth penetrated by GSQ Gympie 7 (Table 5-5). However, there is minimal information on stratigraphy and rock types below the depth penetrated by GSQ Gympie 7, limiting the certainty of these estimations.

A thickness of 450 m was assigned to the Tarong beds. The underlying Maronghi Creek beds are estimated to extend to 2000 m (Day *et al*., 1983), and are comprised of metasedimentary and metavolcanic sequences. Below the Maronghi Creek beds, it is estimated that the Boondooma Igneous Complex extends to 5 km.

The heat flow value of 37.5 ± 1.4 mW/m^2 modelled for GSQ Gympie 7 suggests the region is a low heat flow domain. However, if drilling did not intersect the entirety of the coal sequence, the representative heat flow of the region could be masked.

The cut-off temperature (150°C) is estimated to be at 8063 m, which limits the suitability of Tarong Basin for EGS development.

Stress regime

Field observations of the Maronghi Creek beds (Cranfield *et al*., 2001) were used in conjunction with the structural evolution of the Yarraman Subprovince to infer existing fractures at depth, which may influence reservoir stimulation.

The Maronghi Creek beds are steeply dipping with a well-developed sub-parallel cleavage, and represent an accretionary sequence of the Yarraman Subprovince (Cranfield, *et al*., 2001). The beds have significant internal repetition from imbricate thrust faulting (Donchak *et al*., 2013). Whilst this

is likely to have generated shallow to horizontal fractures initially, subsequent tilting as accretion progressed is likely to have increased the dip of these existing structures.

In contrast, the current stress regime is northeast–southwest-trending compression, which is optimal for shallow to horizontal fracture growth under reservoir stimulation (Figure 5-25). However, the steeply dipping Maronghi Creek beds may also induce vertical fracture growth during reservoir stimulation.

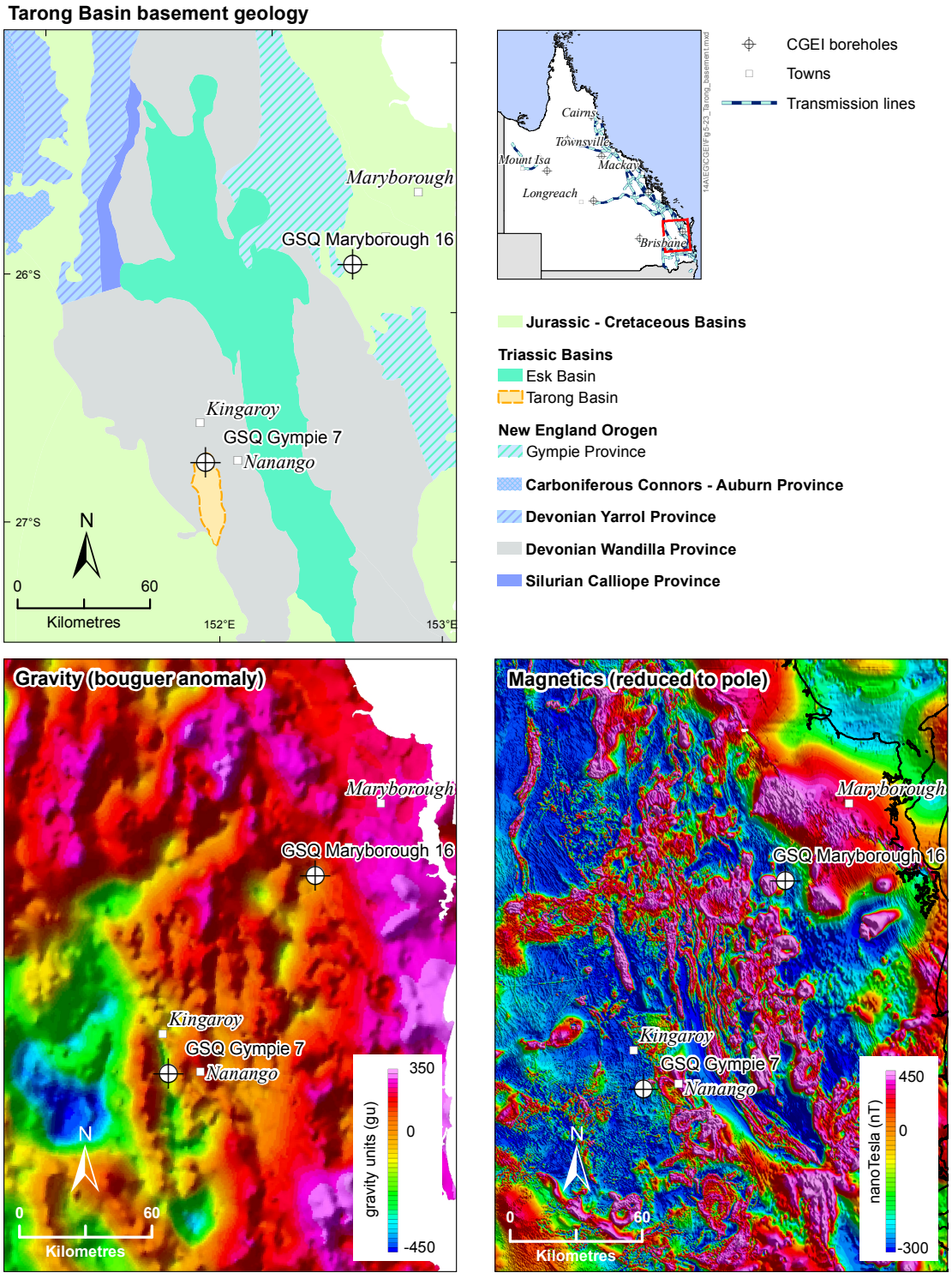

Figure 5-23. Basement geology and geophysics of the Tarong Basin region.

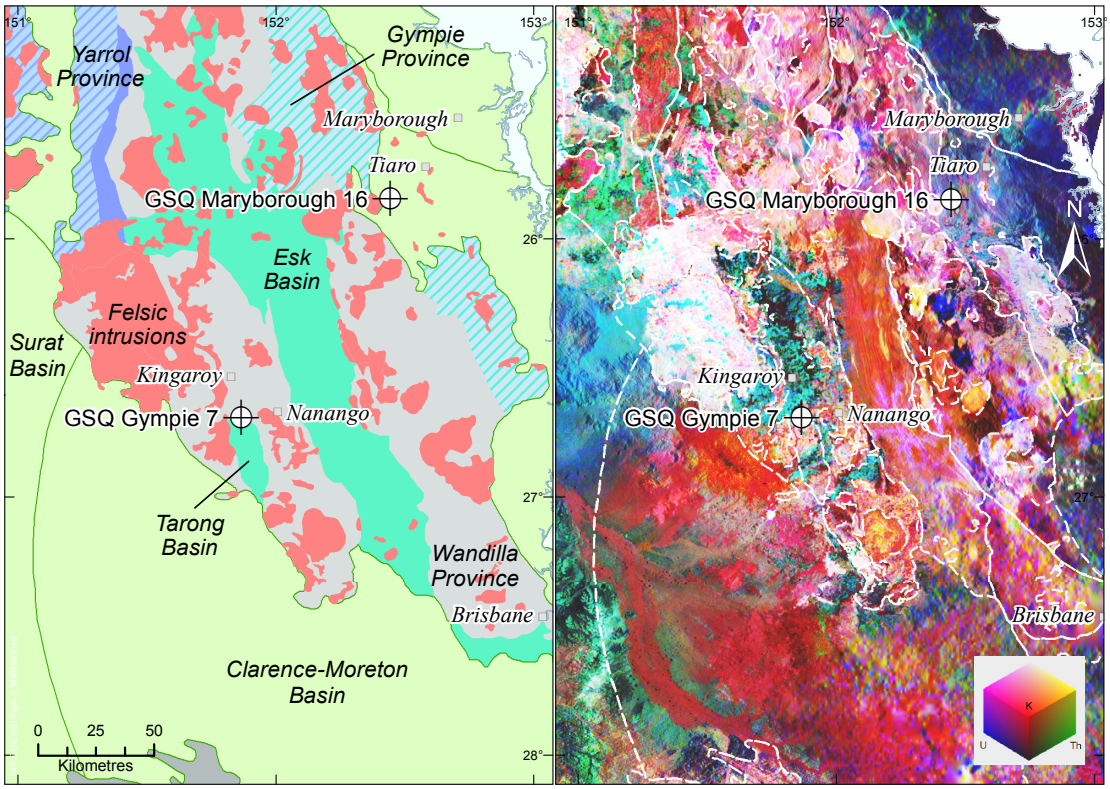

Figure 5-24. Radiometric ternary image of the Tarong Basin region.

Table 5-5. Estimated stratigraphy to 5 km depth beneath GSQ Gympie 7, Tarong Basin.

Borehole name	Depth interval (m)	Tectonic unit	Formation	Rock type	Thermal conductivity (W/mK)
GSQ Gympie 7	54–196[1]	Tarong Basin	Tarong beds	Sandstone, mudstone, coal, tuff[1]	1.08 ± 0.05[1]
	196–247[1]			Mudstone, sandstone, siltstone, tuff, coal[1]	1.21 ± 0.06[1]
	247–281[1]			Mudstone, sandstone, coal, tuff[1]	1.11 ± 0.07[1]
	281–324[1]			Mudstone, sandstone, conglomerate, tuff[1]	1.55 ± 0.38[1]
	324–337[1]			Sandstone, mudstone[1]	1.65 ± 0.07[1]
	337–450[1,2]			Mudstone[1]	1.65 ± 0.07[1]
	450–2000[3]	Yarraman Subprovince	Maronghi Creek beds[3]	Slate[4]	1.88 ± 0.59[5]
	2000–5000[6,7,2]		Boondooma Igneous Complex[6,7,2]	Granite[6]	3.23 ± 0.73[5]

[1] GSQ Gympie 7 (Sargent *et al.*, 2012b)
[2] Pegrem (1995)
[3] Day *et al.* (1983)
[4] Geoscience Australia (2012b)
[5] Beardsmore & Cull (2001)
[6] Cranfield (1999)
[7] Cranfield *et al.* (2001)

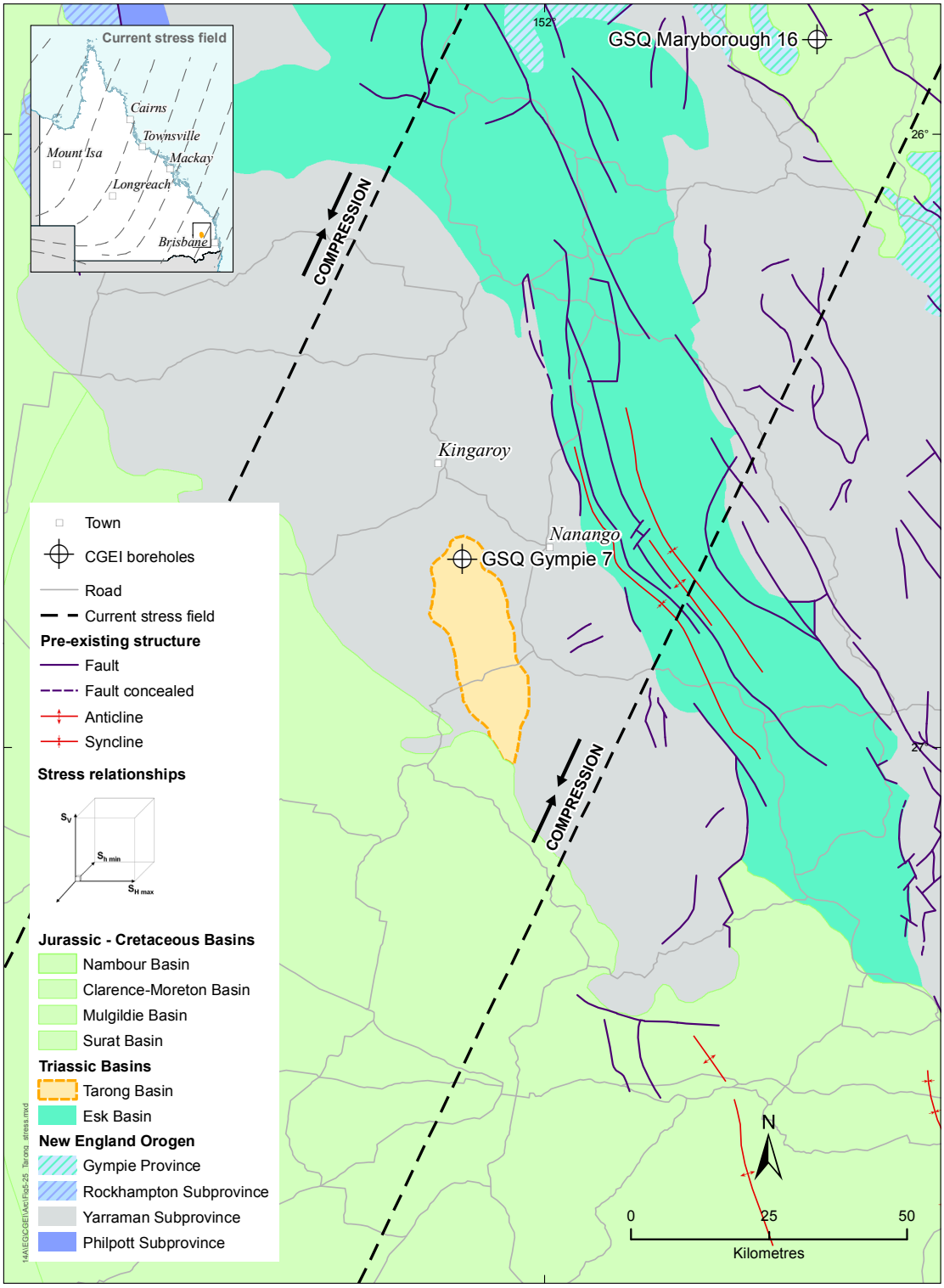

Figure 5-25. Stress regime around the Tarong Basin (adapted from Clark & Leonard, 2003).

5.5.3 Summary

Heat flow	Insulation	Temp @5km	Stress regime	Prospectivity for EGS

Good
Average
Poor

6. Preliminary geothermal resource assessment

6.1 Stored thermal energy in-place

A preliminary geothermal resource assessment was undertaken for five high prospective sites identified through the CGEI program, across Millungera, Surat, Nambour-Maryborough and Hillsborough basins. The volumetric approach was used in this assessment following the method described in Section 2.5. Important assumptions in this approach were:

- Due to the lack of data, and for simplicity, it was assumed that the modelled heat flow values remain constant with depth.
- The modelled temperatures are consequently assumed to be constant with depth.

Based on the modelled temperatures at 5 km, five inferred resource areas have been highlighted with total thermal energy content estimated between 88 000 and 402 000 PJ, using the volumetric approach under the assumptions stated in Section 2.5. The input parameters and resulting estimated stored thermal energy in-place for the five CGEI inferred resource areas are tabulated in Table 6-1 and are shown in Figure 6-1.

Table 6-1. Input parameters and stored thermal energy estimates in the inferred resource areas of CGEI targets.

Tectonic unit		Inferred resource thickness (m)	Resource mean temp. (°C)	Resource surface area (km²)	Rock density (kg/m³)	Rock specific heat capacity (J/kg°C)	Thermal energy estimate (PJ)
Millungera Basin - South		1811	194	848	2880	1000	372 499
Millungera Basin - North	Area A	1761	191	565	2880	1000	231 433
	Area B	1902	195	339	2880	1000	157 805
Surat Basin (Roma Shelf)		959	169	2621	2680	900	355 057
Hillsborough Basin		1120	177	456	2870	900	88 591
Maryborough Basin		1643	179	1465	2680	910	402 565

Note: Reference (base) temperature is assumed 110°C in all cases.

For comparison purposes, and to present a more tangible figure, the estimated thermal energy of CGEI inferred resources is reported in terms of equivalent electric power generation potential and annual electricity generation. The parameters that govern the conversion process of thermal energy to electricity are described in Section 2.5. The resulting equivalent electric power generation and annual electricity generation for the five CGEI inferred resource areas are listed in Table 6-2.

6.2 Monte Carlo simulation

The Monte Carlo analysis, following the method described in Section 2.6, shows a 90 per cent probability that the electric power generation potential of 345–1578 MWe, equivalent to annual electricity generation of 2720–12 441 GWh, can be expected from the inferred resource areas (Table 6-3). The assumed input parameters and the graphical results of the Monte Carlo simulation are presented in Appendix 3.

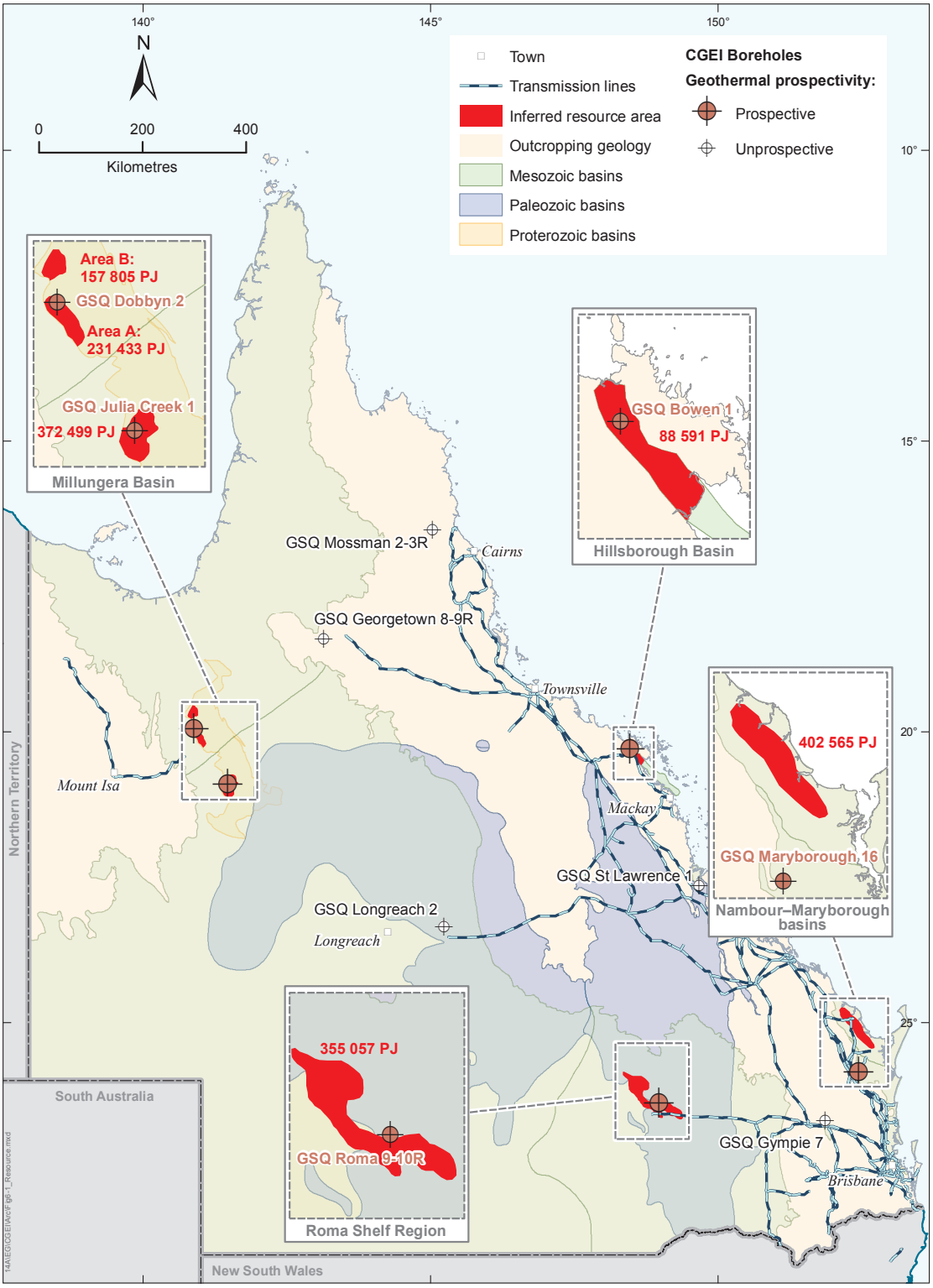

Figure 6-1. Areas of inferred geothermal energy potential highlighted by the CGEI program.

Table 6-2. Estimates of recoverable thermal energy, equivalent electric power potential and annual electricity generation of the inferred resource areas.

Tectonic unit		Inferred resource - recoverable heat estimate (PJ)	Equivalent gross electric power generation potential (MWe)	Estimated annual electricity generation (GWh)
Millungera Basin - South		18 625	1 837	14 483
Millungera Basin - North	Area A	11 572	1 142	9 004
	Area B	7 890	778	6 134
Surat Basin (Roma Shelf)		17 753	1 751	13 808
Hillsborough Basin		4 430	437	3 445
Maryborough Basin		20 128	1 986	15 655

Table 6-3. Result from Monte Carlo simulation, estimation of stored thermal energy, equivalent power output and annual electricity generation for the inferred resource areas at 90% probability.

Tectonic unit		Total stored thermal energy – PJ (90% probability)	Electric power potential – MWe (90% probability)	Annual electricity generation – GWh (90% probability)
Millungera Basin - South		>296 000	>1 460	>11 510
Millungera Basin - North	Area A	>185 000	>912	>7 190
	Area B	>130 000	>640	>5 045
Surat Basin (Roma Shelf)		>280 000	>1 380	>10 880
Hillsborough Basin		>70 000	>345	>2 720
Maryborough Basin		>320 000	>1 578	>12 441

As an example, the Monte Carlo simulation shows that the probability of stored thermal energy in the Millungera Basin - South inferred resource area being greater than 296 000 PJ is 90%. In other words, the risk that the inferred resource could not sustain 296 000 PJ is less than 10%. A similar approach should also be adopted for interpretation of the simulation results for the other inferred resource areas.

However, these estimates are purely hypothetical because of a lack of sufficient quantitative data. They will need to be revised once detailed exploration programs are undertaken and direct measurements at greater depths are obtained. Although there is a high degree of uncertainty in the preliminary geothermal resource assessment, the results from the CGEI program suggest that the selected regions certainly warrant further investigation and detailed exploration for geothermal energy.

The method used here for geothermal resource assessment has its limitations, as it provides no information about the practicalities of development, particularly relating to resource-specific constraints, such as permeability, scaling and corrosion problems. However, the approach provides an understandable, rational basis for comparing the size of different geothermal resources, taking into account both volume and temperature.

7. Discussion and conclusions

7.1 Electricity status in Queensland

With Queensland's growing population and resource industries, there is a need for additional base-load electricity capacity. Queensland has over 14 000 megawatt (MWe) of installed electricity generation capacity, with more than 12 500 MWe connected to the National Electricity Market (NEM) (Somerville *et al*., 2011). The state's maximum demand, annual-growth rate, under a medium economic-growth scenario is approximately double the forecast growth rates for all other jurisdictions (Figure 7-1). Powerlink Queensland's Annual Planning Report (2012) indicates that peak demand in Queensland under a medium economic-growth scenario is forecast to increase at an average rate of 3.5 per cent per annum to 2021–22. The state's energy consumption is also forecast to grow at an average rate of 3.5 per cent per annum over the same period. This equates to an average increase in peak demand to approximately 300 MWe per annum over the next decade. Due to this growth, and to reduce environmental impact, the need for cleaner energy sources is an imperative. Amongst all cleaner energy sources, geothermal energy is the best alternative to provide base-load electricity throughout the year with negligible greenhouse gas emissions.

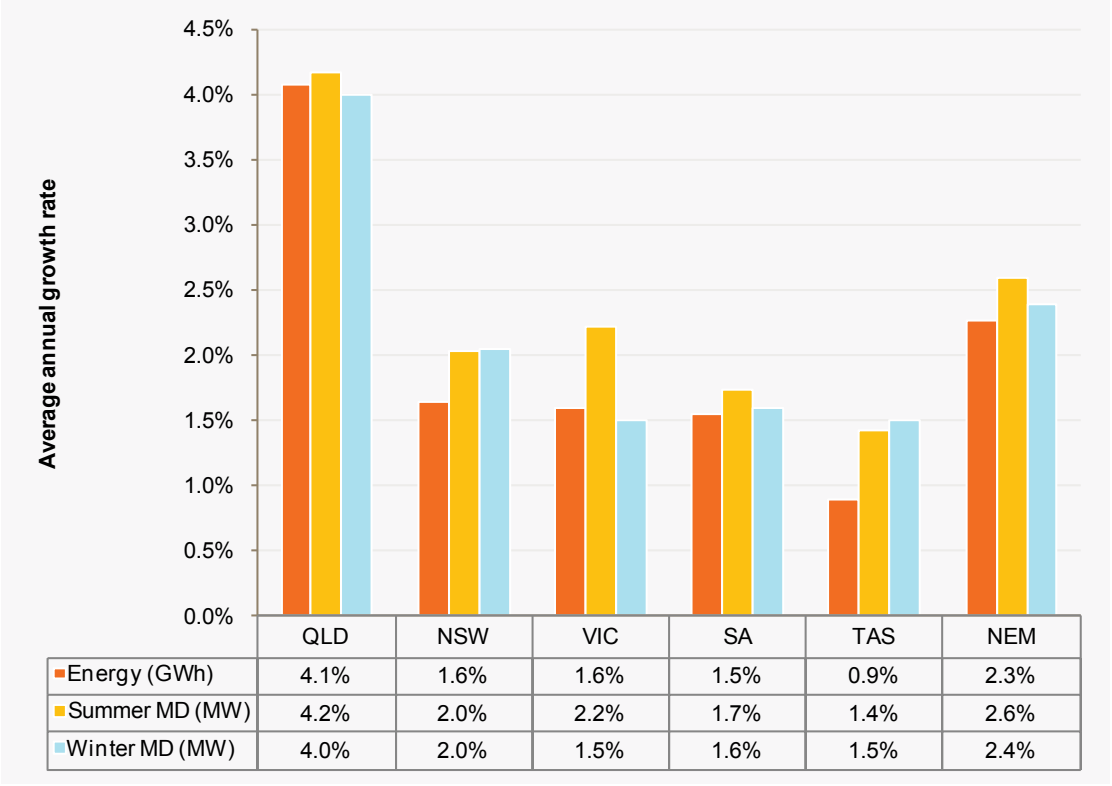

	QLD	NSW	VIC	SA	TAS	NEM
Energy (GWh)	4.1%	1.6%	1.6%	1.5%	0.9%	2.3%
Summer MD (MW)	4.2%	2.0%	2.2%	1.7%	1.4%	2.6%
Winter MD (MW)	4.0%	2.0%	1.5%	1.6%	1.5%	2.4%

Figure 7-1. Average NEM annual electricity and maximum demand growth rate forecasts (Source: AEMO 2011 Electricity Statement of Opportunities).

The equivalent gross electric-power-generation potential of the inferred resource areas identified through the CGEI (the Millungera, Surat, Nambour-Maryborough, and Hillsborough basins) has been estimated using volumetric approach under stated assumptions. The estimates show power-generation potential of 430–1980 MWe, which is equivalent to an annual electricity generation potential of 3440–15 650 GWh (Table 6-2). This potential is sufficient to meet the state's electricity peak demand forecast over the next decade.

In addition, the distribution of heat per unit volume across the inferred resource areas ranges from 140 to 240 PJ/km^3. This is relatively similar to the energy density reported for other geothermal prospects in Australia, such as in the Parachilna and Port Augusta areas in South Australia, and the Murray–Darling and Oaklands basins in New South Wales. The highlighted inferred resource areas may be prospective for both EGS and HSA development depending on the rock type intersected at the target temperature. Other risk factors, such as permeability, will need to be considered in assessing the potential of the resource areas.

7.2 Modelling and data quality

One-dimensional modelling

Steady-state heat flow models for each of the CGEI boreholes were built using 1D heat flow modelling computer code (HF1D) based on an inversion modelling technique. Required input data include precision downhole temperature logs recorded at thermally equilibrated conditions, and thermal conductivity data of the core samples.

The magnitude of the heat flow was adjusted until the computed temperature data best matched the recorded temperature log. The modelling indicated that heat flow for the CGEI boreholes ranges between 37.5 and 113.0 mW/m^2.

Limitation of 1D-modelling

Given the complexity and heterogeneity of geological formations in most geothermal systems, 1D-modelling of heat flow and temperature has limitations in that heat does not always flow vertically in areas where significant lateral contrasts in thermal conductivity exist. Similarly, lateral differences in heat producing elements will also cause local variations in heat flow. For the CGEI targets, lateral contrasts in thermal conductivity as well as heat producing elements were not investigated in more than one dimension. In fact, two- and three-dimensional heat flow modellings are required to understand 2D and 3D distribution of the temperature field, to accurately describe the thermal state of the CGEI targets.

Data quality

As the accuracy of the heat flow modelling is dependent upon the input data, the temperature and conductivity data used to model heat flow needs to represent as closely as possible the actual thermal conditions of the borehole. To ensure that the measurements best reflected the actual thermal conditions, the following procedures were implemented:

- Allowing at least 6-8 weeks before temperature logging to ensure that any perturbation incurred by the drilling process no longer distorted the temperature profile (see Section 2.1.4).
- Preserving the *in situ* condition of the core samples upon recovery of the core (see Section 2.1.3).
- Analysing all core samples at a standard temperature of 25 and 30°C in HDR and GA laboratories respectively. Thermal conductivity is temperature dependent, generally decreasing as temperature increases, and needs to be corrected from laboratory condition to the formation temperature. HF1D computer code accounts for the temperature dependence of rock thermal conductivity, following the method of Sekiguchi (1984).

No terrain corrections were applied for the effect of local topography in the heat flow models, as all the drill site locations were deliberately selected away from any major topographic feature and relief.

7.3 Historical heat flow data set

The CGEI resulted in new pre-competitive geoscientific data sets, including temperature and thermal conductivity data, being collected from selected sedimentary basins and metasedimentary terranes of northern and eastern Queensland. These data were used to determine vertical conductive heat flow, an important parameter for assessing geothermal energy potential. The results gained through the CGEI program were compared with the three heat flow provinces defined by Sass & Lachenbruch (1979).

CGEI targeted diverse geological settings across the Queensland proportion of the Central Shield and Eastern provinces of Sass & Lachenbruch (1979) (Figure 7-2).

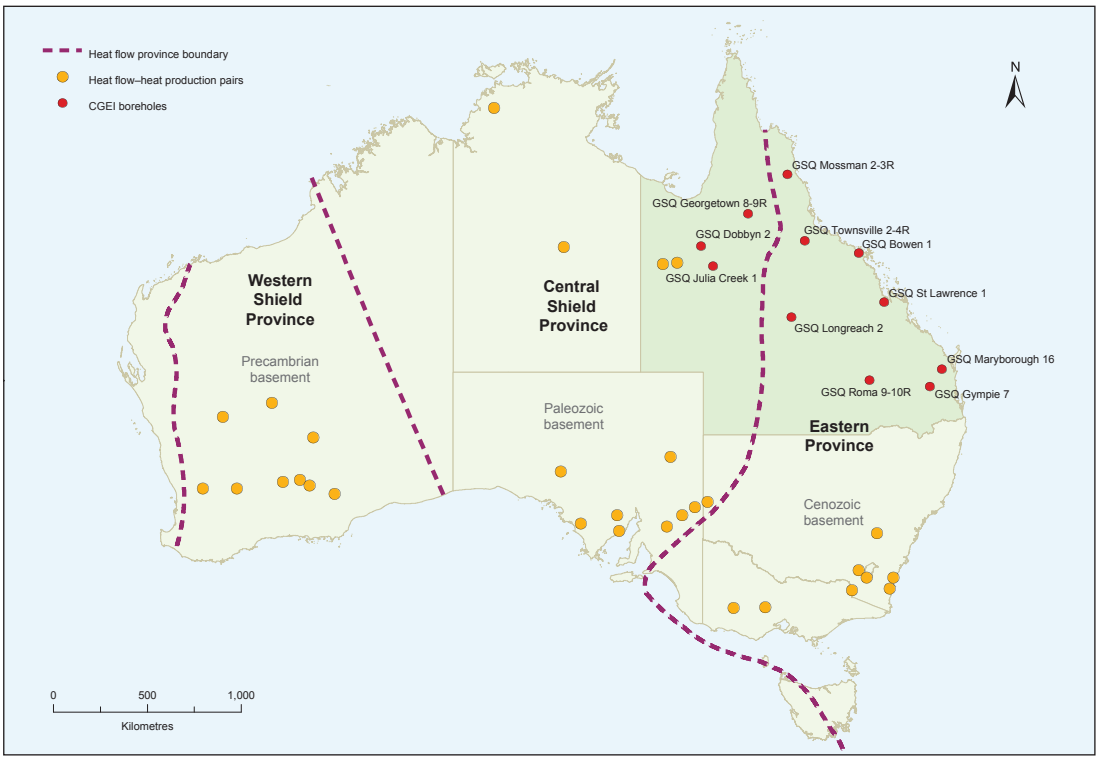

Figure 7-2. The three major Australian heat flow provinces (dashed line), as defined by Sass & Lachenbruch (1979). Circles indicate locations of heat flow-heat production pairs used by Lachenbruch (1968; 1970). The red circles show CGEI boreholes.

Eastern Heat Flow Province

The Eastern Heat Flow Province is characterised by a major period of crustal growth that occurred in the Paleozoic, and widespread Cenozoic magmatism and volcanism. Within this province, CGEI targeted the Nambour-Maryborough, Hillsborough, and Surat basins, where the modelled heat flow values are respectively 67.0, 71.0 and 82.5 mW/m^2 (Sargent *et al*., 2012a; O'Connor *et al*., 2012; Faulkner *et al*., 2012b). These results are consistent with the average heat flow of the Eastern Province (72 ± 27 mW/m^2) and are higher than the averages for Phanerozoic terranes elsewhere in the world (Morgan, 1984). Sass & Lachenbruch suggested that elevated heat flow data in the Eastern Heat Flow Province do not indicate anomalous crustal-heat production, but rather are related to the age of the most recent volcanism in this province. Torgersen *et al*. (1992) suggested that Cenozoic crustal magmatism, including underplating and intrusion, is the likely source of the elevated heat flow, which is indicated by an enhanced helium (^{3}He) flux from modern volcanics in the eastern portion of the Great Australian Basin. Also, independent studies undertaken by Wellman & McDougall (1974) and Hamza (1979) identified that there is an apparent increase in heat flow with latitude within the Cenozoic volcanic regions of eastern Australia. The trend is assumed to relate to hot spot activity in the asthenosphere

associated with the northward movement of the Indo-Australian plate. However, the highest heat flow modelled for the Eastern Heat Flow Province was in the Surat Basin to the south, where the geothermal target is the Devonian Roma granites. This contrasts with the assumed younger Cenozoic age for sources of elevated heat flow in the north.

Several CGEI boreholes targeted the Late Permian to Middle Triassic granites in southeastern Queensland (Figure 7-3). The Nambour-Maryborough basins are partly underlain by these granites, which are low to moderate heat-producing (1.5–3 $\mu W/m^3$). The overlying insulating rocks included up to 1500 m of the Burrum Coal Measures. The coal measures act as a thermal blanket for the intrusives, providing effective insulation and resulting in the development of elevated temperatures at depth. Vitrinite reflectance data from GSQ Maryborough 16 suggest a maximum paleo-geothermal gradient of 98°C/km. This indicates that high temperatures have prevailed sometime in the geological history of Nambour-Maryborough basins and may still exist at the present time based on the temperature estimation at depth presented in this report.

Also, through the Late Triassic – Jurassic, much of the eastern margin of Australia experienced widespread thermal relaxation resulting in the development of sag basins such as the Clarence–Moreton, Surat and Eromanga basins. The Surat and Eromanga basins are known petroleum provinces and also encompass hot aquifers of the Great Artesian Basin with low-enthalpy geothermal energy potential. The Birdsville Geothermal Power Plant, in the southwest corner of the state, is an example of the use of this low-enthalpy geothermal resource.

In the Roma Shelf region, the CGEI targeted the Roma granites, which underlie the Bowen and Surat basins, for a potential heat source. The heat-generation capacity of these granites is largely unknown, but recent geochemical analysis has indicated low to moderate concentrations of radioactive elements, with an average heat-production value of 2.7 $\mu W/m^3$ (Siégel *et al.*, 2012). Additionally, elevated downhole temperature gradients (42–68°C/km) in nearby petroleum wells indicate that high temperature gradients are still present in the region.

In the Hillsborough Basin, residual heat from Cenozoic rifting was the targeted heat source. The basin developed as a graben in response to an extensional regime associated with the opening of the Tasman and Coral seas during the Late Cretaceous – Paleogene (Day *et al.*, 1983; Cook & Jell, 2013). Another potential heat source in the basin is the Campwyn Volcanics, which underlie the basin and comprise a rhyolite ignimbrite dominated upper sequence.

Central Shield Heat Flow Province

In contrast, the Central Shield Heat Flow Province comprises the region of the Australian continent that formed mostly during the Proterozoic, and has a surface heat flow of 49–54 mW/m^2 (Chapman & Furlong, 1977; Morgan, 1984). This is close to the heat flow value of 48.5 mW/m^2 determined for GSQ Georgetown 8-9R. In the northwest portion of Queensland, the Millungera Basin has modelled heat flow values of 107.5 and 113.0 mW/m^2, which are anomalously high for Proterozoic terranes. Drummond (1988) and Collins (1991) have indicated that a compilation of both refraction and reflection seismic data shows that Proterozoic terranes throughout a large proportion of the Central Shield Heat Flow Province contain the thickest crust in the Australian continent, with the Moho discontinuity typically imaged at approximately 45 km. Deep seismic imaging suggests that this thick crust is coupled with a relatively cool, thick lithosphere, with the transition to slow seismic velocities being associated with sub-lithospheric mantle imaged at around 250 km (Kennett & van der Hilst, 1996). Shear wave velocities in the Proterozoic upper lithospheric mantle at 80 km depth beneath the Central Shield Heat Flow Province are about 6 per cent faster than velocities beneath the Eastern Heat Flow Province (Zielhaus & van der Hilst, 1996), where marginally elevated surface heat flow is attributed to anomalous mantle heat flow (Sass & Lachenbruch, 1979).

Consequently, the existence of thick, cold mantle lithosphere beneath much of the Central Shield Heat Flow Province points to low mantle heat flow throughout this region (McLaren *et al.*, 2003). Therefore,

the anomalously high heat flow values determined for the Millungera Basin are a consequence of a contribution from crustal heat sources. These sources are likely to be Proterozoic intrusives, possibly part of the Williams Supersuite, underlying the northwest and southwest portion of the basin (Korsch *et al*., 2011).

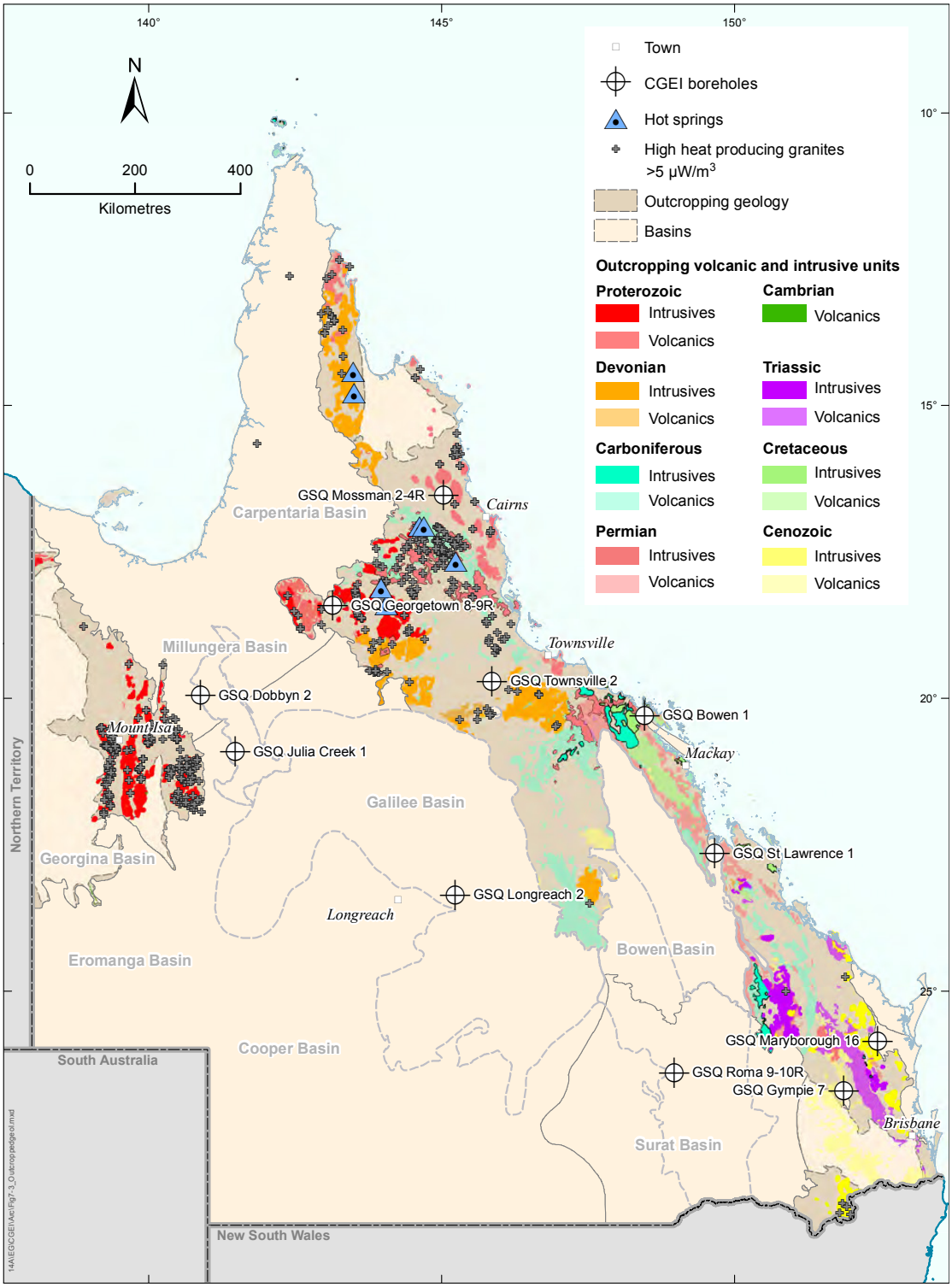

Figure 7-3. Simplified map of magmatic and volcanic units across Queensland.

7.4 Temperature at depth and the importance of a thermal blanket

The temperature values obtained by modelling contrast significantly with existing OzTemp estimates of temperature at depth at the drilling locations. This may be due to the method of estimation used in the CGEI that accounted for influence of thermal resistance of rocks at depth.

The OzTemp estimates for the Millungera Basin area were in the range of 180–220°C at 5 km, whereas the new modelling indicates temperatures up to 240°C. The Hillsborough and Nambour-Maryborough basins produced modelled temperatures in excess of 200°C at 5 km, where earlier estimates were in the range of 100–150°C. These higher temperatures at depth may be attributed to the thick, insulating sedimentary and igneous sequences present at each site.

A good example of the impact of thermal resistance on the estimation of temperature at depth is the comparison of the results obtained for the Hodgkinson Province and the Nambour-Maryborough basins. OzTemp temperature estimates show the Hodgkinson Province to have a significantly higher temperature at 5 km than the Nambour-Maryborough basins. Results from CGEI also show the Hodgkinson Province to have higher heat flow. However, CGEI temperature modelling found the Nambour-Maryborough basins to have a significantly higher temperature at depth in comparison to the Hodgkinson Province. The lower temperature for the Hodgkinson Province is due to the thick, thermally conductive metasediments of the Hodgkinson Province, which offer limited thermal resistance. The higher temperature in the Nambour-Maryborough basins is due to the sedimentary sequences and coal measures, which provide much higher thermal resistance.

The results of the CGEI temperature modelling demonstrate that under sufficient insulation, even moderate heat sources can retain high temperatures at depth. Stacked sedimentary basins, commonly containing coal measures, cover a large portion of Queensland, and typically act as the efficient thermal blanket insulating intrusions and regions of Cenozoic magmatism and volcanism. These results suggest that geothermal energy potential may exist in areas previously overlooked due to the lack of high heat producing intrusives, or no or poor quality temperature data.

7.5 Shallow drilling as a means of assessing geothermal energy potential

Hole completion

The accuracy of using heat flow modelling to estimate temperatures to 5 km depends on how closely the temperature profile from shallow drilling represents the thermal state of the borehole. Whilst the CGEI boreholes were left for a minimum of 6 weeks to achieve thermal stabilisation, it was found the method of hole completion was a crucial component in obtaining reliable temperature profiles.

Two methods of hole completion were used in this program. The first method was to cement aquifers as they were intersected by drilling six metres below and cementing to at least six metres above the permeable zone. However, subsequent temperature logging showed that fluid flow between even minor permeable units distorted the temperature profile. For example, the sharp increase in temperature and steep geothermal gradient between two permeable units are apparent in GSQ Longreach 2 (Figure 7-4). The second method of hole completion involved cementing the annulus from surface to TD. A second temperature profile for GSQ Longreach 2 obtained after the cementation of the annulus had been completed resulted in a steady temperature gradient.

Influence of coal measures

Whilst coal measures are ideal in hot rock geothermal systems due to the excellent insulation they provide, their high thermal resistance can result in localised lower heat flow within and above the coal

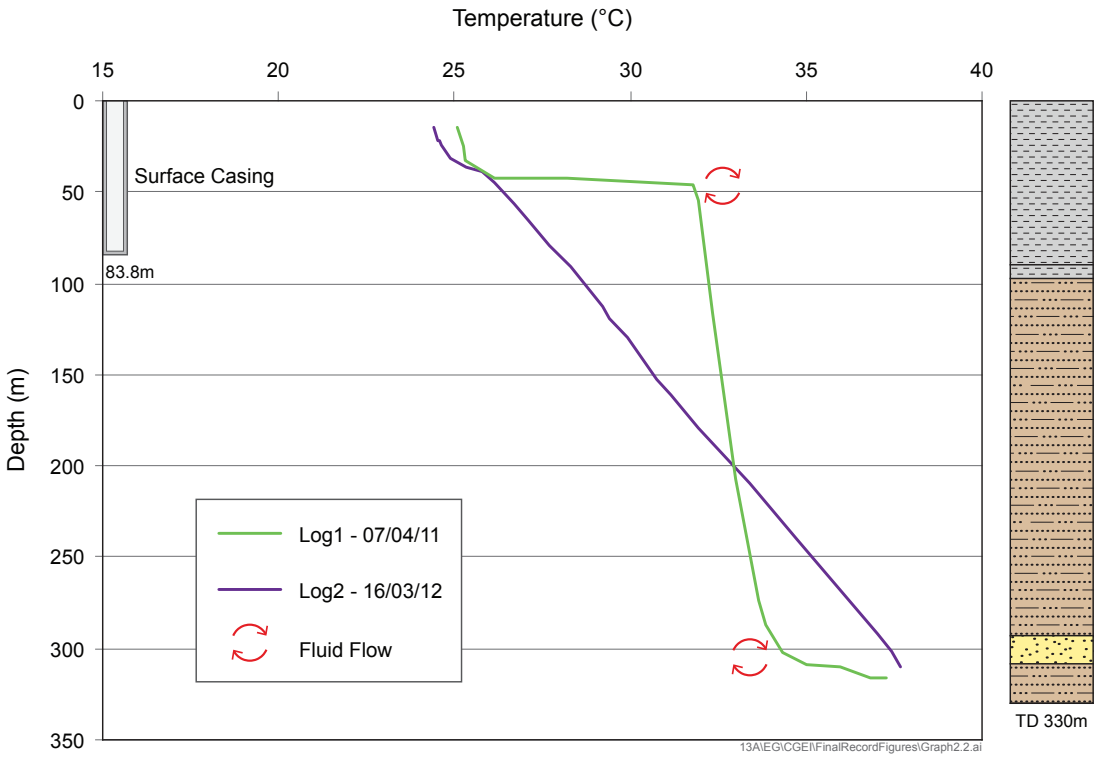

Figure 7-4. Temperature profiles of GSQ Longreach 2 (Brown et al., 2012a). The green line shows temperature profile distorted by minor permeable zones. The purple line is the equilibrated temperature profile of the borehole after work-over by grouting the annulus.

measures. In cases where the coal seams have not been penetrated by drilling, the low heat flow value may not be indicative of poor geothermal energy potential.

Consequently, deeper drilling penetrating the coal measures should be undertaken in order to obtain the data required to determine the geothermal potential in these geological settings.

An example of the influence of coal is the Nambour-Maryborough basins, where a moderate heat flow value of 67.0 mW/m^2 was obtained. Temperature modelling to 5 km factoring in rock types, including over 400 m of coal measures, resulted in a temperature of 204°C indicating a region with high geothermal energy potential.

8. Recommendations

The following recommendations are made in order to better define the geothermal energy potential of the inferred resource areas (Figure 6-1):

- Magnetotelluric (MT) soundings are required to identify subsurface resistivity structure and delineate deep conductive and resistive zones. The application of wide frequency ranges in the soundings over at least a 24-hour cycle of data collection will be required in order to acquire sufficient data to image subsurface structure down to 5 km depth.
- Seismic surveying, in conjunction with the MT survey, could be undertaken to better define the structure (faulting, fracture zones) of the prospect area.
- Spatial distribution of heat flow data needs to be increased in each area, by incorporating temperature and thermal conductivity data from all previously drilled wells as well as drilling new relatively shallow (~500 m) boreholes to improve the data density. A three-dimensional geological model of each area using the results of the magnetotelluric soundings and seismic survey needs to be developed for facilitating 3D heat flow modelling.
- The geological model can be used to better constrain the 3D distribution of the temperature field. Triaxial thermal conductivity analysis of rock samples, to investigate any effects of anisotropy, will be required.
- Extensive stress-field studies are required at both regional and prospect scales, for numerical hydro-mechanical modelling, in order to constrain expected geothermal reservoir growth direction in hydro-fracturing stimulation (EGS type development), and also to understand the effects of stress-dependent fracture permeability.
- Exploratory drilling will be necessary to validate the prospectivity of the identified areas. Initially, this will involve drilling low-cost, slim-holes to a depth of 2–3 km, to verify predicted temperatures at depth, confirm the geological succession, perform down-hole logging, and revise existing geothermal resource assessment.
- Deep drilling and flow testing are required to confirm the viability of the resource area to produce geothermal energy at rates to justify commercial development.
- An engineering feasibility study needs to be undertaken, collating and integrating all the available geoscientific data, drilling and flow testing results, and engineering and economic factors, to individually evaluate the commercial viability of a geothermal-energy-development program.

9. References

AITKINS, A.R.A, SALMON, M.L. & KENNETT, B.L.N., in press: Australia's Moho: A test of the usefulness of gravity modelling for the determination of Moho depth. *Tectonophysics*.

AMOS, B.J. & DE KEYSER, F., 1964: Mossman, Queensland 1:250 000 Geological Series. *Geological Survey of Queensland, Explanatory Notes SE55-01*.

AMPOL EXPLORATION (QLD) PTY LTD, 1965: Proserpine No. 1. Well Completion Report. Unpublished report held by the Geological Survey of Queensland QDEX System as CR1783.

ANDERSON, E.M., 1951: *The dynamics of faulting and dyke formation with application to Britain (2nd edition)*. Oliver and Boyd, Edinburgh, 7–21.

AUSTRALIAN GEOTHERMAL ENERGY GROUP, 2007: The Australian Geothermal Energy Group's submission to the House of Representatives' inquiry into the development of the non-fossil fuel energy in Australia. Viewed 30 June, 2013 <http://www.pir.sa.gov.au/__data/assets/pdf_file/0016/60532/TIG3_AGEG_Submission.pdf>

AUSTRALIAN GEOTHERMAL ENERGY GROUP, 2010: Geothermal Lexicon For Resources and Reserves Definition and Reporting, Edition 2. Viewed 30 June, 2013 <http://www.pir.sa.gov.au/__data/assets/pdf_file/0006/147876/Geothermal_Lexicon_2010.pdf>

BAIN, J.H.C. & DRAPER, J.J., 1997: North Queensland Geology. *Australian Geological Survey Organisation, Bulletin **240**, and Queensland Geology, **9***.

BEARDSMORE, G.R. & CULL, J.P., 2001: *Crustal Heat Flow: A Guide to measurement and modelling*. Cambridge University Press.

BENSTEAD, W.L., 1976: Styx Basin. *In:* Leslie, R.B., Evans, H.J. & Knight, C.L. (Editors): Economic geology of Australia and Papua New Guinea, volume 3, petroleum. *Australasian Institute of Mining and Metallurgy Monograph Series*, **7**, 446–447.

BERTANI, R., 2010: Geothermal power plant efficiency: EUROSTAT consultation. TP Geoelec, 3rd Meeting, Pisa, Italy.

BRADSHAW, B.E., SPENCER, L.K., LAHTINEN, A.C., KHIDER, K., RYAN, D.J., COLWELL, J.B., CHIRINOS, A. & BRADSHAW, J., 2009: *Queensland carbon dioxide geological storage atlas*. Queensland Department of Employment, Economic Development and Innovation.

BROWN, D.D., MAXWELL, M., O'CONNOR, L.K., SARGENT, S.N. & TALEBI, B., 2012a: Coastal Geothermal Energy Initiative GSQ Longreach 2, well completion report and heat flow modelling results. *Queensland Geological Record*, **2012/10**.

BROWN, D.D., MAXWELL, M., O'CONNOR, L.K., SARGENT, S.N. & TALEBI, B., 2012b: Coastal Geothermal Energy Initiative GSQ Mossman 2-3R, well completion report and heat flow modelling results. *Queensland Geological Record*, **2012/15**.

BRYAN, S., 2007: Silicic Large Igneous Provinces. *Episodes*, **30**(1), 20–31.

BRYAN, S.E., ALLEN, C.M., HOLCOMBE, R.J. & FIELDING, C.R., 2004: U-Pb zircon geochronology of the Late Devonian to Early Carboniferous extension-related silicic volcanism in the northern New England Fold Belt. *Australian Journal of Earth Sciences*, **21**, 645–664.

BRYAN, S.E., EWART, A., STEPHENS, C.J., PARIANOS J. & DOWNES, P.J., 2000: The Whitsunday Volcanic Province, Central Queensland, Australia: lithological and stratigraphic investigations of a silicic-dominated large igneous province. *Journal of Volcanology and Geothermal Research*, **99**, 55–78.

BRYAN, S.E., FIELDING, C.R., HOLCOMBE, R.J., COOK, A. & MOFFITT, C.A., 2003: Stratigraphy, facies architecture and tectonic implications of the Upper Devonian to Lower Carboniferous Campwyn Volcanics of the northern New England Fold Belt. *Australian Journal of Earth Sciences*, **50**, 377–401.

BRYAN, S.E., UYSAL, T. & MARSHALL, V., 2010: Seeking high heat-producing granites (HHPG) in Queensland. PowerPoint Presentation presented to the GSQ (unpublished).

BULTITUDE, R.J., DONCHAK, P.J.T., DOMAGALA, J. & FORDHAM, B.J. 1993: The pre-Mesozoic stratigraphy and structure of the western Hodgkinson Province and environs. *Queensland Resource Industries Record*, **1993/29**.

BURNS, K.L., WEBER, C., PERRY, J. & HARRINGTON, H.J., 2000: Status of the geothermal industry in Australia. *Proceedings of the World Geothermal Congress, Japan, May 28 – June 10, 2000*, 99–108.

CHAMPION, D.C. & BULTITUDE, R.J., 2013: Post-orogenic Kennedy Igneous Association. *In:* Jell, P.A. (Editor): *Geology of Queensland.* Geological Survey of Queensland, Department of Natural Resources and Mines, Brisbane.

CHAPMAN, D.S. & FURLONG, K.P., 1977: Continental heat flow — age relationships. *EOS*, **58**, 1240.

CHOPPING, R. & HENSON, P.A., 2009: 3D map and supporting geophysical studies in the North Queensland region. *Geoscience Australia Record*, **2009/29**.

CHOPRA, P.N., 2005: Status of the Geothermal Industry in Australia, 2000–2005. *Proceedings of the World Geothermal Congress 2005, Antalya, Turkey.* International Geothermal Association, Germany.

CLARK, D. & LEONARD, M., 2003: Principal stress orientations from focal-plane solutions: new insight into the Australian intraplate stress field. *In:* Hillis, R.R. & Müller, D. (Editors): Evolution and Dynamics of the Australian Plate. *Geological Society of Australia, Special Publication*, **22**, 91–105.

CLARKE, D.E., PAINE, A.G.L. & JENSEN, A.R., 1971: Geology of the Proserpine 1:250 000 Sheet area, Queensland. *Bureau of Mineral Resources, Australia, Report* **174**.

COLLINS, C.D.N., 1991: The nature of the crust–mantle boundary under Australia from seismic evidence. *Geological Society of Australia, Special Publication*, **17**, 67–80.

COOK, A.G., BRYAN, S.E. & DRAPER, J., 2013: Post-orogenic Mesozoic basins and magmatism. *In:* Jell, P.A. (Editor): *Geology of Queensland.* Geological Survey of Queensland, Department of Natural Resources and Mines, Brisbane.

COOK, A.G. & JELL, P.A., 2013: Paleogene and Neogene. *In:* Jell, P.A. (Editor): *Geology of Queensland.* Geological Survey of Queensland, Department of Natural Resources and Mines, Brisbane.

CRANFIELD, L.C., 1982: Stratigraphic drilling in the southern Maryborough basin 1978–1980. *Queensland Government Mining Journal*, **83**(963), 15–29.

CRANFIELD, L.C., 1992: *Maryborough Sheet SG 56–6, Queensland, 1:250 000 geological map series, first edition.* Department of Resource Industries, Queensland.

CRANFIELD, L.C., 1994: Maryborough, Queensland 1:250 000 Geological Series. *Geological Survey of Queensland Explanatory Notes SG56-06.*

CRANFIELD, L.C., 1999: *Gympie Special, Sheet 9445, Part 9545, Queensland 1:100 000 Geological Map Commentary.* Queensland Department of Mines and Energy, Brisbane.

CRANFIELD, L.C., DONCHAK, P.J.T., RANDALL, R.E. & CROSBY, G.C., 2001: Geology and mineralisation of the Yarraman Subprovince, southeast Queensland. *Queensland Geology*, **10**.

CULL, J.P., 1982: An appraisal of Australian Heat Flow. *BMR Journal of Australian Geology and Geophysics*, **7**, 11–21.

DAY, R.W., WHITAKER, W.G., MURRAY, C.G., WILSON, I.H. & GRIMES, K.G., 1983: Queensland geology. A companion volume to the 1:2 500 000 scale geological map (1975). *Geological Survey of Queensland Publication*, **383**.

DEHNAM, D., ALEXANDER, L.G. & WOROTNICKI, G. 1979: Stresses in the Australian crust: evidence from earthquake and in-situ stress measurements. *BMR Journal of Australian Geology & Geophysics*, **4**, 289–295.

DENARO, T.J., CRANFIELD, L.C., FITZELL, M.J., BURROWS, P.E. & MORWOOD, D.A., 2007: Mines, mineralisation and mineral exploration in the Maryborough 1:250 000 Sheet area, south-east Queensland. *Queensland Geological Record*, **2007/01**.

DEPARTMENT OF TRADE AND INVESTMENT OF NSW, 2010: Geothermal Energy Potential in the Murray-Darling and Oaklands Basins of New South Wales (webpage). Viewed 30 June 2013 at <http://www.resources.nsw.gov.au/__data/assets/pdf_file/0004/384331/Geothermal-Energy-Potential-in-the-Murray-Darling-and-Oaklands-Basins-of-NSW-by-Hot-Dry-Rocks-PL.pdf>

DERRINGTON, S.S., 1981: POG Gregory River 2 QLD, Well Completion Report. Unpubished report held by the Geological Survey of Queensland QDEX System as CR10767.

DONCHAK, P.J.T., PURDY, D.J., WITHNALL, I.W., BLAKE, P.R. & JELL, P.A., 2013: New England Orogen. *In:* Jell, P.A. (Editor). *Geology of Queensland.* Geological Survey of Queensland, Department of Natural Resources and Mines, Brisbane.

DOUTCH, H.F., 1973: Carpentaria Basin. *In:* Leslie, R.B., Evans, H.J. & Knight, C.L. (Editors): Economic geology of Australia and Papua New Guinea, volume 3, petroleum. *Australasian Institute of Mining and Metallurgy Monograph Series*, **7**, 374–379.

DRUMMOND, B.J., 1988: A review of crust/upper mantle structure in the Precambrian areas of Australia and implications for Precambrian crustal evolution. *Precambrian Research*, **40**, 101–116.

EGHBAL, M. & SAHA, T.K., 2011: Large scale integration of geothermal energy into the Australian transmission network. *Proceedings of the Australian Geothermal Energy Conference*, **2011**, 69–72.

ELLIS, P.L., 1968: Geology of the Maryborough 1:250 000 sheet area. *Queensland Geological Report*, **26**.

ENTER, M. & GRANT, N., 2007a: A-P 613P, Map Burrum 1, Well Completion Report. Unpublished report held by the Geological Survey of Queensland QDEX System as CR47789.

ENTER, M. & GRANT, N., 2007b: A-P 613P, Map Burrum 2, Well Completion Report. Unpublished report held by the Geological Survey of Queensland QDEX System as CR47790.

EVANS, P.A., 1996: Fluoride anomalies in aquifers of the Queensland sector of the Great Artesian Basin and their Significance. *Geological Society of Australia, Extended Abstracts*, **43**, 172.

EWART, A., SCHON, R.W. & CHAPPELL, B.W., 1992: The Cretaceous volcanic-plutonic province of central Queensland (Australia) coast—a rift-related 'calc-alkaline' province. *Transactions of the Royal Society of Edinburgh: Earth Sciences*, **83**, 327–345.

EXON , N.F., 1976: Geology of the Surat Basin in Queensland. *Bureau of Mineral Resources, Australia, Bulletin* **166**.

FARRINGTON, R.J., STEGMAN, D.R., MORESI, L.N, SANDIFORD, M. & MAY, D.A., 2010: Interactions of 3D mantle flow and continental lithosphere near passive margins. *Tectonophysics*, **483**, 20–28.

FAULKNER, S.P., MAXWELL, M., O'CONNOR, L.K., SARGENT, S.N. & TALEBI, B., 2012a: Coastal Geothermal Energy Initiative GSQ Julia Creek 1, well completion report and heat flow modelling results. *Queensland Geological Record* **2012/05**.

FAULKNER, S.P., MAXWELL, M., O'CONNOR, L.K., SARGENT, S.N. & TALEBI, B., 2012b: Coastal Geothermal Energy Initiative GSQ Roma 9-10R, well completion report and heat flow modelling results. *Queensland Geological Record* **2012/09**.

FERGUSSON, C.L. & HENDERSON, R.A., 2013: Thomson Orogen. *In:* Jell, P.A. (Editor): *Geology of Queensland.* Geological Survey of Queensland, Department of Natural Resources and Mines, Brisbane.

FIELDING, C.R., STEPHENS, C.J. & HOLCOMBE, R.J. 1997: Permian stratigraphy and palaeogeography of the eastern Bowen Basin, Gogango Overfolded Zone and Strathmuir Synclinorium in the Rockhampton–Mackay region, central Queensland. *Geological Society of Australia, Special Publication*, **19**, 80–95.

FINLAYSON, D.M. (Editor), 1990: The Eromanga-Brisbane Geosience Transect: a guide to basin development across Phanerozoic Australia in southern Queensland. *Bulletin of the Bureau of Mineral Resources, Australia*, **232**, 1–261.

FISHWICK, S., HEINTZ, M., KENNETT, B.L.N., READING, A.M. & YOSHIZAWA, K., 2008: Steps in lithospheric thickness within eastern Australia, evidence from surface wave tomography. *Tectonics*, **27**(4).

FITZELL, M.J., MAXWELL, M., O'CONNOR, L.K., SARGENT, S.N. & TALEBI, B., 2012: Coastal Geothermal Energy Initiative GSQ Dobbyn 2, well completion report and heat flow modelling results. *Queensland Geological Record* **2012/04**.

FLOOD, P.G. & GARCES, B., 1986: A late Triassic strike-slip (pull-apart) basin containing alluvial fan and coal-rich fluviatile sediments. *In:* Willmott, W.F. (Editor): Geological Society of Australia, Queensland Division. *1986 Field Conference, South Burnett District*, 77–81.

FOSTER, D.A. & GRAY, D.R., 2000: Evolution and structure of the Lachlan Fold Belt (Orogen) of eastern Australia. *Annual Review of Earth and Planetary Sciences*, **28**, 47–80.

GARCES, B. & FLOOD, P.G., 1984: Alluvial and braided stream sedimentation within the late Triassic Tarong Basin, S.E. Queensland. *Proceedings of the Eighteenth Symposium on Advances in the Study of the Sydney Basin. Department of Geology, University of Newcastle*, 81–84.

GEARY, G.C., 1983: LMN Bellara-1 Well completion report ATP-239P, Queensland. Leighton Mining NL. Unpublished report held by the Geological Survey of Queensland QDEX System as CR11433.

GEODYNAMICS, 2014a: Geothermal Frequently Asked Questions (webpage). Viewed 13 February, 2014. <http://www.geodynamics.com.au/Resource-Centre/Geothermal-FAQ.aspx>

GEODYNAMICS, 2014b: Innamincka Deeps (EGS) Project (webpage). Viewed 13 February, 2014. <http://www. geodynamics.com.au/Our-Projects/Innamincka-Deeps.aspx>

GEOLOGICAL SURVEY OF QUEENSLAND, 2011: North-west Queensland Mineral and Energy Province Report. Queensland Department of Employment, Economic Development and Innovation, Brisbane.

GEOSCIENCE AUSTRALIA, 2008a: Carpentaria Basin (webpage). Viewed 30 June 2013. <http://www.ga.gov.au/energy/province-sedimentary-basin-geology/petroleum/onshore-australia/carpentaria-basin.html>

GEOSCIENCE AUSTRALIA, 2008b: Nambour Basin (webpage). Viewed 30 June 2013. <http://www.ga.gov.au/energy/province-sedimentary-basin-geology/petroleum/onshore-australia/nambour-basin.html>

GEOSCIENCE AUSTRALIA, 2008c: Surat Basin (webpage). Viewed 30 June 2013. <http://www.ga.gov.au/energy/province-sedimentary-basin-geology/petroleum/onshore-australia/surat-basin.html>

GEOSCIENCE AUSTRALIA, 2012a: Mount Urah Granodiorite (webpage). Viewed 30 June 2013. <http://dbforms.ga.gov.au/pls/www/geodx.strat_units.sch_full?wher=stratno=13158>

GEOSCIENCE AUSTRALIA, 2012b: Maronghi Creek beds (webpage). Viewed 30 June 2013. <http://dbforms.ga.gov.au/pls/www/geodx.strat_units.sch_full?wher=stratno=11343>

GERNER, E.J & HOLGATE, F.L., 2010: OzTemp – Interpreted Temperature at 5 km Depth Image. Geoscience Australia. Available from: <http://www.ga.gov.au/metadata-gateway/metadata/record/gcat_71143>

GLEN, R.A., 2005: The Tasmanides of eastern Australia. *In:* Vaughan, A.P.M., Leat, P.T. & Pankhurst, R.J.: Terrane Processes at the Margins of Gondwana. *Special Publication of the Geological Society*, **246**, 23–96.

GORTON, J., 2010: A-P 787P, AEL HB 2P, Well Completion Report. Unpublished report held by the Geological Survey of Queensland QDEX System as CR64554.

GOSCOMBE, P.W. & COXHEAD, B.A., 1995: Clarence-Moreton, Surat, Eromanga, Nambour, and Mulgildie Basins. *In:* Ward, C.R., Harrington, H.J., Mallett, C.W. & Beeston, J.W. (Editors): Geology of Australian coal basins. *Geological Society of Australia, Coal Geology Group, Special Publication*, **1**, 465–470.

GRAY, A.R., 1976: Hillsborough Basin. *In:* Leslie, R.B., Evans, H.J. & Knight, C.L. (Editors): Economic geology of Australia and Papua New Guinea, volume 3, petroleum. *Australasian Institute of Mining and Metallurgy Monograph Series*, **7**, 460–464.

GRAY, A.R.G. & DRAPER, J.J., 2002: Petroleum geology, Cooper and Eromanga basins. *In:* Draper, J.J. (Editor): Geology of the Cooper and Eromanga Basins. *Queensland Minerals and Energy Review Series*, Queensland Department of Natural Resources and Mines, Queensland, 63–85.

GREEN, P.M. (Editor), 1997: The Surat and Bowen Basins, southeast Queensland. *Queensland Minerals and Energy Review Series*, Queensland Department of Mines and Energy, Queensland.

GREEN, P.W. & LINDNER, A.W., 1981: Final Report, ATP2245M. Unpublished report held by the Geological Survey of Queensland QDEX System as CR8580.

HAMZA, V.M., 1979: Variation of continental mantle heat flow with age: Possibility of discriminating between thermal models of the lithosphere. *Pure and Applied Geophysics*, **117**(1/2), 65–74.

HAWKINS, P.J. & GREEN, P.M., 1993: Exploration results, hydrocarbon potential and future strategies for the northern Galilee Basin. *APEA Journal*, **33**, 280–280.

HENDERSON, R.A., DONCHAK, P.J.T. & WITHNALL, I.W., 2013: Mossman Orogen. *In:* Jell, P.A. (Editor): *Geology of Queensland*. Geological Survey of Queensland, Department of Natural Resources and Mines, Brisbane.

HODGKINSON, J., GRIGORESCU, M., HORTLE, A.L., McKILLOP, M.D., DIXON, O. & FOSTER, L.M., 2010: The potential impact of carbon dioxide injection on freshwater aquifers: The Surat and Eromanga Basins in Queensland. *Queensland Minerals and Energy Review*, Department of Employment, Economic Development and Innovation, Queensland.

HOFFMANN, K.L., 1989: The influence of pre-Jurassic tectonic regimes on the structural development of the southern Eromanga Basin, Queensland. *In:* O'Neil, B.J. (Editor): The Cooper and Eromanga Basins, Australia. *Proceedings of Petroleum Exploration Society of Australia*, **1989**, 315–328.

HOLCOMBE, R.J., STEPHENS, C.J., FIELDING, C.R., GUST, D.A., LITTLE, T.A., SLIWA, R., KASSAN, J., McPHIE, J. & EWART, A., 1997a: Tectonic evolution of the northern New England Fold Belt: the Permian–Triassic Hunter–Bowen event. *Geological Society of Australia, Special Publication*, **19**, 52–65.

HOLCOMBE, R.J., STEPHENS, C.J., FIELDING, C.R., GUST, D.A., LITTLE, T.A., SLIWA, R., McPHIE, J. & EWART, A., 1997b: Tectonic evolution of the northern New England Fold Belt: Carboniferous to early Permian transition from active accretion to extension. *Geological Society of Australia Special Publication*, **19**, 66–79.

HOUSTON, R.R., 1964: Petrology of intrusives of the Roma Shelf. *Geological Survey of Queensland Report*, **7**.

HUDDLESTONE-HOLMES, C. & GERNER, E., (Editors), 2012: *Proceedings of the 2012 Australian Geothermal Energy Conference*. Record 2012/73. Geoscience Australia: Canberra.

KENNETT, B.L.N. & van der HILST, R.D., 1996: Using a synthetic continental array in Australia to study the Earth's interior. *Journal of Physics of the Earth*, **44**, 669–674.

KENNETT, B.L.N., SALMON, M., SAYGIN, E. & AUSMOHO WORKING GROUP, 2011: AusMoho: the variation of Moho depth in Australia. *Geophysical Journal International*, **187**, 946–958.

KORSCH, R.J., STRUCKMEYER, H.I.M., KIRKBY, A., HUTTON, L.J., CARR, L.K., HOFFMANN, K.L., CHOPPING, R., ROY, I.G., FITZELL, M., TOTTERDELL, J.M., NICOLL, M.G. & TALEBI, B., 2011: Energy potential of the Millungera Basin: a newly discovered basin in north Queensland. *APPEA Journal*, **51**, 295–332.

KORSCH, R.J., WITHNALL, I.W., HUTTON, L.J., HENSON, P.A., BLEWETT, R.J., HUSTON, D.L., CHAMPION, D.C., MEIXNER, A.J., NICOLL, M.G. & NAKAMURA, A., 2009: Geological interpretation of deep seismic reflection line 07GA-IG1: The Cloncurry to Croydon transect. *Australian Institute of Geoscientists, Bulletin*, **49**, 153–157.

LACHENBRUCH, A.H., 1968: Preliminary geothermal model of the Sierra Nevada. *Journal of Geophysical Research*, **73**(22), 6977–6989.

LACHENBRUCH, A.H., 1970: Crustal temperature and heat production: implications of the linear heat-flow relation. *Journal of Geophysical Research*, **75**(17), 3291–3300.

LESLIE WARREN, C., 1970: Beaver-Pexa, Coreena No. 1, Well Completion Report, A-P 138P. Unpublished report held by the Geological Survey of Queensland QDEX System as CR3123.

LONGREACH OIL, 1964: Well Completion Report, Saltern Creek No. 1, Longreach Oil Ltd, A-P 87P, QLD. Unpublished report held by the Geological Survey of Queensland QDEX System as CR 1469.

LONGREACH OIL, 1990: Well Completion Report, Marchmont No. 1, Longreach Oil Ltd, A-P 87P, QLD. Unpublished report held by the Geological Survey of Queensland QDEX System as CR 1482.

McCONACHIE, B.A., FILATOFF, J. & SENAPATI, N., 1990: Stratigraphy and petroleum potential of the onshore Carpentaria Basin, north Queensland. *The APEA Journal*, **30**(1), 149–165.

McDONAGH, G.P., 1967: Phillips - Sunray Glenaras No. 1, A-P 106P, QLD, Well Completion Report. Unpublished report held by the Geological Survey of Queensland QDEX System as CR2049.

McKELLAR, J.L., 1993: Stratigraphic relationships in the Nambour Basin, southeastern Queensland. *Queensland Geology*, **5**, 1–17.

McLAREN, S., SANDIFORD, M., HAND, M., NEUMANN, N., WYBORN, L. & BASTRAKOVA, I., 2003: The hot southern continent: heat flow and heat production in Australian Proterozoic terranes. *In:* Hillis, R.R. & Müller, D. (Editors): Evolution and dynamics of the Australian Plate. *Geological Society of Australia, Special Publication*, **22**, 151–161.

MAGELLAN PETROLEUM AUSTRALIA LIMITED, 1992: ATP504P Maryborough Basin technical summary. Unpublished report held by the Geological Survey of Queensland QDEX System as CR24488.

MALONE, E.J., 1970. St Lawrence, Queensland 1:250 000 Geological Series. *Geological Survey of Queensland, Explanatory Notes* SF55-12.

MALONE, E.J. & PAINE, A.G.L., 1961: Bowen, Queensland 1:250 000 Geological Series. *Bureau of Mineral Resources, Australia, Explanatory Notes* SF55-03.

MANIAR, O.D. & PICCOLI, P.M., 1989: Tectonic discrimination of granitoids. *Geological Society of America Bulletin*, **101**, 635–643.

MAXWELL, M., O'CONNOR, L.K., SARGENT, S.N. & TALEBI, B., 2012: Coastal Geothermal Energy Initiative GSQ Georgetown 8-9R, well completion report and heat flow modelling results. *Queensland Geological Record*, **2012/16**.

MORGAN, P., 1984: The thermal structure and thermal evolution of the continental lithosphere. *Physics and Chemistry of the Earth*, **15**, 107–185.

MUFFLER, P., 1979: Assessment of geothermal resources of the United States - 1978. *USGS Circular*, **790**.

MULLIGAN, P.R., PETKOVIC, P. & DRUMMOND, B.J., 2003: Potential-field datasets for the Australian region: their significance in mapping basement architecture. *In:* Hillis, R.R. & Müller, D. (Editors): Evolution and dynamics of the Australian Plate. *Geological Society of Australia Special Publication*, **22**, 129–140.

MURRAY, C.G., 1994: Basement cores from the Tasman Fold Belt system beneath the Great Artesian Basin in Queensland. *Queensland Geological Record*, **1994/10**.

MURRAY, C.G. & KIRKEGAARD, A.G., 1978: The Thomson Orogen of the Tasman Orogenic Zone. *In:* Scheibner, E. (Editor): The Phanerozoic Structure of Australia and variations in tectonic style. *Tectonophysics*, **48**, 299–325.

O'CONNOR, L.K., MAXWELL, M., SARGENT, S.N. & TALEBI, B., 2012: Coastal Geothermal Energy Initiative GSQ Bowen 1, well completion report and heat flow modelling results. *Queensland Geological Record*, **2012/08**.

PAINE, A.G.L., 1972: Proserpine, Queensland 1:250 000 Geological Series. *Geological Survey of Queensland, Explanatory Notes* SF55-04,

PAINE, A.G.L. & BROWN, P.J., 1971: Proserpine, Queensland 1:250 000 Geological Series. *Bureau of Mineral Resources, Australia, Explanatory Notes* SF55-04.

PAINE, A.G.L., CAMERON, R.L., 1972: Bowen, Queensland 1:250 000 Geological Series. *Geological Survey of Queensland, Explanatory Notes* SF55-03.

PEGREM, B.J., 1995: Tarong Basin. *In:* Ward, C.R., Harrington, H.J., Mallett, C.W. & Beeston, J.W. (Editors): Geology of Australian coal basins. *Geological Society of Australia, Coal Geology Group, Special Publication*, **1**, 465–470.

PINDER, B., 2007: A-P 700P, ARM Styx River 1 Well Completion Report. Unpublished report held by the Geological Survey of Queensland QDEX System as CR49882.

POWERLINK QUEENSLAND, 2012: Viewed 28 January 2013, <http://www.powerlink.com.au/About_Powerlink/Publications/Annual_Planning_Reports/Annual_Planning_Report_2012.aspx>

PURDY, D. & BROWN, D., 2011: Peeking under the covers – the new 'geology of the Thomson Orogen' project. *Queensland Geological Record*, **2011/09**.

QUEENSLAND DEPARTMENT OF MINES AND ENERGY, TAYLOR WALL & ASSOCIATES, SRK CONSULTING PTY LTD & ESRI AUSTRALIA, 2000: *North-west Queensland Mineral Province Report*. Queensland Department of Mines and Energy, Brisbane.

RADKE, B.M., FERGUSON, J., CRESSWELL, R.G., RANSLEY, T.R. & HABERMEHL, M.A., 2000: *Hydrochemistry and implied hydrodynamics of the Cadna-owie–Hooray Aquifer, Great Artesian Basin, Australia*. Bureau of Rural Sciences, Canberra.

ROBERTSON, A.D., 1990: Rifting, transfer faulting, and resultant Cainozoic volcanism, Maryborough Basin, southeast Queensland. *In: Proceedings Volume II, Pacific Rim Congress 90,* The Australian Institute of Mining and Metallurgy, Melbourne, 265–270.

RYBACH, L., 1988: Determination of Heat Production Rate. *In:* Haenel, R., Rybach, L. & Stegena, L. (Editors): *Handbook of Terrestrial Heat-Flow Density Determination*, Kluwer Academic Publishers, Dordrecht, 125–142.

SANDIFORD, M., HAND, M. & MCLAREN, S., 1998: High geothermal gradient metamorphism during thermal subsidence. *Earth and Planetary Science Letters*, **163**, 149–165.

SANYAL, S.K. & BUTLER, S.J., 2005: An Analysis of Power Generation Prospects from Enhanced Geothermal Systems. *Geothermal Resources Council Transactions*, **29**, 131–137.

SANYAL, S.K. & SARMIENTO, Z.F., 2005: Booking Geothermal Energy Reserves. *Geothermal Resources Council Transactions*, **29**, 467–474.

SARGENT, S.N., BOWDEN, S., MAXWELL, M., O'CONNOR, L.K. & TALEBI, B., 2012a: Coastal Geothermal Energy Initiative GSQ Maryborough 16 well completion report and heat flow modelling results. *Queensland Geological Record*, **2012/01**.

SARGENT, S.N., MAXWELL, M., O'CONNOR, L.K. & TALEBI, B., 2012a: Coastal Geothermal Energy Initiative GSQ Gympie 7, well completion report and heat flow modelling results. *Queensland Geological Record*, **2012/12**.

SASS, J.H. & LACHENBRUCH, A.H., 1979: Thermal regime of the Australian continental crust. *In:* McElhinny, M.W. (Editor): *The Earth—its Origin, Structure and Evolution*. Academic Press, London, 301–351.

SAYGIN, E., McQUEEN, H., HUTTON, L.J., KENNETT, B.L.N., & LISTER, G., 2013: Structure of the Mount Isa region from seismic ambient noise tomography. *Australian Journal of Earth Sciences*, **60**(6–7), 707–718.

SCOTT, S.G., BEESTON, J.W. & CARR, A.F., 1995: Galilee Basin. *In:* Ward, C.R., Harrington, H.J. & Beeston, J.W. (Editors): Geology of Australian coal basins. *Geological Society of Australia, Coal Geology Group, Special Publication*, **1**, 341–352.

SEKIGUCHI, K., 1984: A method for determining terrestrial heat flow in oil basinal areas. *Tectonophysics*, **103**, 67–79.

SHELL DEVELOPMENT, 1967: SDA Gregory River No. 1 well, QLD, Well Completion Report, A-P 70P, SDA Report No. 71. Unpublished report held by the Geological Survey of Queensland QDEX System as CR2160.

SIEGEL, C., BRYAN, S. PURDY, D., ALLEN, C., SCHRANK, C., UYSAL, T., GUST, D. & BEARDSMORE, G., 2012: Evaluating the role of deep granitic rocks in generating anomalous temperatures in south-west Queensland. *In:* Geological Survey of Queensland: Digging Deeper 10 seminar extended abstracts. *Queensland Geological Record* **2012/14**, 95–101.

SIEGEL, C., SCHRANK, C.E., BRYAN, S.E., BEARDSMORE G.R. & PURDY, D.J., 2013: Heat-producing crust regulation of subsurface temperatures: a stochastic model re-evaluation of the geothermal potential in southwestern Queensland, Australia. Geothermics (under review).

SILLER, C.W., 1965: A-P 6P, Report On LSD Cherwell 1 Well. Unpublished report held by the Geological Survey of Queensland QDEX System as CR17.

SLIWA, R., HAMILTON, S., HODGKINSON, J. & DRAPER, J., 2008: Bowen Basin structural geology 2008, an interpretation based on airborne geophysics and open file exploration data. CSIRO and Queensland Government Department of Mines and Energy.

SOMERVILLE, D., CAMP, J. & BLANCH, S., 2011: Electricity Network Capital Program Review 2011 - Detailed report of the independent panel. Queensland Government – Business and industry portal, available from: <http://www.business.qld.gov.au/__data/assets/pdf_file/0018/9117/ENCAP_Review_Final_Report_3_new.pdf>

STRECKEISEN, A.L., 1973: Plutonic rocks. Classification and nomenclature recommended by the IUGS Subcommission on the Systematics of Igneous Rocks. *Geotimes*, **18**(10), 26–30.

TANG, J.E.H., 2003: *Goomeri, Sheet 9345, Queensland, 1:100 000 Geological Map Commentary*. Department of Natural Resources and Mines, Queensland, Brisbane.

TORGERSEN, T., HABERMEHL, M.A. & CLARKE, W.B., 1992: Crustal helium fluxes and heat flow in the Great Artesian Basin, Australia. *Chemical Geology*, **102**, 139–152.

TROUP, A.J., MAXWELL, M., O'CONNOR, L.K., SARGENT, S.N. & TALEBI, B., 2012: Coastal Geothermal Energy Initiative GSQ St Lawrence 1, well completion report and heat flow modelling results. *Queensland Geological Record*, **2012/11**.

TURCOTTE, D.L. & SCHUBERT, G., 1982: *Geodynamics: Applications of continuum physics to geological problems*. Wiley.

TURNER, S., BEAN, L.B., DETTMAN, M., McKELLAR, J.L., McLOUGHLIN, S. & THULBORN, T., 2009: Australian Jurassic sedimentary and fossil successions: current work and future prospects for marine and non-marine correlation. *GFF*, **131**(1-2), 49–70.

TZIMAS, E., MOSS, R.L. & NTAGIA, P., 2011: 2011 Technology Map of the European Strategic Energy Technology Plan (SET-Plan). Available from: http://setis.ec.europa.eu/about-setis/technology-map/2011_Technology_Map1.pdf/view

van HEESWIJCK, A., 2010: Late Paleozoic to Early Mesozoic deformation in the northeastern Galilee Basin, Australia. *Australian Journal of Earth Sciences*, **57**(4), 431–451.

VINE, R.R., 1973: Eromanga Basin. *In:* Leslie, R.B., Evans, H.J. & Knight, C.L. (Editors): Economic geology of Australia and Papua New Guinea, volume 3, petroleum. *Australasian Institute of Mining and Metallurgy, Monograph Series*, **7**, 306–309.

von GNIELINSKI, F. (Compiler), 2011: *Queensland Minerals, a summary of major mineral resources, mines, and projects 2011*. Queensland Department of Employment, Economic Development and Innovation, Brisbane.

VOSTEEN, H-D. & SCHELLSCHMIDT, R., 2003: Influence of temperature on thermal conductivity, thermal capacity and thermal diffusivity for different types of rock. *Physics and Chemistry of the Earth*, **28**, 499–509.

WAPLES, D.W. & WAPLES, J.S., 2004: A review and evaluation of specific heat capacities of rocks, minerals and subsurface fluids. Part 1: Minerals and nonporous rocks. *Natural Resources Research*, **13**(2), 97–122.

WEBER, R.D. & KIRKBY, A.L., 2011: Thermal Conductivity Dataset. Geoscience Australia.

WECKER, H.R.B., 1972: PL 4, AAO Pleasant Hills 1A, Well Completion Report. Unpublished report held by the Geological Survey of Queensland QDEX System as CR4362.

WELLMAN, P. & McDOUGALL, I., 1974. Cainozoic igneous activity in Eastern Australia. *Tectonophysics*, **23**, 49–65.

WHITE, D.A., 1962: Einasleigh, 1:250 000 Geological Series. *Bureau of Mineral Resources, Australia Explanatory Notes* SE/55-9.

WILLEY, E.C., 1998: The Maronghi Creek beds: A preliminary appraisal. *Queensland Government Mining Journal*, **99**(1161), 49–56.

WILLIAMS, C.F., 2007: Updated methods for estimating recovery factors for geothermal resources. *Proceedings of the 32nd Workshop on Geothermal Reservoir Engineering (SGP-TR-183)*, Stanford University.

WITHNALL, I.W., 1985: Geochemistry and tectonic significance of Early Proterozoic mafic rocks from the Etheridge Group, Georgetown Inlier. North Queensland. *BMR Journal of Australian Geology and Geophysics*, **9**, 339–351.

WITHNALL, I.W., 1996: Stratigraphy, structure, and metamorphism of the Proterozoic Etheridge and Langlovale Groups, Georgetown region, North Queensland. *Australian Geological Survey Organisation Record*, **1996/15**.

WITHNALL, I.W., BLAKE, P.R., CROUCH, S.B.S., TENISON WOODS, K., HAYWOOD, M.A., LAM, J.S., GARRAD, P. & REES, I.D., 1995: Geology of the southern part of the Anakie Inlier, central Queensland. *Queensland Geology*, **7**.

WITHNALL, I.W. & HUTTON, L.J, 2013: North Australian Craton. *In:* Jell, P.A. (Editor).): *Geology of Queensland.* Geological Survey of Queensland, Department of Natural Resources and Mines, Brisbane.

WITHNALL, I.W., HUTTON, L.J., BULTITUDE, R.J., von GNIELINSKI, F.E. & REINKS, I.P., 2009: Geology of the Auburn Arch, Southern Connors Arch and adjacent parts of the Bowen Basin and Yarrol Province, Central Queensland. *Queensland Geology*, **12**.

WITHNALL, I.W., HUTTON, L.J., GARRAD, P.D., JONES, M.R. & BLIGHT, R.L. 2002: North Queensland Gold and Base Metal Study Stage 1 Preliminary data release – Georgetown GIS. Geological Survey of Queensland, Department of Natural Resources and Mines, digital data released on CD-ROM.

WITHNALL, I.W., HUTTON, L.J., GARRAD, P.D. & REINKS, I.P., 1997: Pre-Silurian rocks of the Lolworth-Pentland area, North Queensland. *Queensland Geological Record*, **1997/6**.

WITHNALL, I.W. & MACKENZIE, D.E., 1980: New and revised stratigraphic units in the Proterozoic Georgetown Inlier, north Queensland. *Queensland Government Mining Journal*, **81**(939), 28–43.

WITHNALL, I.W., NEUMANN, N.L. & LAMBECK, A., 2009: Palaeoproterozoic to Mesoproterozoic geology of north Queensland. *Bulletin of the Australian Institute of Geoscientists*, **49**, 129–34.

WITHNALL, I.W., NIEUWENBERG, A., BLIGHT, R.L. & YARROL-SCAG Project Teams, 2005: Central Queensland Geoscience Data set Version 2, Yarrol-Connors-Auburn GIS. Geological Survey of Queensland, Department of Natural Resources and Mines, digital data released on DVD.

WYBORN, L., 1998: Younger ca 1500 Ma granites of the Williams and Naraku Batholiths, Cloncurry district, eastern Mt Isa Inlier: geochemistry, origin, metallogenic significance and exploration indicators. *Australian Journal of Earth Sciences*, **45**, 397–411.

YARROL PROJECT TEAM, 1997: New insights into the geology of the northern New England Orogen in the Rockhampton–Monto Region, Central Coastal Queensland: Progress Report on the Yarrol Project. *Queensland Government Mining Journal*, **98**(1146), 11–26.

ZIELHAUS, A. & van der HILST, R.D., 1996: Upper-mantle shear velocity beneath eastern Australian from inversion of waveforms from SKIPPY portable arrays. *Geophysical Journal International*, **127**, 1–16.